Pteropod Shell Condition, Locomotion, and Long-term Population Trends in the Context of Ocean Acidification and Environmental Change

By

Alexander Bergan

B.S., University of California San Diego, 2010

Submitted in partial fulfillment of the requirements for the degree of

Doctor of Philosophy

at the

MASSACHUSETTS INSTITUTE OF TECHNOLOGY

and the

WOODS HOLE OCEANOGRAPHIC INSTITUTION

June 2017

Signature of Author

_____

Joint Program in Biological Oceanography

Massachusetts Institute of Technology and Woods Hole Oceanographic Institution

May 24, 2017

Certified by

_____

Gareth L. Lawson

Thesis Supervisor, Joint Committee for Biology Department

Woods Hole Oceanographic Institution

Accepted by

_____

Ann M. Tarrant

Chair, Joint Committee for Biology Department

Woods Hole Oceanographic Institution

Pteropod Shell Condition, Locomotion, and Long-term Population Trends in the Context of Ocean Acidification and Environmental Change

By

Alexander Bergan

Submitted to the MIT-WHOI Joint Program in Oceanography and Applied Ocean Science and Engineering, in partial fulfillment of the requirements for the degree of Doctor of Philosophy in Biological Oceanography

Abstract

Thecosome pteropods are planktonic mollusks that form aragonite shells and that may experience increased dissolution and other adverse effects due to ocean acidification. This thesis focuses on assessing the possible biological effects of ocean acidification on the shells and locomotion of pteropods and examining the response of a local pteropod population to environmental change over time. I analyzed shell condition after exposing pteropods to elevated CO_2 as well as in natural populations to investigate the sensitivity of the shells of different species to aragonite saturation state (Ω_A). The pteropods (*Limacina retroversa*) from laboratory experiments showed the clearest pattern of shell dissolution in response to decreased Ω_A, while wild populations either had non-significant regional trends in shell condition (*Clio pyramidata*) or variability in shell condition that did not match expectations due to regional variability in Ω_A (*Limacina helicina*). At locations with intermediate Ω_A (1.5-2.5) the variability seen in *L. helicina* shell condition might be affected by food availability more than Ω_A. I examined sinking and swimming behaviors in the laboratory in order to investigate a possible fitness effect of ocean acidification on pteropods. The sinking rates of *L. retroversa* from elevated CO_2 treatments were slower in conjunction with worsened shell condition. These changes could increase their vulnerability to predators in the wild. Swimming ability was mostly unchanged by elevated CO_2 after experiments that were up to three weeks in duration. I used a long-term dataset of pteropods in the Gulf of Maine to directly test whether there has been a population effect of environmental change over the past several decades. I did not observe a population decline between 1977 and 2015, and *L. retroversa* abundance in the fall actually increased over the time series. Analysis of the habitat use of *L. retroversa* revealed seasonal associations with temperature, salinity, and bottom depths. The combination of laboratory experiments and field surveys helped to address gaps in knowledge about pteropod ecology and improve our understanding of the effects of ocean acidification on pteropods.

Thesis supervisor: Gareth L. Lawson
Title: Associate Scientist, Woods Hole Oceanographic Institution

Acknowledgements

I would like to thank my adviser, G. Lawson, who provided me with all of the opportunities that made this research possible. Also, I would like to thank the other members of my thesis committee, C. Asjian, G. Flierl, and L. Mullineaux, for their guidance and support and M. Neubert for chairing the defense. I would like to acknowledge the help of J. Kellner who served on the thesis committee for most of my candidacy. I would like to thank Captain K. Houtler and Mate I. Hanley of the R/V *Tioga*, Captain D. Mello and crew of OC473, and Captain I. Lawrence and the crew of NH1208 for all of their efforts that allowed us to collect data and pteropods. I appreciate the help I received at sea and in the lab collecting and rearing the pteropods from P. Alatalo, L. Blanco Bercial, T. Bolmer, S. Chu, N. Copley, T. Crockford, S. Crosby, J. Edebeli, M. Edenius, J. Fincke, K. Hoering, G. Lawson, R. Levine, M. Lowe, C. Luttazi, A. Maas, K. Manganini, C. Pagniello, E. Roberts, L. Roger, A. Schlunk, A. Tarrant, A. Thabet, N. Tuttle, M. Uddin, B. Voss, Z. Wang, T. White, P. Wiebe, K. Wurtzell. I thank R. Galat and D. McCorkle for their help setting up the CO_2 exposure system and S. Chu, K. Hoering, K. Morkeski, and Z. Sandwich for their invaluable help measuring carbonate chemistry. I would like to thank K. Young and D. Adhikari for providing insight into how to measure pteropod movements. I also thank S. Colin, J. Costello, H. Jiang, and L. Mullineaux for loaning equipment used for filming. I would like to thank A. Solow for his invaluable help with statistics used for comparing shell condition and habitat usage. I thank L. Kerr, A. Kuzirian, S. Senft, and the technicians at the Central Microscopy Facility at MBL for teaching me how to use their SEM. I would also like to thank V. Le Roux and A. Helbling for teaching me how to use the micro-CT. I would like to acknowledge C. Charette, V. Caron, L. Fraser, K. Kipp, R. Schwartz, M. Tivey, J. Westwater, and J. Yoder for all of their help in the Academic Programs Office. Finally, I would like to thank my family and friends for all of their support along the way.

Funding Sources

Funding for this research was provided by a National Science Foundation grant to Lawson, Lavery, Wang, and Wiebe (OCE-1041068), a National Science Foundation grant to Lawson, Maas, and Tarrant (OCE-1316040), a WHOI Coastal Ocean Institute Student Research Proposal Award to Bergan (COI-27040178), the Pickman Foundation, the Tom Haas Fund at the New Hampshire Charitable Foundation, and the WHOI Academic Programs Office.

Table of Contents

Abstract 3

Acknowledgments 5

Table of Contents 7

List of Figures 9

List of Tables 10

1. Introduction 11

    1.1 Pteropod Biology 11
    1.2 Ocean Acidification 15
    1.3 Calcification and Dissolution 17
    1.4 Pteropod Time Series 20
    1.5 Study Regions 21
    1.6 Objectives 22

2. The effect of elevated carbon dioxide on the sinking and swimming of the shelled pteropod *Limacina retroversa* 29

    2.1 Abstract 29
    2.2 Introduction 30
    2.3 Methods 32
    2.4 Results 41
    2.5 Discussion 52
    2.6 Supplementary Materials 60

3. Shell condition of three thecosome pteropod species (*Limacina retroversa*, *Limacina helicina*, and *Clio pyramidata*) from CO_2 exposure experiments and wild populations 65

    3.1 Abstract 65
    3.2 Introduction 66
    3.3 Methods 70
    3.4 Results 79
    3.5 Discussion 99

4. Variability in the abundance, distribution, and habitat use of *Limacina retroversa* in the Gulf of Maine 109

    4.1 Abstract 109
    4.2 Introduction 110
    4.3 Methods 114

4.4 Results 120
4.5 Discussion 131
4.6 Supplementary Materials 142

5. Conclusions.....143

5.1 Pteropod Fitness and Ocean Acidification 144
5.2 Shells from Wild Populations of Pteropods 148
5.3 Population Changes 153
5.4 Broader View 155

References 159

List of Figures

Chapter 2 Figures

1 The filming set up 37
2 Examples of swimming speed and trajectory 40
3 Transmittance and opacity of *L. retroversa* shells from the April 2015 experiment 44
4 Terminal sinking speed with wings withdrawn and wings extended 47
5 Log_{10} terminal sinking speed with wings withdrawn vs log_{10} shell length 49
6 Mean swimming speed, wing beat frequency, and tortuosity 50
S1 Shell dry mass with animal tissue present normalized to individual length 60
S2 Log_{10} mean swimming speed vs log_{10} shell length 60

Chapter 3 Figures

1 Regions of study in the Northeast Pacific and Northwest Atlantic 72
2 Aperture and protoconch regions of *C. pyramidata* shells 78
3 Converting a SEM image to black and white 78
4 The percent transparency from day 4 of the experiments during different seasons 81
5 The percent transparency vs dry mass from the ambient treatment 81
6 Calcein intensity for the April 2014 experiment 83
7 Representative images of transparency, calcein stained shells, and SEM images 83
8 Shell condition of *L. retroversa* from day 7 of the November 2014 experiment 84
9 Shell condition metrics vs Ω_A for multiple pteropod species 85
10 Vertical profiles of temperature, salinity, aragonite saturation state, and pH in the North Pacific where *L. helicina* were caught 88
11 Fluorescence vs depth at the stations where *L. helicina* were caught 89
12 The porosity of wild-caught *L. helicina* in the North Pacific from each of the nets 89
13 The shell condition of wild-caught small *L. helicina* across different stations 90
14 The shell condition of wild-caught small *L. helicina* across different depths 91
15 A comparison of shell condition between two size classes of wild-caught *L. helicina* 92
16 Vertical profiles of temperature, salinity, Ω_A, and pH at Atlantic and Pacific stations where *C. pyramidata* were caught 95
17 Morphological and shell condition measurements of wild caught *C. pyramidata* 96
18 Relationships between the percent transparency vs. porosity and mean pore size vs. porosity for multiple species of pteropod 97

Chapter 4 Figures

1 The study region in the Gulf of Maine 116
2 The location and density of pteropods between 1977 and 2015 121
3 The temperature and salinity plots from 1977-2015 122
4 Plots of *L. retroversa* density vs hydrography or bathymetry in the Gulf of Maine 124
5 Annual abundance, temperature, and salinity anomalies of in the Gulf of Maine 126
6 Annual climate indices and Gulf of Maine water mass composition from 1977-2015 128
7 Temperature and salinity averages from 150-200 m from 1977-2015 129
8 Fall weighted mean latitude and mean bottom depth vs year 130
S1 Annual anomalies of *L. retroversa* abundance, temperature, and salinity in the CCMB 142

List of Tables

Chapter 2 Tables

1 The carbonate chemistry parameters pCO_2, pH, and Ω_A between treatments 42
2 Representative images showing the changes in shell appearance from day 2 to day 15 45
3 Cruise and experiment details and associated statistics 46
4 Correlation coefficients among the swimming variables.....52
S1 Carbonate chemistry parameters over the course of the four experiments.....61

Chapter 3 Tables

1 Summary of each experiment 72
2 The pCO_2, pH, and Ω_A in the first week of experiments 80
3 The Ω_A, temperature, and salinity for each latitude and depth ranges of the nets where *L. helicina* were examined 88
4 Results from the ANCOVA (transparency, porosity, and pore size) with covariates: station, depth, and size.....94
5 The Ω_A, temperature, salinity, and depth of the saturation horizon for each station where *C. pyramidata* were examined.....95

Chapter 4 Tables

1 The mean bottom depth, distance to coast, temperature, and salinity weighted by the density of pteropods in the spring and fall.....121
2 Results for the linear regression model of the binary presence-absence of *L. retroversa* 123
3 Results for the linear regression model of the log-normal *L. retroversa* density 123
4 The correlation coefficients between annual time series of *L. retroversa* abundance, temperature, salinity, water mass composition, and climate indices 127
5 The correlation coefficients between lagged climate indices and the annual time series of *L. retroversa* abundance, temperature, salinity, water mass composition 128

Chapter 1

Introduction

Shelled pteropods (thecosomes) are holoplanktonic gastropods that have been receiving attention in the context of ocean acidification in recent years. In particular, there is concern that the shells will be subjected to enhanced dissolution as carbon dioxide concentrations increase in the ocean. Since the shells are likely to be important to the ecology of pteropods, adverse effects on the individual finesses and populations of pteropods might occur due to ocean acidification. These effects may be occurring already or may only become apparent in the future. This thesis focuses on assessing the possible biological effects of ocean acidification on the shells and locomotion of pteropods and examining the response of a local pteropod population to environmental change over time. In this thesis, I address 1) how might ocean acidification affect the fitness of pteropods, 2) does the shell condition of pteropod species vary regionally in response to environmental conditions, 3) have population scale changes occurred to pteropods in the Gulf of Maine, and 4) what associations do pteropods have with the hydrography and climate oscillations in the Gulf of Maine? By addressing these questions, I aim to further the fields of pteropod ecology and ocean acidification research.

Pteropod Biology

All pteropods are gastropod mollusks that live an entirely planktonic life and have parapodia, or wings, that allow them to swim (Lalli and Gilmer 1989). Pteropods (Class Gastropoda, subclass: Opisthobranchia) are split into two orders Thecosomata, the shelled pteropods, and Gymnosomata, the shell-less pteropods (Lalli and Gilmer 1989). Thecosomes are

further divided into the suborders Euthecosomata and Pseudothecosomata. In some species of Pseudothecosomata the adults do not have calcium carbonate shells, but instead a hard gelatinous pseudoconch. Euthecosomata has received the most research in the context of ocean acidification since all of its members produce aragonite (a calcium carbonate mineral form) shells that may be susceptible to dissolution. The families that comprise Euthecosomata are Limacinidae and Cavoliniidae (Lalli and Gilmer 1989). Members of Limacinidae have spiraling shells with a sinistral (left hand) coil. The growth of aragonite crystals form distinct layers in the shells. For the limacinids, shells are composed of inner and outer prismatic layers and a cross-lamellar middle layer (with the exception of *Heliconoides inflatus*, Gerhardt *et al.* 2000, Teniswood *et al.* 2013, Wall-Palmer *et al.* 2013). Cavoliniids have shells that do not coil and have a helical growth pattern in the middle layer (Bé *et al.* 1972, Zhang *et al.* 2011). Forma, or subspecies, have been classified based on morphological differences of the shells, and multiple forma can be co-located or geographically separated (McGowan 1963, Van der Spoel 1969, Burridge *et al.* 2015). Due to advances in the genetics analysis of pteropods, there have been some recent developments in the definition of pteropod species (Hunt *et al.* 2010, Maas *et al.* 2013, Gasca and Janssen 2014). Even in light of new evidence of speciation, species ranges can be very large with some species existing in multiple oceans (e.g. *Clio pyramidata*, *H. inflatus*) or having a bipolar distribution (e.g. *Limacina retroversa*).

Pteropods are protandrous hermaphrodites, developing from male to female once they have reached a certain size (e.g. Hsiao 1939). They produce egg masses that form gelatinous ribbons, and continually produce eggs throughout maturity (Thabet *et al.* 2015). The number of eggs and frequency of release varies by species and region (Lalli and Gilmer 1989). The life

spans of pteropods are believed to be between 6 months to 2 years (Bednaršek *et al.* 2012b, Thabet *et al.* 2015).

Pteropods can affect the carbon cycle and energy transfer to higher trophic levels. Thecosome pteropods are microphages, feeding mostly on particles <2 μm in diameter (Noji *et al.* 1997). The repackaging of organic matter by pteropods into larger fecal pellets is an important component of biological carbon pump, which exports carbon to the deep sea (Fortier *et al.* 1994). Thecosomes feed by forming mucous webs that trap suspended particles, including phytoplankton, small zooplankton, and detritus, which can then be ingested (Gilmer and Harbison 1986). Stable isotope and gut analyses have found that thecosomes are truly omnivorous (Gilmer and Harbison 1991, Richoux and Froneman 2009, Fanelli *et al.* 2011, Letessier *et al.* 2012). Gilmer and Harbison (1986) observed that disturbed thecosomes will abandon the mucous webs, which can then act as nuclei for other sinking organic matter. After being disturbed, pteropods will swim or sink away from the perceived threat, suggesting that this is how they try to escape from predators (Gilmer and Harbison 1986). Any change to the locomotive ability of pteropods due to ocean acidification could therefore affect susceptibility to predation.

The sinking shells of dead pteropods is another important way that pteropods sequester carbon to depth (Byrne *et al.* 1984). Pteropods account for about 20-42% of the carbonate produced in the ocean (Bednaršek *et al.* 2012c). Depending on the depth and carbonate chemistry of the water column, pteropod shells will sink to the seafloor and contribute to the sediments or they will dissolve in the water column (Berger 1978). The amount of pteropod aragonite that sinks into the deep ocean could be affected by ocean acidification in two ways. Firstly, pteropods might produce less aragonite as the favorability of conditions for shell formation decreases.

Secondly, the rate of dissolution of shells might increase throughout the water column resulting in more carbonate ions returning to the dissolved state at shallower depths. This process is known as the carbonate pump, and changes to its efficiency may be an important feedback to climate change (Passow and Carlson 2012). The amount of time that carbon remains in the deep ocean before returning to the atmosphere and surface ocean depends on how deep the organic (e.g. fecal pellets) or inorganic carbon (e.g. calcium carbonate) sinks before being respired or dissolved respectively (Fortier *et al.* 1994).

Shelled pteropods are prey to many predators. Gymnosomes feed exclusively on thecosomes (Lalli 1972, Conover and Lalli 1974). Thecosomes are also found in the diets of large organisms, including seabirds and bowhead whales (Karnovsky *et al.* 2008, Pomerleau *et al.* 2012). There are several commercially valuable fish that consume thecosomes, such as salmon, trout, mackerel, herring, and cod (LeBrasseur 1966, Armstrong *et al.* 2005, Sturdevant *et al.* 2013). Fish that consume large numbers of thecosomes can accumulate dimethyl sulfide and develop black gut which makes the fish meat smell foul (Ackman *et al*. 1972, Levasseur *et al.* 1994). Also, thecosomes can accumulate dinoflagellate toxins which can kill fish or cause health problems for humans (White 1977). Thecosomes may be important for mesopelagic food webs as well and are eaten by mid-water myctophids (Pakhomov *et al.* 1996, Hunt *et al.* 2008). However, the degree to which pelagic food webs rely on pteropods is not well understood. Stomach content analyses have uncertainty from variability in digestion rates and unidentifiable material (LeBrasseur 1966). Some species may be able to switch to other prey if pteropods are rare, while others may be obligate predators on shelled pteropods, such as gymnosomes. Since pteropods are wide-spread in the world's oceans, the possible effects of ocean acidification on pteropods are a concern for marine ecosystems.

Ocean Acidification

The ocean has taken up approximately 30% of the carbon dioxide (CO_2) emitted as a result of human activity since pre-industrial times, causing ocean acidification (Sabine *et al.* 2004). Increased dissolved CO_2 (pCO_2) decreases the pH and shifts the equilibrium between carbonate (CO_3^{2-}) and bicarbonate (HCO_3^-) to favor the latter (equation 1). It has been estimated that ocean acidification might lower the average global surface pH by 0.3 – 0.4 and that the availability of CO_3^{2-} might decrease by 60% by the end of the century (Feely *et al.* 2004, Orr *et al.* 2005).

$$CO_3{}^{2-} + H_2O + CO_2 \rightleftharpoons 2HCO_3^- \qquad 1$$

Equation 1. A simplified representation of the equilibrium between dissolved carbon dioxide, carbonate, and bicarbonate.

$$\Omega_A = \frac{[Ca^{2+}] \times [CO_3^{2-}]}{K'_{sp}} \qquad 2$$

Equation 2. Aragonite saturation state is calculated as the product of available dissolved calcium and carbonate ion concentrations divided by the apparent solubility product.

The thermodynamic favorability of $CaCO_3$ (in the form of aragonite) is determined by the saturation state (Ω_A; equation 2). Aragonite is approximately 50% more soluble than calcite, another common biogenic $CaCO_3$ form, under the same seawater conditions, due to a higher solubility product (K'_{sp}; Mucci 1983). When the product of the calcium and carbonate ion concentrations exceed the K'_{sp} of aragonite, then precipitation is favored and $\Omega_A>1$ (super-saturated). When $\Omega_A<1$, seawater is under-saturated and aragonite is prone to dissolution. Ca^{2+} concentrations are relatively similar across depths and in different regions of the oceans (Emerson and Hedges 2008). Thus spatial differences in Ω_A depend on the concentration of CO_3^{2-} ions and apparent solubility product (K'_{sp}). Due to equilibrium effects of the carbonate

system, CO_3^{2-} concentrations vary inversely with pCO_2. The K'_{sp} increases when seawater is colder, more saline, and at higher pressure (depth), which lowers the saturation state (Mucci 1983).

There are two notable depths in relation to aragonite, the saturation horizon and compensation depth. The saturation horizon is the depth at which Ω_A=1, and below the saturation depth Ω_A continues to decrease since K'_{sp} increases at higher pressure and lower temperature (e.g. Fabry *et al.* 2008). Aragonite can still exist below the saturation horizon if the rate of sinking aragonite exceeds the rate of dissolution. The compensation depth is deeper than the saturation horizon and is the depth below which no aragonite is found because it has all been dissolved (Manno *et al* 2007). Millman *et al.* (1999) estimated that the aragonite compensation depth is approximately where Ω_A=0.8. Ocean models and direct measurements indicate that the saturation horizon and the compensation depth will shoal over time due to ocean acidification (e.g. Fabry *et al.* 2008, Chu *et al.* 2016).

The Ω_A varies in space and time because of biological activities and the movement of water masses. Dissolved inorganic carbon (DIC) and total alkalinity (TA) are variables that can be used to calculate the Ω_A. Seawater with higher DIC will have lower Ω_A and seawater with higher TA will have higher Ω_A. Seasonal cycles in primary production and remineralization affect the DIC and TA (e.g. Wang *et al.* 2017). Photosynthesis consumes CO_2 to form sugars, which draws down the DIC, whereas remineralization of organic matter (i.e. respiration) releases CO_2, thus increasing DIC. Respiration below the euphotic zone and subsequent upwelling of this water can bring DIC rich water to the surface and decrease the Ω_A (e.g. Fabry *et al.* 2008). Calcification decreases the DIC but also decreases TA by twice as a result of the consumption of CO_3^{2-}. Known as the carbonate counter pump, calcification can increase the concentration of

CO_2 by affecting the carbonate system equilibria, whereas dissolution of $CaCO_3$ will have the opposite effect (Passow and Carlson 2012).

Calcification and Dissolution

Calcifying organisms are less able to build and maintain calcium carbonate structures (e.g. the shells of mollusks, tests of foraminifera, liths of coccolithophores, and the skeletons of hard corals) as the saturation state declines (e.g. Fabry *et al.* 2008, Kroeker *et al.*, 2010). Organisms calcify within an enclosed space separated from the external seawater by a membrane across which they actively transport ions to favor the precipitation of $CaCO_3$ (Waldbusser *et al.*, 2011, Lischka and Riebesell, 2012). For mollusks, this calcifying space is called the extrapallial cavity and the organic covering is called the periostracum (Ries *et al.*, 2009, Ivanina *et al.*, 2013, Gazeau *et al.*, 2013). The transport of ions into or out of the extrapallial cavity against existing chemical gradients is necessary for calcification, but requires energy. Some studies hypothesize that the energetic demands of calcifying in sub-optimal condition can be met if the food consumption is sufficiently high (Langdon and Atkinson 2005, Cohen and Holcomb 2009, Melzner *et al.* 2011, Drenkard *et al.* 2013, Thomsen *et al.* 2013). Early life stages of calcifying animals might be more vulnerable to low pH and low saturation state, including larval sea urchins and bivalves, perhaps due to having a limited energy budget (Kurihara 2008, Clark *et al.* 2009, Kurihara *et al.* 2009, Gazeau *et al.* 2013, White *et al*. 2013).

Some species may be better adapted to exposure to high levels of dissolved CO_2 and may be more resilient to changes in the carbonate chemistry. These might include species in upwelling environments, those that live in estuaries, and those that live buried in low pH sediments (Gazeau *et al.* 2007, Miller *et al.* 2009, Waldbusser *et al.* 2011, Amaral *et al.* 2011,

Range *et al.* 2012). For instance, *Mytilus galloprovicialis* has been a successful invasive mussel species from the Mediterranean to the western coast of the US, it thrives in estuaries and lagoons, and it is relatively resilient to decreased pH (Fernández-Reiriz *et al.*, 2012). Within a species, genetic diversity may be an important factor for resilience to ocean acidification (Parker *et al.* 2011, Burridge *et al.* 2015). Some species may not be able to cope with changing conditions if they are already living at their physiological limits. Other environmental changes that may have adverse effects on calcifying organisms include warming and deoxygenation (Parker *et al.* 2010, Talmage and Gobler 2011, Dickinson *et al.* 2013, Hiebenthal *et al.* 2013, Ivanina *et al.* 2013, Matoo *et al.* 2013).

Pteropods have been receiving attention in the context of ocean acidification, especially in regards to dissolution of the shell (e.g. Orr *et al.* 2005, Fabry et al. 2008, Bednaršek *et al.* 2012a). In experiments that change pCO_2 to concentrations forecasted by the end of the century, the shells of live pteropods have been observed to partially dissolve (Comeau *et al* 2010a, Comeau *et al.* 2010b, Comeau *et al.* 2012a, Lischka and Riebesell 2012). At high pCO_2 (1700 µatm), Comeau *et al.* (2010b) observed that larval *Cavolinia inflexa* were incapable of forming shells. Experiments using juvenile and adult *Limacina helicina* found that shell growth was reduced under low Ω_A (Comeau *et al.* 2009, Lischka *et al.* 2011). To investigate whether ocean acidification might already be affecting the shells of pteropods, one study compared the shells of live pteropods reared under pre-industrial and modern CO_2 concentrations, and did not observe a significant change in growth or dissolution (Lischka *et al.* 2011, Manno *et al.* 2012).

Dissolution of pteropod shells has been examined in laboratory experiments and wild caught specimen using optical techniques. The Limacina Dissolution Index (LDX) was established for paleoceanography, using the appearance of shells under light microscopy from

cores of pteropod oozes, a type of calcareous sediment, to examine past climate and hydrography (Almogi-Labin *et al.* 1986, Haddad and Droxler 1996, Gerhardt *et al.* 2000, Gerhardt and Henrich 2001). The LDX has also been used for examining the shells of live pteropods from experiments that manipulate the level of CO_2 to understand the potential effects of ocean acidification (Lischka *et al.* 2011, Lischka and Riebesell 2012). Higher magnification Scanning Electron Microscopy (SEM) has been used on thecosomes collected in sediment traps, those from CO_2 experiments, and pteropods caught in the wild (Manno *et al.* 2007, Roberts *et al* 2011, Bednaršek *et al.* 2012b, Bednaršek *et al.* 2014a, Bednaršek and Ohman 2015, Johnson *et al.* 2016). Overall, dissolution of pteropod shells increases as Ω_A decreases.

Analogies between wild populations of pteropods and laboratory experiments are possibly hindered by captivity effects (Howes *et al.* 2014). In order to directly test for threshold effects of Ω_A on pteropod shells in the wild, regional variability in shell condition can be compared across a range of naturally occurring Ω_A. Studies have been conducted in regions influenced by coastal upwelling of under-saturated water, off the coast of California (Bednaršek *et al.* 2014a, Bednaršek and Ohman 2015) and in coastal regions in the Southern Ocean (Bednaršek *et al.* 2012b, Johnson *et al.* 2016). These studies found regional differences in the shells of pteropods that could be mostly explained by regional variability in Ω_A. Even in marginally super-saturated waters ($1< \Omega_A<1.2$), shell dissolution can be in an advanced state (Bednaršek *et al.* 2012b, Bednaršek *et al.* 2014a, Bednaršek and Ohman 2015, Johnson *et al.* 2016). However, only the shells of *L. helicina* and *L. helicina antarctica* were examined in these studies and other species might respond differently to *in situ* Ω_A. Furthermore, there is a need for more quantitative measurements of shell condition because categorical methods do not lend themselves well to comparison between studies or allow for the measurement of more subtle

changes in shell condition. Pteropod shells should also be compared across open ocean environments, which cover the majority of the world's surface and where pteropods have largest impact on the global carbon cycle (Bednaršek *et al.* 2016a).

Pteropod Time Series

Long-term time series of pteropods allow for the assessment of population scale responses to environmental change. Multi-decade sampling programs are needed in order to reveal trends that can be obscured by natural ecological variability. Of the time series of pteropods that have been examined, the results have shown different directional long-term trends with datasets that span between 16 and 58 years. Specifically, studies observed a decrease in *Limacina spp.* in the North Sea (Beare *et al.* 2013, Beaugrand *et al.* 2013) and Northeast Pacific (Mackas and Galbraith 2011), an increase in *Clio pyramidata* in the Northeast Pacific (Mackas and Galbraith 2011), increases in overall pteropods in the California Current Ecosystem (Ohman *et al.* 2009) and the Mediterranean Sea (Howes *et al.* 2015), no directional trend in *Limacina spp.* in the Northwest Atlantic (Head and Pepin 2010), and no directional trends in the assemblage of pteropod species in the Southern Ocean (Loeb and Santora 2013) or in regions of the Northeast U.S. Continental Shelf (Kane 2007, Kane 2011a). Ideally, studies would examine the dynamics of species individually, but sometimes the taxonomic resolution has not been at the species level.

There is furthermore a lack of knowledge about the conditions (e.g. temperature and salinity) at which pteropods reside. Most of the studies on pteropod time series focus on temporal trends using large regional averages to represent the environmental conditions. Studies that address the conditions in pteropod habitats are relatively few and some have methodological issues, especially in the earlier years (Bigelow 1924, Redfield 1939, Chan and Bé 1964,

Vecchione and Grant 1983, Dadon 1990, Gallager *et al.* 1996). It is important to understand the associations between temperature, salinity, and pteropods since these factors might act synergistically with ocean acidification to have adverse effects on the fitness of pteropods (Lischka *et al.* 2011, Lischka and Riebesell 2012, Manno *et al.* 2012, Lischka and Riebesell 2016).

Study Regions

In this thesis, pteropods were studied in the Gulf of Maine, offshore Northwest Atlantic and Northeast Pacific. The Gulf of Maine has overall low buffering ability to coastal acidification and experiences large seasonal swings in Ω_A (Wang *et al.* 2013, Wanninkhof *et al.* 2015). Coastal acidification differs from ocean acidification in the open ocean due to the geochemical complexity of nearshore environments, where coastal processes vary DIC, TA, and nutrient loads at higher frequencies than open ocean environments (e.g. Glendhill *et al.* 2015). The circulation and bathymetry in the Gulf of Maine results in long residence times for the deep water (below 100 m ~1.5 years, Wang *et al.* 2017) allowing for the build-up of respiratory CO_2. During phytoplankton blooms, the DIC decreases and Ω_A increases, but as a bloom is grazed, respiration increases DIC and decreases Ω_A. Due to water column mixing and the annual cycles of productivity and respiration, the average Ω_A in the upper 60 m of the GOM decreases in the fall and winter (Wang *et al.* 2017). Seasonal changes in Ω_A might affect the shell condition of pteropods in this region. The dominant pteropod species in this region, *L. retroversa*, is readily available year round, making it a suitable model organism for laboratory experiments. Furthermore, regional surveys of the Gulf of Maine that began in 1977 provide an opportunity to

characterize the habitat of *L. retroversa* and examine population scale changes in abundance and distribution.

This thesis also compares pteropods sampled in the Northwest Atlantic and Northeast Pacific as well as across different latitudes. Deep water formation in the North Atlantic, but not in the Pacific, is largely responsible for basin scale differences in Ω_A (Talley *et al*. 2011). Over large spatial scales, variability in Ω_A is affected by the thermohaline circulation, which connects the deep water current of all the oceans. The North Pacific has lower Ω_A than the North Atlantic because in the Pacific there is gradual upwelling of deep water that is high in DIC due to the gradual build-up of respiratory CO_2. Additionally, the Ω_A generally decreases and the saturation horizon shoals at higher latitudes in the North Pacific due to this upwelling of deep water. Large-scale spatial patterns in Ω_A and the wide-spread (in some cases cosmopolitan) distributions of pteropod species allows for the comparison of shells across a natural gradient in Ω_A.

Objectives and Approach

The overarching context of this work was to understand the effects of climate change on pteropods, with a particular emphasis on ocean acidification. Other studies have observed changes to the shells and physiology of pteropods under elevated pCO_2 concentrations, but linking the effects of ocean acidification to fitness is still tenuous. One way that ocean acidification could affect organismal fitness is by affecting the way in which pteropods move through the environment. I used laboratory experiments to evaluate changes in the shells and locomotion of pteropods. Next, I examined wild populations of pteropods to measure the shell condition across large regions with varying Ω_A in order to measure the sensitivity of pteropod species to changes in Ω_A. Inspecting the shell condition of three species of pteropod allowed me

to compare species-specific patterns of shell dissolution in relation to Ω_A. Finally, I used a time series of pteropod abundances in the Gulf of Maine from 1977-2015 to directly test for possible population effects of climate change up to the present day. This dataset also provided me with the opportunity to examine the physical conditions associated with the distribution and abundance of *L. retroversa* in the Gulf of Maine and how this species responds to large scale climate patterns.

Chapter 2: The effect of elevated carbon dioxide on the sinking and swimming of the shelled pteropod *Limacina retroversa*

In this chapter, I measured the sinking and swimming behaviors of the pteropod *L. retroversa* using high speed video, and then compared the movements of *L. retroversa* across varying levels of dissolved CO_2 to changes in shell condition in order to address the following questions:

1. How does the appearance of shells change after exposure to elevated CO_2?
2. Does *L. retroversa* sinking speed differ in relation to exposure to elevated CO_2?
3. Is the swimming ability of *L. retroversa* affected by exposure to elevated CO_2?

Limacina retroversa were captured on expeditions into the Gulf of Maine over multiple seasons, which allowed for repeat testing of the response of shells, sinking, and swimming to elevated CO_2. This was the first study to examine the sinking rates of pteropods after exposure to experimentally elevated CO_2 in order to investigate a possible effect of ocean acidification. With the use of a high speed camera and a mirrored tank, I was able to measure speed in 3D, the shell lengths, and the terminal speed, thus improving upon the methods for measuring pteropod sinking rates used previously (Kornicker 1959, Vingradov 1961, Diester-Haass 1973, Davenport

and Bebbington 1990). I expected that the shells would partially dissolve when exposed to elevated CO_2, since this had been observed already for *L. retroversa* (Lischka and Riebesell 2012, Manno *et al.* 2012), and that this would be associated with slowing in the sinking speed of individuals reared under elevated CO_2. I also expected the swimming of *L. retroversa* to be affected by elevated CO_2 due to physiological stress and/or changes to the ballast. Previous studies have yielded mixed results concerning whether mortality is increased for pteropods kept under elevated CO_2 (Lischka *et al.* 2011, Lischka and Riebesell 2012, Manno *et al.* 2012), but I expected that there would be a sub-lethal effect of elevated CO_2 on swimming speeds.

Unlike prior studies, my aim was to test the shell and locomotion responses of *L. retroversa* after different durations of exposure to elevated CO_2 to understand the time-scale at which effects occur. I developed quantitative tools for examining shell condition that could replace the categorical methods that have been previously used (e.g. LDX) in order to compare the shell condition response over time. Quantitative measurements were important throughout this thesis because they are objective and continuous.

Chapter 3: Shell condition of three thecosome pteropod species (*Limacina retroversa*, *Limacina helicina*, and *Clio pyramidata*) from CO_2 exposure experiments and wild populations

In this chapter, I used quantitative measurements of shell condition to examine the extent of dissolution of shells during laboratory experiments and on the shells of individuals preserved directly after being captured in the wild. Examining the shells of pteropods across different regions is a relatively new approach for assessing the vulnerability of pteropods to ocean acidification. Unlike other studies, I focused on open ocean populations and used spatial

variability in Ω_A over a large spatial scale that results from the thermohaline circulation. Specifically, I addressed the following questions:

1. How do methods for measuring shell condition using standard light microscopy compare to using scanning electron microscopy?
2. Are there seasonal differences in the shell condition of *L. retroversa*?
3. Does the shell condition of wild-caught *L. helicina* vary latitudinally and does the variability relate to differences in Ω_A?
4. Are there differences between the *L. helicina* shells that are caught at different depths?
5. Are there differences between the *L. helicina* shells of large and small individuals?
6. Do *C. pyramidata* from the North Atlantic and North Pacific and from different latitudes have differences in shell condition that are related to Ω_A?
7. Are there species-specific threshold values of Ω_A that cause severe changes in shell condition?

By examining shells from laboratory experiments and wild populations, I aimed to measure how shell condition responds to different Ω_A and therefore understand how vulnerable pteropod shells are to ocean acidification. As shells dissolve, there is increased pitting in the outer prismatic layer that manifests as more and larger pores. Porosity is a measure of the proportion of shell's surface that is pores (Roger *et al.* 2011). I first used laboratory experiments to examine how exposure to elevated CO_2 affects shell condition in *L. retroversa*, measuring shell transparency with light microscopy and porosity with SEM. The elevated CO_2 experiments with *L. retroversa* were conducted over several seasons, which allowed me to investigate

seasonality in shell condition that could be due to temporal variability in Ω_A in the Gulf of Maine (where the *L. retroversa* were collected). Furthermore, the response of the shells to elevated CO_2 could be affected by seasonal changes in sensitivity, either due to acclimatization or differences in the health, feeding history, and developmental state of the individuals. Additionally, I investigated how calcification differs due to exposure to elevated CO_2 by calcein staining live *L. retroversa*. Next, I looked at the shell condition of the congeneric species *L. helicina* across wild-caught individuals from regions in the North Pacific and individuals caught at different depths. Furthermore, I examined different sized *L. helicina* to test whether there was a size based difference in shell condition. Lastly, I examined the shells of *C. pyramidata* between sampling locations in the Atlantic and Pacific comparing the porosity and shell thickness. I expected that the shells of wild caught individuals would reflect the regional differences in Ω_A. Regional variability in the shell condition of pteropods could reveal whether there is a relationship between shell condition and Ω_A or whether other factors may be important. By comparing shells across different Ω_A, I sought to determine if there was a threshold Ω_A value that caused elevated dissolution and if there were species-specific sensitivities to Ω_A.

Chapter 4: Variability in the abundance, distribution, and habitat use of *Limacina retroversa* in the Gulf of Maine

In this chapter, I used a long-term dataset describing the population of *L. retroversa* in the Gulf of Maine to investigate how *L. retroversa* associate with physical conditions in space and time. Furthermore, I sought to determine whether there had been a decline in the local pteropod species that might have been caused by ocean acidification or other environmental change in this region. The specific questions addressed are:

1. Does *L. retroversa* associate with water of a certain temperature, salinity, or bottom depth?
2. Have *L. retroversa* densities in the Gulf of Maine declined over the course of the time series?
3. Has there been a range shift in the distribution of *L. retroversa* within the Gulf of Maine over the course of the time series?
4. Are there inter-annual cycles of *L. retroversa* abundance and can they be explained by the physical environment, climate oscillations, or water masses in the Gulf of Maine?

I used co-located measurements of *L. retroversa* densities, temperature, and salinity to describe the habitat and distribution of pteropods. The dataset that I used was from 1977 to 2015 and was collected as part of ecosystem monitoring programs (EcoMon and MARMAP) in the Gulf of Maine operated by the Northeast Fisheries Science Center (NEFSC). Using this time series I sought to describe how the abundance and distribution of pteropods in the Gulf of Maine was related to environmental conditions in this region. I expected that environmental changes had led to a long-term population decline in *L. retroversa*. The population of *L. retroversa* might also exhibit cyclical inter-annual patterns that relate to climate variability, which is known to shift the relative abundances of different members of the zooplankton community in this region (e.g. Greene *et al.* 2003, Greene and Pershing 2007).

Chapter 2

The effect of elevated carbon dioxide on the sinking and swimming of the shelled pteropod *Limacina retroversa*

Reprinted with permission from Oxford University Press.

Abstract

Shelled pteropods are planktonic mollusks that may be affected by ocean acidification. *Limacina retroversa* from the Gulf of Maine were used to investigate the impact of elevated carbon dioxide (CO_2) on shell condition as well as swimming and sinking behaviors. *Limacina retroversa* were maintained at either ambient (ca. 400 µatm) or two levels of elevated CO_2 (800 and 1200 µatm) for up to four weeks, and then examined for changes in shell transparency, sinking speed, and swimming behavior assessed through a variety of metrics (e.g., speed, path tortuosity, wing beat frequency). After exposures to elevated CO_2 for as little as four days, the pteropod shells were significantly darker and more opaque in the elevated CO_2 treatments. Sinking speeds were significantly slower for pteropods exposed to medium and high CO_2 in comparison to the ambient treatment. Swimming behavior showed less clear patterns of response to treatment and duration of exposure, but overall, swimming did not appear to be hindered under elevated CO_2. Sinking is used by *L. retroversa* for predator evasion, and altered speeds and increased visibility could increase the susceptibility of pteropods to predation.

Introduction

The chemistry of the oceans is rapidly changing due to the infiltration of anthropogenic carbon dioxide (CO_2) into the surface ocean, a process known as ocean acidification. One of the effects of ocean acidification is a decrease in the availability of carbonate ion (CO_3^{2-}) which affects calcifying organisms that use calcium carbonate ($CaCO_3$) to build shells and other structures (e.g. Orr *et al.* 2005, Raven *et al.* 2005). A shifting balance of dissolution and calcification as saturation state decreases due to ocean acidification jeopardizes the shell structure that, in many cases, provides protection from predators (e.g. Fabry *et al.* 2008). Ocean acidification could also change the way that some organisms move in the environment since calcified structures govern the movements of certain planktonic organisms, including echinoderms and mollusks (e.g. Chan *et al.* 2011, Wheeler *et al.* 2013).

Thecosomes, or shelled pteropods (Order Euthecosomata; henceforth referred to simply as pteropods), are planktonic mollusks that build calcium carbonate shells in the crystal form of aragonite, which is less stable than the other common form, calcite. Pteropod shells are becoming increasingly soluble in some regions of their habitat due to ocean acidification (e.g. Fabry *et al.* 2008). The shells of many species of pteropod are transparent, but turn darker and more opaque when exposed to seawater under-saturated with respect to aragonite, possibly due to an increased roughness of the shell's surface associated with partial dissolution (Almogi-Labin *et al.* 1986, Haddad and Droxler 1996, Lischka *et al.* 2011, Lischka and Riebesell 2012, Wall-Palmer *et al.* 2013). Laboratory experiments have also shown that lowering the saturation state decreased calcification, leading to impaired shell growth (Comeau *et al.* 2009, Comeau *et al.* 2010a, Bednaršek *et al.* 2014b). Wild caught *Limacina helicina* from regions naturally low in aragonite saturation state have also shown signs of dissolution under scanning electron microscopy (Bednaršek, *et al.* 2012b, Bednaršek, *et al.* 2014a, Bednaršek, and Ohman. 2015).

Shelled pteropods are a food source for many marine organisms, including seabirds, whales, salmon, trout, mackerel, cod, myctophids, and other zooplankton (LeBrasseur 1966, Ackman *et al.* 1972, Conover and Lalli 1974, Levasseur *et al.* 1996, Pakhomov *et al.* 1996, Armstrong *et al.* 2005, Hunt *et al.* 2008, Karnovsky *et al.* 2008, Pomerleau *et al.* 2012, Sturdevant *et al.* 2013), and hence any effects of ocean acidification on pteropod populations also could have effects on a wide range of marine species. The ability of pteropods to move through the water column could be affected by ocean acidification via changes to the shell. Pteropods have evolved wings, or parapodia, to propel themselves through the water. The spiral shaped pteropod species (Limacinidae) swim in a zig-zag motion, rotating their shell between a power stroke followed by a recovery stroke to provide lift (Chang and Yen 2012, Murphy *et al.* 2016). Many species of pteropods make daily migrations to depth during the day to avoid visual predators and to the surface at night to feed (Wormuth 1981, Comeau *et al.* 2012, Maas *et al.* 2012); sinking of the negatively buoyant shell is presumed to be an important component of the downward part of this diel vertical migration. Pteropods can also use swimming and sinking to escape from predators that are in their immediate proximity (Comeau *et al.* 2012). Harbison and Gilmer (1986) observed both swimming and sinking behaviors when pteropods were disturbed. Furthermore, after pteropods die, their sinking shells sequester inorganic carbon to the deep ocean (Byrne *et al.* 1984) and pteropod shells are estimated to account for 20-42% of the global carbonate flux (Bednaršek *et al.* 2012c). Changes in the fitness, abundance, and sinking of pteropods under ocean acidification thus also have consequences to the carbon cycle.

The species examined in this study, *Limacina retroversa*, is found in the Gulf of Maine, a region that is particularly susceptible to ocean acidification (Wang et al. 2013). Due to deep water formation in the North Atlantic, the infiltration of anthropogenic CO_2 into intermediate and

deep water is pronounced in this region and is causing the carbonate chemistry throughout the water column to change more quickly than the average global rate (Sabine *et al.* 2004). Furthermore, recent studies along the length of the U.S. East Coast found that the Gulf of Maine had the lowest saturation states observed as well as the lowest total alkalinity to dissolved inorganic carbon ratio, indicative of strong sensitivity to continued acidification (Wang *et al.* 2013; Wanninkhof *et al.* 2015). Although found year round in the Gulf of Maine, *L. retroversa* is also found in the open ocean, in the temperate and subpolar Atlantic of the Northern and Southern hemispheres. As a broadly distributed species that is also readily available relatively close to shore, it serves as a useful model species for examining the response of pteropods to ocean acidification.

In this study, *L. retroversa* were captured and reared under different concentrations of CO_2 over the course of multiple seasons to examine the impacts on shell condition and locomotion, testing the hypotheses that 1) The appearance of shells changes after exposure to elevated levels of CO_2; 2) *L. retroversa* sinking speed differs among CO_2 treatments; and 3) The swimming ability of *L. retroversa* is affected by exposure to elevated CO_2.

Methods

Four cruises into the Gulf of Maine allowed for the capture of shelled pteropods, *Limacina retroversa*. The pteropods were brought back to the laboratory and reared in seawater modified by bubbling with three different levels of CO_2, an ambient treatment (nominally 400 ppm) and two elevated treatments, 800 and 1200 ppm, hereafter referred to as the ambient, medium, and high CO_2 treatments, respectively. These were intended to yield over-saturated, marginal, and strongly under-saturated conditions with respect to aragonite. The actual pCO_2

levels and saturation states achieved via bubbling were calculated from measured dissolved inorganic carbon (DIC) and total alkalinity (TA) using CO2SYS (see below). The condition of shells along with swimming performance and sinking rates of animals was examined after 2 days to 4 weeks of exposure.

Animal Sampling

Limacina retroversa were collected in water depths of ca. 45-260 m in the Gulf of Maine near Provincetown, MA aboard the R/V *Tioga* during four cruises in April, August, and November 2014 and April 2015, with each expedition lasting one to three days. Oblique tows were conducted with a 1-m diameter Reeve net with 333 µm mesh size. The net was equipped with a large cod-end and hauled at slow speeds (ca. 5 m/min) to collect animals in healthy condition. *Limacina retroversa* were isolated from the rest of the plankton sample and placed into 1-L jars filled with Gulf of Maine seawater pumped *in situ* from a depth of ca. 30 m and filtered through a 64 µm sieve. The pteropods were kept at densities of ca. 30-40 individuals per liter and maintained in a refrigerator at ca. 8°C and later in coolers for transfer to the laboratory.

Culturing and Experimental Set-up

Upon returning to the laboratory, *L. retroversa* were moved with a soft pipette into 13-L carboys with 2-3 replicate carboys per treatment. The carboys were filled with *in situ* seawater collected during the cruise that had been transferred a day earlier to the laboratory and filtered to 1µm. For the duration of each experiment, as well as for ca. 8-16 hours prior to the addition of animals, each carboy was bubbled continuously using one of the three CO_2 concentrations, ambient (nominally ca. 400 ppm), 800, and 1200 ppm. For the medium and high treatments, the

target air-balanced CO_2 gases used for bubbling were achieved by mixing pure CO_2 gas and CO_2-free air using mass-flow controllers. The ambient treatment was not controlled but rather was derived from the CO_2 content of ambient air drawn from outside the building.

The carboys were kept in a cold room at 8°C at a density of ca. 15 individuals per liter. The pteropods were fed a mixed diet of *Rhodomonas lens* (1500-4000 cells/mL) and *Heterocapsa triquentra* (150-500 cells/mL) with lower concentrations provided over the course of each experiment as the pteropod culture density decreased due to mortality and use for various measurements. Water and pteropods were siphoned out of the carboys every week so that the seawater could be replaced with clean pre-bubbled water (collected *in situ* in the Gulf of Maine and kept after the cruise in a holding tank filtered continuously at 1 µm) and dead pteropods could be separated from the live ones. Additional details on culturing protocols can be found in Thabet *et al.* (2015).

During water changes, samples of the water leaving each carboy and the water entering the carboys were collected in 250 mL borosilicate glass bottles, poisoned with 100 µL saturated mercuric chloride, and then capped with a greased stopper for later analysis of TA and DIC. TA was measured using an Apollo SciTech alkalinity auto-titrator (AS-ALK2, Apollo SciTech, Newark, DE, USA), an Orion 3 Star pH meter, and a Ross combination pH electrode based on a modified Gran titration method (Wang and Cai 2004). DIC was analyzed with a DIC auto-analyzer (AS-C3, Apollo SciTech, Newark, DE, USA) via acidification and non-dispersive infrared CO_2 detection (LiCOR 7000: Wang and Cai 2004). The saturation state of aragonite (Ω_A), pCO_2, and pH were calculated from DIC and TA with the CO2SYS software (Pierrot *et al.* 2006), using constants K_1 and K_2 from Mehrbach *et al.* (1973) refitted by Dickson and Millero (1987), and the $KHSO_4$ dissociation constant from Dickson (1990).

In order to monitor conditions and adjust bubbling rates accordingly between water changes, pH in each carboy was measured every 2-3 days using a USB 4000 spectrometer with an LS-1 light source and a FIA-Z-SMA-PEEK 100-mm flow cell (Ocean Optics, Dunedin, FL, USA), and 2 mM m-Cresol indicator dye (50 µL in 20 mL of sample). The DIC/TA-based calculations of Ω_A and pCO_2 described above were used as the primary means of assessing the carbonate chemistry of the experimental treatments, but Ω_A and pCO_2 were also calculated using CO2SYS from measurements of pH along with the nearest measurement of TA in time, as a means of assessing variability between water changes.

Shell Condition

Ten live animals were removed from each of the ambient, medium, and high treatments at days 2, 4, 8, and 15 during the April 2015 experiment. They were rinsed in de-ionized water, weighed wet and dry with a Cahn C-33 microbalance with a precision of 1 µg, then placed in 8.25% hypochlorite bleach for 24-48 hours to remove tissue, rinsed in de-ionized water again, and dried.

Using a light microscope, the empty shells were photographed at 2.5X magnification for transparency, opacity, and length measurements. For transparency, the shell was positioned in a glass petri dish with the aperture facing up and the light coming from below and through the shell. A photograph was taken through the microscope with a 2-ms exposure, and with white balance, contrast, and brightness values conserved across images. Similarly, opacity was measured from images of shells placed with the aperture up with 2-ms exposure, but with the lighting coming from two incandescent lights that illuminated the shell parallel to the camera in

order to measure reflected light. The lights were positioned opposite each other to reduce shadows, and about 10 cm away from the shell's location at the center of the petri dish.

Images were analyzed in MATLAB to calculate transmittance and opacity. For transmittance, the shell was identified against the white background by thresholding the image to black and white. The aperture as well as any holes were manually cropped from the object. The transmittance was calculated as the mean grayscale value (range: 0-255) of the pixels of the shell divided by 255 to get a scale of 0 (black) to 1 (white). The image analysis was similar for opacity, but instead the shell was identified by thresholding the brighter shell from a dark background. For opacity the mean grayscale value of the shell, after cropping out the aperture and any holes, was calculated on the same scale of 0 (black) to 1 (white), like transmittance.

Videography

Live and active *L. retroversa* (shell lengths ranging from 0.56 mm to 2.37 mm) were removed from each of the CO_2 treated carboys for filming during the 1^{st}, 2^{nd}, 3^{rd}, and 4^{th} weeks of exposure to the different CO_2 treatments. Due to the length of time needed to make a sufficient number of observations, filming was done over two to five days for each week. The exact numbers removed from the treatments for each week as well as which weeks were sampled varied among experiments due to variability in the number of live animals available and needs for companion studies of physiology and gene expression. The removed animals were moved to another cold room at 8°C, in 1-L jars of filtered seawater at the ambient CO_2 concentration. Videos were recorded with a Photron Fastcam SA3 high speed camera at 500 frames per second. A triangular prism tank with a mirrored face on the hypotenuse of the isosceles right triangle was used so that both the animal and its orthogonal projection were visible in the field of view and

the 3D position and velocity of the pteropod could be recorded (Figure 1a). Illumination was delivered by an LED panel with the light diffusing through a thin plastic sheet. The mirrored tank was filled with filtered seawater with a density between 1024-1026 kg/m^3. Density was measured with a digital seawater refractometer (Hanna Instruments, model 96822). Three types of movements were examined: sinking with wings withdrawn, sinking with wings extended, and upward swimming.

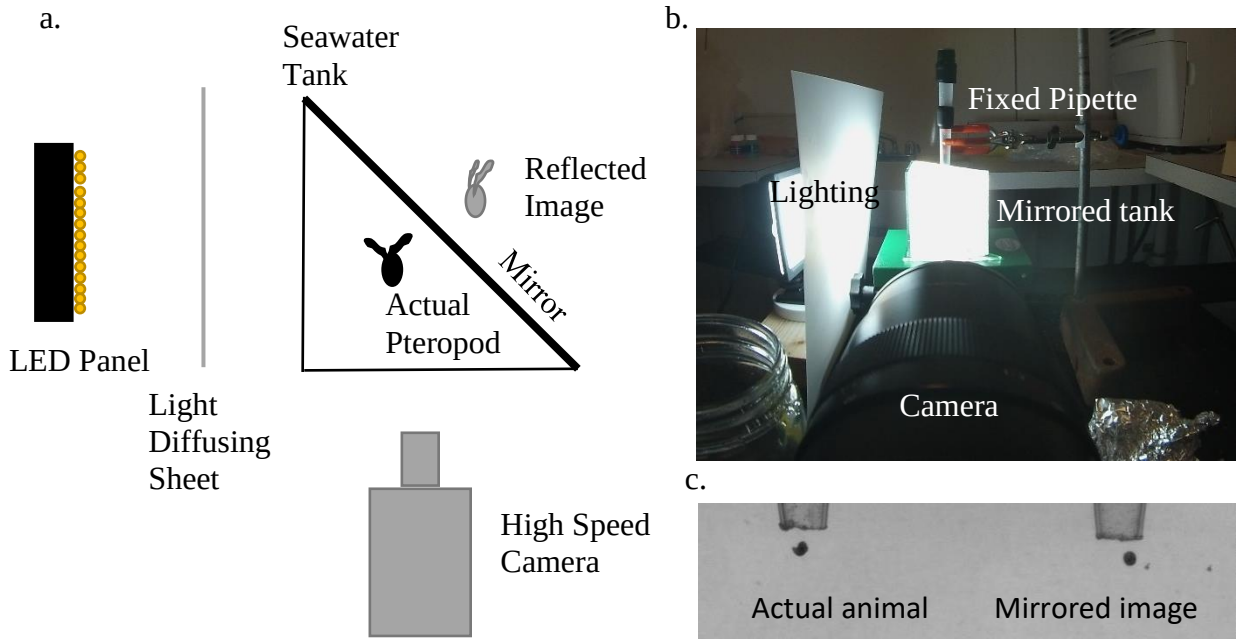

Figure 1. (a) Schematic of the filming set up. The seawater tank had a mirror to show the actual and reflected image of an animal sinking or swimming, allowing position to be determined in three dimensions. A high speed camera was used for filming and illumination was provided by an LED panel. The tank was 10 cm long, 10 cm wide, and 10 cm high. (b) Filming set up showing the mirrored tank with the fixed pipette that was used to drop the pteropods through for sinking trials. (c) One frame of a video shows the actual image and mirrored image of a sinking pteropod with wings withdrawn, shortly after exiting the fixed pipette.

Sinking

For quantification of sinking rates, a rigid pipette was attached to a ring stand and placed so that the narrow end was in the water and at the top of the camera's frame (Figure 1b,c). The camera was focused and a ruler used to calibrate distance in the tank. The field of view for sinking trials was 5.7 cm x 5.7 cm. Each *L. retroversa* was sucked into a soft pipette and then

released into the fixed pipette. The constriction in the fixed pipette caused the animal to slow and then accelerate as it left the fixed pipette and sank through the frame. Individual animals were filmed for 3-6 repeat sinking trials, which were used to calculate average sinking rates for each experimental animal later used in statistical comparisons among treatments. In April, August, and November of 2014, animals were filmed sinking with their wings extended and also with their wings withdrawn. In April 2015, only animals sinking with wings withdrawn were recorded in order to dedicate more time and generate a larger sample sizes for this behavior, since by then the difference between wings withdrawn and wings extended during sinking had already been determined.

The videos were analyzed in MATLAB by converting the frames to black and white. With the pteropod and its reflection isolated as objects, the length and position of the animal and its reflection were measured. Over successive frames, the difference in position was used to calculate speed. Since the animals rotated slightly about the horizontal axis the maximum length of the animal or reflection observed over the course of the video was used to estimate the length of the long axis. Speed vs. time plots were fit with a hyperbolic tangent function, giving an analytical solution for terminal speed. The hyperbolic tangent function solves for sinking velocity for a high Reynolds number regime (Owen and Ryu 2005). The Reynolds number is a non-dimensional number describing the ratio of inertial to viscous forces and is calculated here as animal length multiplied by the speed of the pteropod divided by the kinematic viscosity of water. Although *L. retroversa* move at low to intermediate Reynolds numbers (ca. 5-50), the hyperbolic tangent function fit the data better than the low Reynolds number solution (negative exponential function).

Swimming

Swimming trials were conducted by placing animals below the camera's field of view via soft pipette and filming their swimming up through the frame. The size of the field of view was calibrated with a ruler and was 2.7 cm x 2.7 cm, with the bottom of the field of view 2-3 cm above the floor of the tank. In the April 2014 and August 2014 experiments, multiple pteropods from the same treatment were placed in the tank together and swimming trials were recorded. Each of these swimming trials was included separately in statistical comparisons among treatments, but since the exact identity of swimmers was not known, the more active individuals could have contributed multiple swimming observations. Therefore, for improved accuracy, in November 2014 and April 2015, a single individual was placed in the tank and multiple swimming trials were recorded for each animal; swimming metrics averaged over the multiple trials for each individual were then used in statistical comparisons among treatments.

Video analysis was done in MATLAB with similar protocols as for sinking. The frames were converted to black and white to allow for the identification of the pteropod and its reflection to track its properties (length, position) from one frame to the next. These properties were used to determine the speed, distance travelled, and trajectory. Path tortuosity was measured as the total cumulative distance travelled over a video segment divided by the direct distance between the last and first frame; each video segment was at least 0.5 seconds and recorded at least three wing beats (power and recovery strokes). The swimming metrics examined were the mean speed (calculated in 3D), frequency of wing beats, path tortuosity, ratio of horizontal to vertical displacement, and asymmetry of speed between the power and recovery strokes (Figure 2).

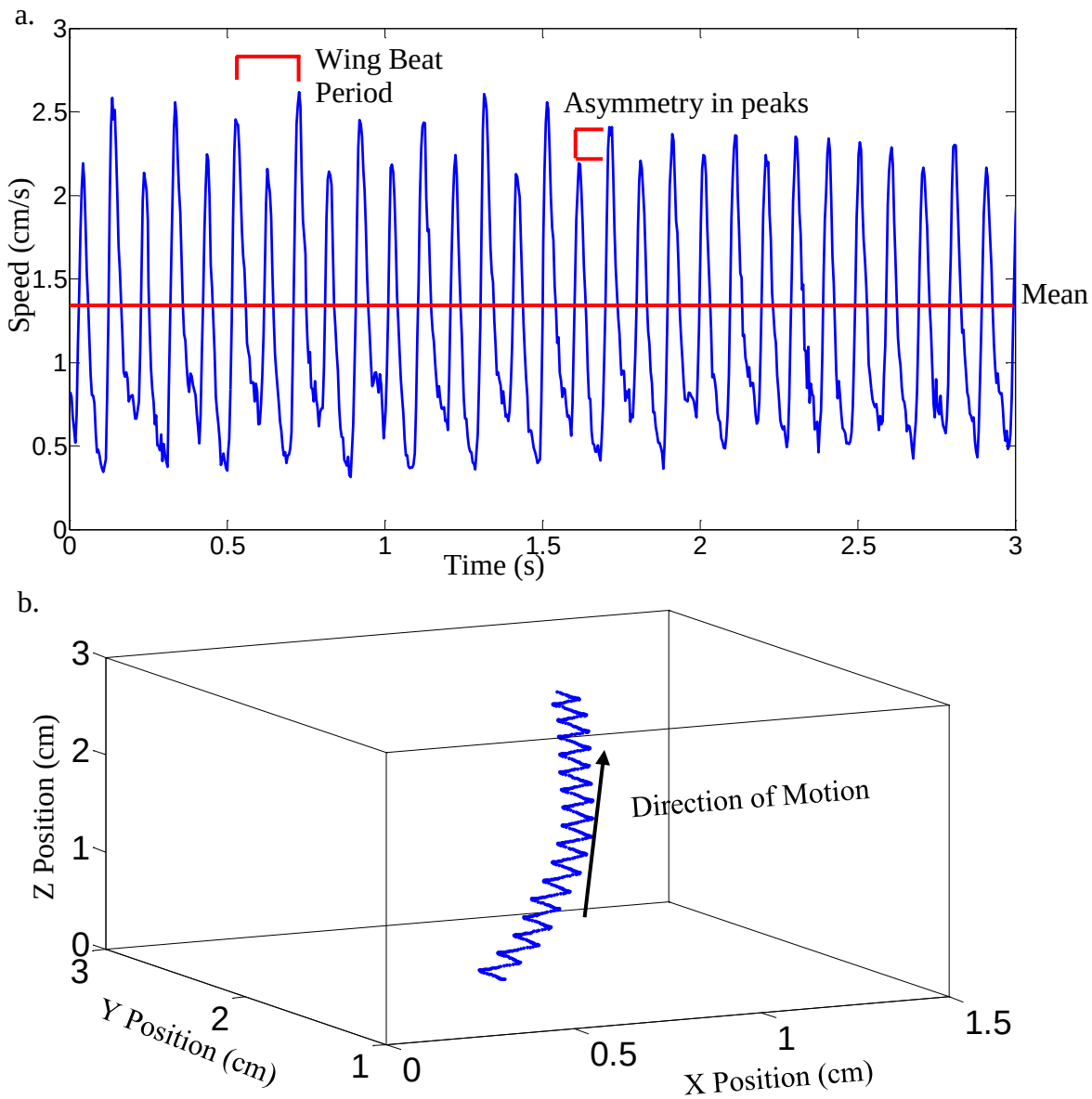

Figure 2. (a) Speed vs time plot of a swimming trial, showing the full time series of speed from the 3 second video segment (blue), along with calculated mean speed (red line), a wing beat period, and the asymmetry in peaks. The wing beat frequency was calculated as 1/(beat period) and included both the power and recovery strokes. Power strokes were consistently associated with greater speeds and asymmetry between the peak speeds of the power and recovery stroke was measured as the difference between subsequent peaks of speed divided by the larger of the two. (b) The 3D trajectory of a swimming *L. retroversa* shows the pattern of motion. Note that this is a scatter plot but the high frame rate of the camera leads to the points appearing essentially as a line. Tortuosity was calculated as the total cumulative distance traveled divided by the direct distance from starting point to finish.

Statistics

One-way analyses of variance (ANOVA), or a Kruskal-Wallis one-way ANOVA on ranks when the data failed either the equal variance or normality tests, were used to test for differences among treatments in shell transmittance and opacity, sinking speeds (separately for wings withdrawn and extended), swimming speed, wing beat frequency, swimming path tortuosity, ratio of horizontal to vertical displacement, and asymmetry in speed between the power stroke and recovery stroke. If there were significant effects from these tests, post-hoc pairwise comparison tests were conducted using the Holm-Sidak method for one-way ANOVAs and Dunn's method for Kruskal-Wallis one-way ANOVAs. Sinking speed with wings withdrawn was compared to sinking speed with wings extended using a Wilcoxon Paired-Sample Signed-Rank signed rank test. Correlation coefficients were also calculated among swimming metrics.

Results

Experimental Treatments

The nominal target values for pCO_2 of 400, 800, and 1200 µatm were not always achieved and calculated values varied among experiments, but overall the carbonate chemistry measurements indicated clear distinctions among treatments (summarized in Table 1 and see Supplementary Table S1 for full details). The ambient treatment had higher levels than the nominal 400 µatm (the approximate global average atmospheric concentration), closer to 450 µatm. Calculations of achieved pCO_2 for the medium and high treatments also indicated variability, likely due to a combination of uncertainty in the sampling and measurements of DIC and TA, uncertainty in the mixture of gas by the mass-flow controllers, and variability in the degree of bubbling. In April and August 2014 the calculated pCO_2 of pre-bubbled water that was

entering the carboys at the onset of the experiment was consistently lower than that calculated for the outgoing water, suggesting incomplete pre-equilibration (Supplementary Table S1). Subsequent measurements of pH made between water changes, however, indicated that the seawater chemistry for these treatments attained their target values after less than 24 h.

Table 1. The carbonate chemistry parameters partial pressure of CO_2 (pCO_2), pH, and aragonite saturation state (Ω_A) are average values for the water leaving the treatment carboys at days 7 and 14 during water changes. TA and DIC were directly measured and were used for calculation of the other parameters. Measurements of ingoing water at the start of each week of exposure in April and August 2014 appeared to indicate insufficient pre-equilibration, although target levels were reached by day 1 (see text and Supplementary Table S1). The values are reported as the mean ± standard deviation.

Experiment	**Treatment**	**pCO_2 (µatm)**	**pH**	**Ω_A**
April 2014	Ambient	470±20	7.96±0.02	1.54±0.06
	Medium	850±40	7.73±0.02	0.94±0.03
	High	1190±120	7.59±0.04	0.70±0.07
Aug 2014	Ambient	440±40	7.98±0.03	1.58±0.11
	Medium	650±170	7.84±0.11	1.21±0.30
	High	990±100	7.66±0.04	0.80±0.08
Nov 2014	Ambient	480±50	7.95±0.04	1.49±0.11
	Medium	1100±290	7.63±0.10	0.76±0.15
	High	1320±160	7.55±0.05	0.63±0.07
April 2015	Ambient	440±30	7.99±0.03	1.61±0.09
	Medium	740±100	7.78±0.05	1.05±0.12
	High	1180±190	7.59±0.07	0.70±0.11

Measurements of outgoing water made during water changes indicated that the ambient treatments always had over-saturated conditions with respect to aragonite (Ω_A=1.49-1.61), medium treatments were near the threshold of saturation (0.76 in November 2014, 1.21 in August 2014, and otherwise 0.94-1.05), and the high treatment had strongly under-saturated conditions (Ω_A=0.63-0.80, Table 1). The medium treatment showed the greatest variability, likely due to a combination of sampling error, issues with the mass-flow controllers (in November 2014, where saturation states were overly low), and insufficient bubbling (in August 2014, where saturation states were overly high). The ambient treatment was significantly different in aragonite saturation state from both of the elevated CO_2 treatments in three of the

experiments (one-way ANOVA, $p<0.001$), while in the August 2014 experiment only the ambient and high treatments were significantly different (Kruskal-Wallis one-way ANOVA, $H=11.7$, $p=0.003$). The medium and high treatments were also significantly different from one another in April of 2014 and 2015 (Holm-Sidak, $p<0.05$), though not in August or November 2014. TA showed relatively small differences between experiments, presumably related to natural seasonal processes in the Gulf of Maine region (Supplemental Table S1).

Shell Condition

Shell condition from the April 2015 experiment for the ambient treatment was mostly unchanged relative to duration of exposure, while the medium and high CO_2 treatments showed decreased transmittance and increased opacity over the course of 15 days of exposure (Figure 3, Table 2). On day 2, there was not a significant difference in the appearance of shells among treatments, but both shell transmittance and opacity were significantly different among treatments on days 4, 8, and 15 (Table 3). Post-hoc pairwise comparisons showed that the transmittance from the ambient and high treatments were significantly different on days 4, 8, and 15 ($p<0.05$), the medium and high treatments were never significantly different, and the medium and ambient treatments were only significantly different on day 15 ($p<0.05$). For opacity, on days 4 and 8 only the ambient and high treatments were significantly different ($p<0.05$), whereas on day 15, each treatment was significantly different from the others ($p<0.05$).

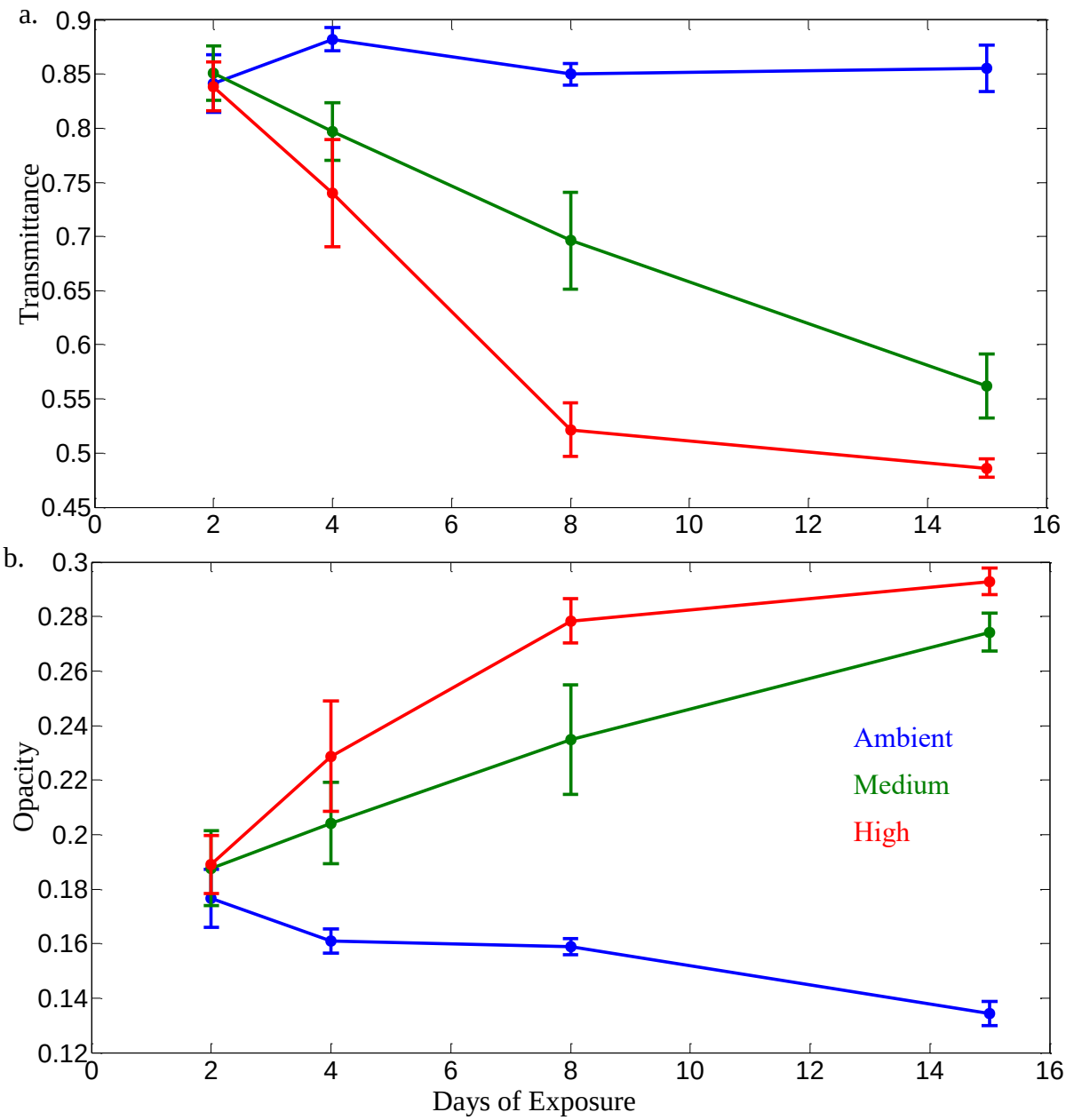

Figure 3. (a) Transmittance (proportion of transmitted light) and (b) opacity (proportion of reflected light) of *L. retroversa* shells from the April 2015 experiment relative to duration of exposure for each of the three CO_2 treatments.

Table 2. Representative images showing the changes in shell appearance from day 2 to day 15 for each treatment during the April 2015 experiment. Transmittance images are taken when light is shining from below the sample, and opacity images are taken when light is illuminating the sample from the sides.

	Treatment	Day 2	Day 15
Transmit-tance	Ambient	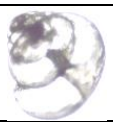	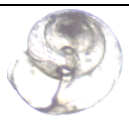
	Medium	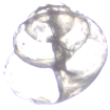	
	High	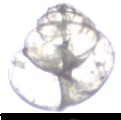	
Opacity	Ambient	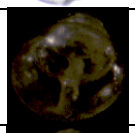	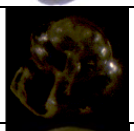
	Medium	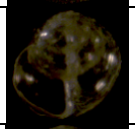	
	High	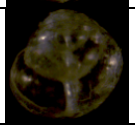	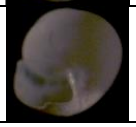

The dry masses of the shells (with animal body tissue present) from April 2015, normalized to length, indicated an overall decrease over the course of the 15 days of exposure and also substantial overlap among treatments (Supplementary Figure S1). Mass normalized to length was significantly different between the CO_2 treatments at days 8 (Kruskal Wallis one-way ANOVA, $H=6.1$, $p=0.048$) and 15 (one-way ANOVA, $F=4.1$, $p=0.037$), but not for the earlier time points. At day 8, there were not significant pairwise differences in mass normalized to length among treatments (Dunn's method, $p>0.05$), and on day 15 only the medium and high treatment were significantly different from one other (Holm-Sidak method, $p<0.05$).

Table 3. Cruise and experiment details and associated statistics. For each type of observation of *L. retroversa* (shell condition, sinking, or swimming) and each duration of exposure the sample sizes are listed (ambient, medium, high). Test statistics (F for one-way ANOVAs and H for Kruskal-Wallis one-way ANOVAs on ranks) are reported for comparisons among treatments for multiple sinking, swimming, and shell variables abbreviated as follows: "Sinking wings in" is sinking speed with wings withdrawn, "Sinking wings out" is sinking speed with wings extended, "Swim speed" is mean swimming speed, "Beat" is wing beat frequency, and "Tort" is tortuosity. * $p<0.05$, ** $p<0.01$, *** $p<0.001$, NS=Non-Significant

Experiment	Cruise Dates	Type of Observation	Exposure Duration	Sample Size Amb., Med., High	One-way ANOVA: F Kruskal-Wallis one-way ANOVA: H
April 2014	25 April – 27 April 2014	Sinking	4 Weeks	10, 10, 7	Sinking wings in: F=9.8***; Sinking wings out: F=9.0**
		Swimming	3 Weeks	11, 7, 10	Swim speed: $F=0.9^{NS}$, Beat: $H=1.7^{NS}$, Tort: H=8.4*
August 2014	19 August 2014	Sinking	1 Week	10, 12, 13	Sinking wings in: $H=1.1^{NS}$, Sinking wings out: $F=1.0^{NS}$
		Swimming	1 Week	13, 21, 17	Swim speed: F=4.6*, Beat: $H=2.1^{NS}$, Tort: H=10.6**
November 2014	4 November – 6 November 2014	Sinking	1 Week	20, 22, 20	Sinking wings in: $F=0.3^{NS}$, Sinking wings out: $F=0.4^{NS}$
		Sinking	2 Weeks	25, 20, 18	Sinking wings in : F=4.2*, Sinking wings out : F=6.4**
		Swimming	2 Weeks	3, 10, 10	Speed: $H=1.6^{NS}$, Beat: $F=1.6^{NS}$, Tort: $H=2.3^{NS}$
April 2015	26 April – 27 April 2015	Sinking	1 Week	25, 26, 25	Sinking wings in: F=5.8**
		Sinking	2 Weeks	26, 26, 22	Sinking wings in: H=11.6**
		Sinking	3 Weeks	26, 22, 16	Sinking wings in: F=19.0***
		Swimming	1 Week	15, 18, 16	Swim speed: F=3.7*, Beat: F=9.5***, Tort: $H=4.7^{NS}$
		Swimming	2 Weeks	8, 14, 18	Swim speed: $F=0.1^{NS}$, Beat: $F=1.5^{NS}$, Tort: $H=5.1^{NS}$
		Shells	2 Days	8, 9, 8	Transmittance: $F=0.1^{NS}$, Opacity: $H=0.8^{NS}$
		Shells	4 Days	8, 8, 8	Transmittance: H=9.0*, Opacity: H=8.1*
		Shells	8 Days	8, 7, 5	Transmittance: H=14.5***, Opacity: H=13.0**
		Shells	15 Days	7, 7, 5	Transmittance: F=60***, Opacity: F=212***

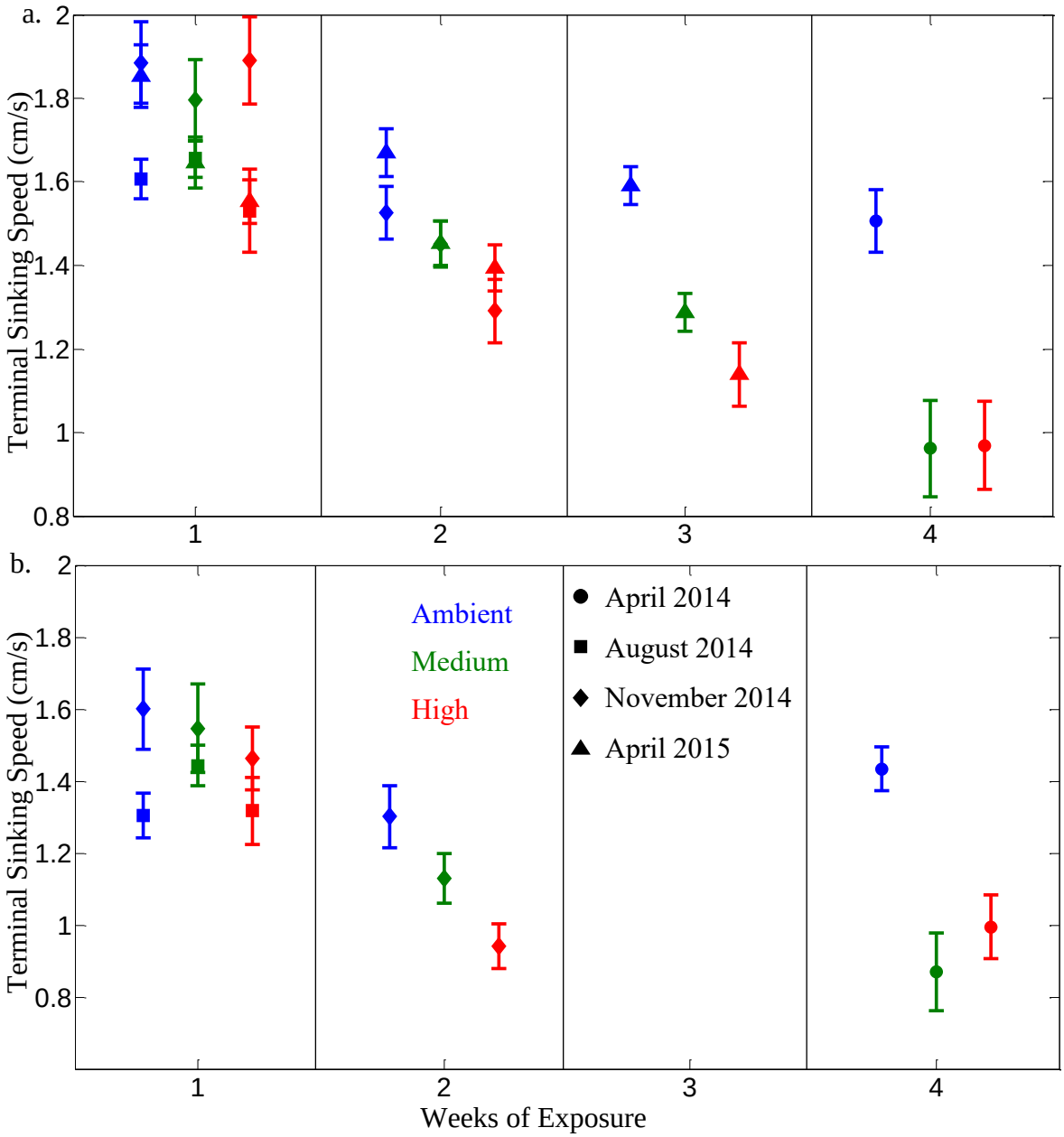

Figure 4. (a) Terminal sinking speed for *L. retroversa* with wings withdrawn for the four experiments (circle: April 2014; square: August 2014; diamond: November 2014; triangle: April 2015) after durations of exposure of 1-4 weeks. From left to right within each weekly bracket the ambient, medium, and high treatment are plotted, although the treatments were measured together of the course of 2-5 days, and are spaced along the x-axis simply for easier visualization. The error bars denote standard error. (b) The terminal sinking speed with wings extended for the April 2014, August 2014, and November 2015 experiments. No measurements of sinking with wings extended were made in April 2015 or in week 3 of any of the experiments.

Sinking

Sinking rates showed differences associated with treatment, duration of exposure, experiment, and behavior (i.e. wings extended or withdrawn). After one week of exposure,

sinking rates for animals with wings withdrawn were similar among treatments and showed no significant differences for two of three experiments (Figure 4a, Table 3), while during week one of the third experiment (April 2015) sinking rates differed significantly among treatments. Sinking rates were significantly slower for animals in the elevated CO_2 treatments than in the ambient treatment after two or more weeks of exposure during every experiment. In all pairwise comparisons, the ambient treatment was significantly different from both the medium and high treatments, except for the second week of the November 2014 when only the ambient and high treatments were significantly different ($p<0.05$).

On average there was an 16% reduction in sinking speed for animals holding their wings extended compared to wings withdrawn, and sinking speeds with wings withdrawn and wings extended measured for the same individuals were significantly different (Wilcoxon Paired-Sample Signed Rank, $Z=-8.981$, $p<0.001$). Sinking rates for animals with wings extended also showed similar trends to those with wings withdrawn with respect to treatment and duration of exposure (Figure 4b). While there were no significant differences among the treatments after one week of exposure, significant differences were observed among treatments after an exposure duration of two weeks and onwards, with significantly faster sinking rates evident for the *L. retroversa* exposed to ambient CO_2 compared with the high treatment (November 2014 week 2) or to the medium and high treatments (April 2014 week 4).

In order to account for possible uncertainty introduced by any differences in the size of animals among treatments and time points, attempts were also made to normalize the sinking rate measurements relative to individual size. Linear regressions based on log-log plots were used to examine the effect of length on sinking speed of animals with wings withdrawn. The resulting power law scaling relationships between sinking speed and length for the ambient, medium, and

high treatments were 0.45, 0.74, and 0.52 respectively (Figure 5), suggesting that normalizing the sinking speeds by the square root of length (0.50 scaling) was appropriate. In all but one case, normalizing sinking speed by length in this way did not affect the significance of the differences among treatments, with the exception of week one for November 2014. In this case, in contrast to the initial test, when normalized, the Kruskal-Wallis one-way ANOVA showed significant differences among treatments in sinking speeds (H=7.3, p=0.026) due to faster sinking in the high treatment, followed by the medium, then ambient.

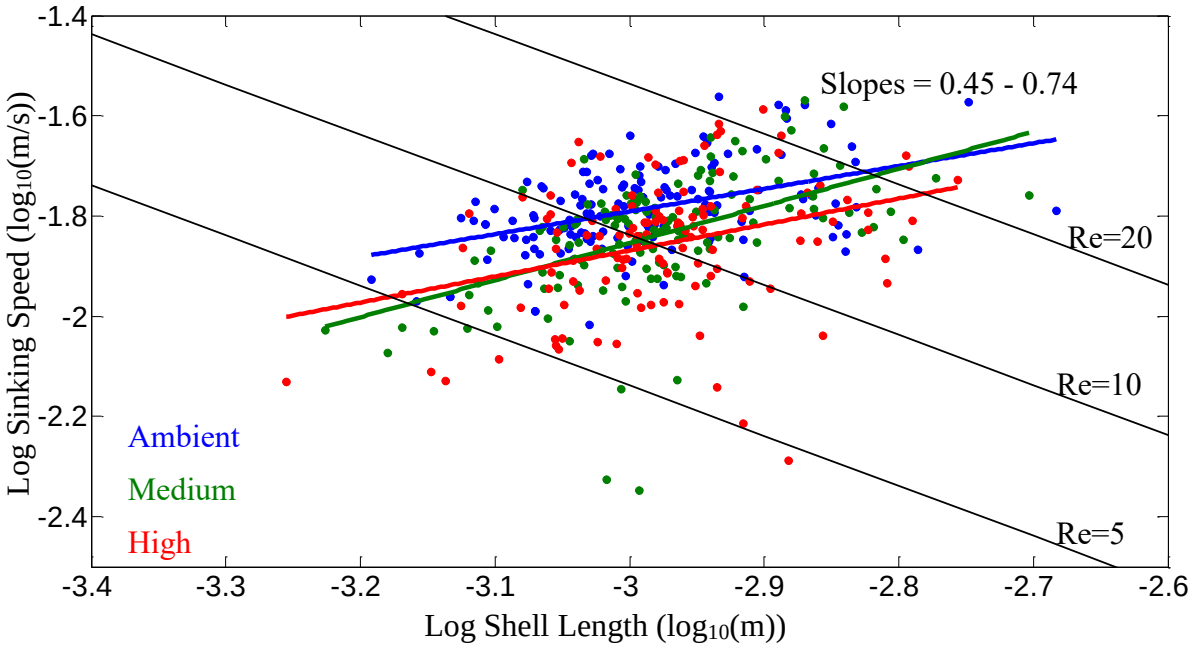

Figure 5. Log_{10} terminal sinking speed with wings withdrawn vs log_{10} shell length for each treatment (points) along with a linear regression for each treatment (lines). The slope of the linear regressions shows the power scaling between sinking speed and shell length. Contours of constant Reynolds numbers (Re) of 5, 10, and 20 are shown in black.

Swimming

In contrast to sinking, swimming rates did not differ in a consistent manner among treatments and durations of exposure. For the two experiments (August 2014 and April 2015) where observations were made after one week, mean swimming speed was significantly different among treatments but differed in which treatment showed the fastest swimming (Figure 6a,

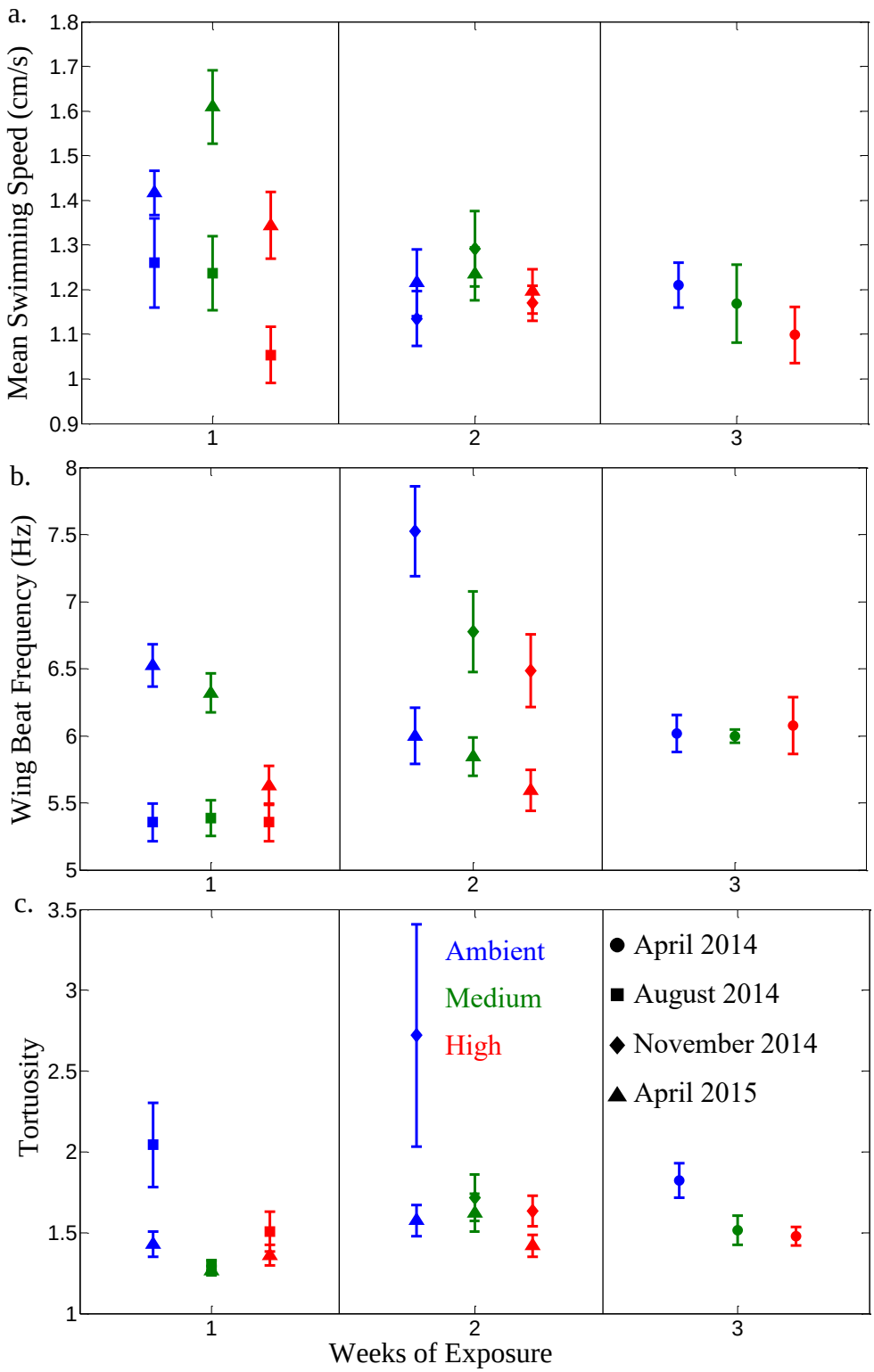

Figure 6. (a) Mean swimming speed, (b) wing beat frequency, and (c) tortuosity for *L. retroversa* for the four experiments (circle: April 2014; square: August 2014; diamond: November 2014; triangle: April 2015) after durations of exposure of 1-3 weeks. From left to right within a week the ambient, medium, and high treatment are plotted, although treatments were measured together over the course of 2-5 days. The error bars denote standard error. Both the power and recovery stroke are included in each wing beat in calculating wing beat frequency.

Table 3). Significant differences were not seen among treatments at two or three weeks. There was also not a significant correlation between swimming speed and animal length (Table 4): in the log-log plot of swimming speed vs. animal length the slopes of the linear regressions were nearly zero (see Supplementary Figure S2) and hence no attempts were made to normalize swimming measurements to animal size.

For the initial two experiments (April and August 2014) where multiple animals were together in the filming tank and individual swim analyses were not possible, wing beat frequency showed no differences among treatments (Figure 6b, Table 3). For the two later experiments (November 2014 and April 2015), where individual animals were measured separately, a trend of decreasing flapping frequency under elevated CO_2 was evident, and the frequency of wing beats was significantly higher in the ambient treatment compared to the medium and high treatments in week one of the April 2015 experiment, although not in week two of the November 2014 experiment or week two of April 2015.

Tortuosity only differed significantly during the initial experiments (April 2014 and August 2014), where multiple animals were placed together during filming (Figure 6c, Table 3). In the November 2014 and April 2015 experiments, no significant differences were seen in tortuosity among the treatments, although there was a high degree of variability during the November 2014 week two experiment, where the ambient treatment had the highest tortuosity due to an outlier (4.05) and low sample size (n=3). The average ratio of horizontal to vertical displacement averaged over all the experiments was 0.35±0.15 (±standard deviation) and similar to tortuosity there were only significant differences between treatments in April 2014 (Kruskal-Wallis one-way ANOVA, $H=8.7$, $p=0.013$) and August 2014 (Kruskal-Wallis one-way ANOVA, $H=6.9$, $p=0.032$). The asymmetry between the peak speeds of the power and recovery strokes did

not differ among treatments for any of the experiments (one-way ANOVA). The average and standard deviation of asymmetry between the power/recovery strokes over all the experiments was 7.2±5.1% (n=191).

There was a significant positive correlation between mean swimming speed and wing beat frequency and a significant negative correlation between wing beat frequency and length (Table 4). The mean swimming speed also had significant negative correlations with both tortuosity and the asymmetry between the speeds of the power and recovery strokes. There were no significant correlations between tortuosity or the asymmetry of the strokes and length.

Table 4. Correlation coefficients (r) among the swimming variables: mean swimming speed, wing beat frequency, path tortuosity, and asymmetry between the peaks of speed (i.e. the difference between the power and recovery stroke). Bold indicates significant correlations. * p<0.05, ** p<0.01, *** p<0.001, NS=Non-Significant

Correlation coefficient	**Length**	**Wing Beat frequency**	**Tortuosity**	**Asymmetry in peaks**
Speed	0.0005^{NS}	**0.2395 *****	**-0.4357*****	**-0.18233***
Length		**-0.3785*****	-0.1418 ^{NS}	0.110331 ^{NS}
Wing Beat			0.1209 ^{NS}	-0.13198 ^{NS}
Tortuosity				0.059909 ^{NS}

Discussion

The condition of *Limacina retroversa* shells and sinking speeds of live animals were significantly affected by exposure to elevated carbon dioxide. Since the passive motion of sinking was slower in the elevated CO_2 treatments, even for animals with wings withdrawn, this indicates that the slower sinking rates likely relate to differences in the shells. Swimming behavior showed less clear patterns of variability in relation to treatment and duration of exposure, and overall swimming ability did not appear to be hindered under elevated CO_2.

Shell Condition

The appearance of shells changed significantly in the elevated CO_2 treatments. Differences in transmittance and opacity of the shells from the medium and high treatments relative to the ambient treatment were apparent from day four of exposure, while in contrast the shells from the ambient treatment did not change significantly over time. Other studies have found that short exposures to similar CO_2 concentrations (750, 880, and 1000 ppm for 7-8 days) can cause changes in shell condition of *L. retroversa* (Lischka and Riebesell 2012, Manno *et al.* 2012) and in the congeneric species *L. helicina* (Lischka *et al.* 2011, Bednaršek *et al.* 2012a, Busch *et al.* 2014, Bednaršek *et al.* 2014b). The present study adds to these earlier observations by offering a new, quantitative metric for assessing shell condition based on transparency to light-based microscopy and by extending the duration over which effects on shell condition were examined. Although they were measured and considered separately, transmittance and opacity are highly related optical properties and as such expectedly showed very similar patterns (though in opposing directions). Future studies employing this light microscopy-based approach might thus focus on transmittance, since the transverse lighting used for opacity measurements causes some glare on the shells regardless of condition which may affect the sensitivity of this metric.

A loss of transparency could have a negative impact on shelled pteropods since transparency is a form of camouflage in the open ocean environment. Although some pteropod predators, notably the gymnosome (or shell-less) pteropods, are non-visual, the decrease in transparency could potentially serve to increase visibility to visual predators known to feed on pteropods, such as fish and birds (LeBrasseur 1966, Levasseur *et al.* 1996, Armstrong *et al.* 2005, Hunt *et al.* 2008, Karnovsky *et al.* 2008, Sturdevant *et al.* 2013). It is not known how small of a change in CO_2 concentration will elicit a response in shell condition, but it is noteworthy that changes were evident here in the medium treatment, which in April 2015 was just above an

aragonite saturation state of one, a potential environmental threshold. The loss of transparency is likely caused by dissolution of the calcium carbonate matrix, as has been seen at higher resolution using scanning electron microscopy (e.g. Bednaršek *et al.* 2012a). It is possible that the more gradual change in CO_2 concentrations that will occur as a result of climate change could allow for adaptation, although shell dissolution has already been documented for wild populations of *L. helicina* exposed to naturally low saturation state conditions (Bednaršek *et al.* 2012b, Bednaršek *et al.* 2014a). The methods provided here for examining the transparency of shells could be applied to natural populations to look for seasonal and inter-annual changes.

Sinking

Although sinking speeds have been previously quantified in some pteropod species (Lalli and Gilmer 1989), the effect of elevated CO_2 on pteropod sinking has not previously been examined, despite the important role that sinking plays in pteropod locomotion and carbonate flux. In this study, the sinking speeds of *L. retroversa* were slower during the second week of exposure to elevated CO_2 and onwards. Measurements of mass made for the April 2015 experiment, normalized to length to account for variability in size, did not indicate a clear pattern among treatments indicative of dissolution due to exposure to elevated CO_2. It is thus not clear whether the change in sinking speed are due to the shells changing in mass, density, or if they are modified in a way that increases drag. It is also not known whether the experimentally manipulated chemical conditions had any impacts on the mass of the animal bodies, separate from the shells. Given the relatively massive shells and direct linkage between under-saturated conditions and calcium carbonate dissolution, however, it seems likely that changes in sinking speed relate primarily to changes in the shells. The ambient treatment also showed slower

sinking with increased duration of exposure, but nonetheless the effect of elevated CO_2 treatment was persistent and sinking both with wings withdrawn and extended showed a similar treatment effect. The decrease in sinking speed for the ambient treatment could indicate a captivity effect, where animals in all treatments might decrease in overall health and vigor with increased duration of time in captivity. It could also be due to removal of larger individuals earlier in the experiments, leading to smaller pteropods being tested in the later weeks, although the effect of exposure on sinking speed was consistent when normalized by the square root of length (based on the observed relationship between size and sinking speed) so this is less likely. In an earlier study, the scaling between shell length and sinking speed for the congeneric species *L. helicina* was between 0.3 and 0.4 (Chang and Yen, 2012), similar to the scaling of 0.5 found in this study. Animal length and speed are also important in determining the Reynolds number (Re). Since *L. retroversa* moves in a transitional regime of Re between ca. 5 and 50, decreases in sinking and swimming speeds might lead to a decrease in Re that could result in increased viscous drag (Walker 2002).

Extended wings slowed sinking, presumably as an adaptation to minimize energetic expenditure on swimming to maintain position in the water column. In the laboratory, pteropods alternate between periods of swimming upwards and sinking, while in the field, the production of mucous webs is thought to slow or even halt sinking, although the prevalence of this behavior is not well known (Gilmer and Harbison 1986). The bio-energetic consequences to pteropods in the wild of reduced sinking speeds are thus somewhat difficult to assess, but it may be that metabolic costs of maintaining position in the water column are overall reduced under exposure to enhanced CO_2. In contrast, changes in sinking speed may have negative consequences in terms of vulnerability to predation. The gymnosome pteropods feed exclusively on shelled pteropods

and for this monospecific predator-prey relationship, withdrawing wings into the shell might make it harder for the predatory shell-less pteropods to successfully capture and consume their prey (Conover and Lalli 1974). Sinking behavior in the wild is also believed to be a mode of predator avoidance: a response to a disturbance was noted for the pteropod species *Diacria quadridentata*, which withdrew its wings presumably to achieve a faster sinking speed (Gilmer and Harbison 1986). Overall, there are only a few field observations of pteropod behavior in the wild, but along with the decrease in transparency and camouflage, a decrease in sinking speed with increased CO_2 is another way that *L. retroversa* and other shelled pteropods might have increased vulnerability to predators due to ocean acidification.

Post-mortem sinking of pteropod shells is important for the biogeochemical cycling of carbon (Berner and Honjo 1981). The solubility of aragonite increases with depth, dropping below a saturation state of one at a depth known as the aragonite compensation depth, which is shoaling due to ocean acidification (Fabry *et al.* 2008). Dissolution is not immediate below the aragonite compensation depth, however, and shells that sink more slowly have more time to be dissolved before reaching deeper water (Byrne *et al.* 1984). The combination of the slower sinking rates observed here with the shoaling of the compensation depth and the elevated rate of dissolution expected from ocean acidification is likely to cause pteropod dissolution and redistribution of carbonate to occur at increasingly shallower depths.

Swimming

Although the degradation of the shell after exposure to elevated CO_2 might have been expected to have consequences to the animal's weight and ballast, swimming behavior did not show clear changes when *L. retroversa* were exposed to elevated CO_2. In particular, unlike

sinking speed, swimming speed did not show any clear reduction in the elevated CO_2 treatments. It may be that the differences among the experiments in swimming behavior and the sensitivity of the various swimming metrics to CO_2 relate to seasonal differences in the overall condition, developmental state, and vigor of the animals prior to capture that persisted through the experiments; these differences may also be influenced by overall low sample sizes. It should also be noted that variability in individual swimming performance may have affected the patterns evident in the April and August 2014 experiments, where multiple animals were present in the filming tank concurrently, relative to the multiple runs done on individual animals in the November 2014 and April 2015 experiments. This methodological change was unfortunate and introduces the possibility of pseudo-replication in the earlier two experiments if swimming was observed for the same animal more than once. Given the overall low sample sizes and dearth of previous information, I have presented the observations from both the initial sub-optimal experiments as well as the latter two more rigorous investigations. No consistent differences across the measured swimming metrics were evident associated with the change in method.

The significant differences in swimming speed in the first week of exposure may be spurious, as the treatment with the fastest swimmers was not consistent among experiments and significant differences among treatments did not persist after longer exposure durations. A previous study by Manno *et al.* (2012) manipulated CO_2 and salinity to examine how swimming was affected in *L. retroversa* and found that elevated CO_2 alone did not cause a change in swimming speed or wing beat frequency after eight days of exposure, while decreased salinity combined with increased CO_2 conditions slowed the swimming and increased the beat frequency. This supports the idea that the findings at one week are spurious.

More consistent in the present study than the patterns in swimming speed was a trend towards decreased wing beat frequency in the medium and high treatments relative to ambient, albeit only significant in one of the experiments. This reduction in wing beat frequency is interesting in its not being accompanied by an associated difference between treatments in swimming speed (although at the individual level, wing beat frequency was positively correlated with swimming speed). A reduction in beat frequency may suggest a reduced metabolic cost of swimming in the animals exposed to elevated CO_2, and is perhaps associated with a less massive shell. While there was not a good correlation between swimming speed and length, there was a significant negative correlation between wing beat frequency and length, which has also been noted in another study where larger *L. helicina* beat their wings less frequently but achieved greater speeds (Chang and Yen 2012). That more detailed study of swimming kinetics also found that across sizes the trajectory and timing of the wing strokes varied, possibly as a response to changing Reynolds number regimes.

Tortuosity often, but not always, showed differences associated with treatment in the present study, with greatest tortuosity in the ambient treatment. Tortuosity was significantly negatively correlated to swimming speed, as animals tended to exhibit more horizontal movements that often appeared helical in nature when swimming at lower speeds. Tortuosity and length were also negatively related, though not quite significantly, whereas Chang and Yen (2012) found that the helical component of *L. helicina* swimming paths was greater for larger individuals. Pteropod swimming relies on the rotation of the shell between the power and recovery strokes and differential dissolution along the elongate shells of individual *L. retroversa* could conceivably influence swimming efficiency. Examining the asymmetry in swimming speed induced by the power and recovery strokes, however, did not show any effect of CO_2

exposure. In general it is possible that the limited effects observed on the swimming metrics examined here in relation to CO_2 exposure are due to shell dissolution (and associated potential impacts on weight and ballast) not being advanced enough to result in discernible consequences to swimming. If future studies can overcome limitations in the durations over which pteropods can be maintained in captivity, the longer-term effects on locomotion of enhanced CO_2 might be examined.

Conclusions

This study observed decreased sinking speeds in pteropods exposed to conditions of elevated CO_2 that could exist by the end of the century, suggesting that ocean acidification could affect pteropod fitness, as sinking is a mode of predator avoidance. Decreased sinking speeds will likely also slow the passive transport of calcium carbonate to depth. Ocean acidification could potentially also increase the visibility of pteropods to predators, since increased CO_2 significantly affected the transparency of shells. Longer perturbation experiments or greater replication may be needed to understand whether ocean acidification affects swimming. The cues that pteropods respond to that motivate their upward swimming are not known, and whether these cues are influenced by CO_2 treatment is also uncertain. Overall, more behavioral experiments on pteropods are needed to understand the consequences of ocean acidification, although this relies on the development of improved culture techniques in order to achieve adequately large sample sizes and to examine impacts over longer time periods (Howes *et al.* 2014).

Supplementary Materials

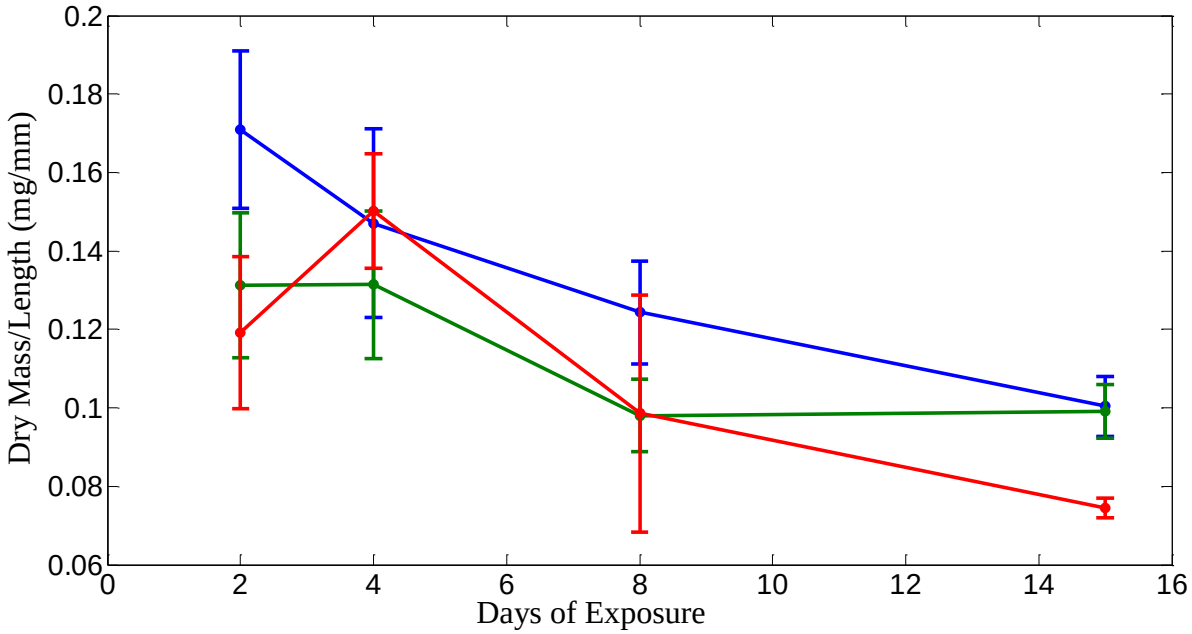

Supplementary Figure S1. Shell dry mass with animal tissue present (i.e., prior to digestion with bleach) normalized to individual length from the April 2015 experiment relative to duration of exposure for each of the three CO_2 treatments.

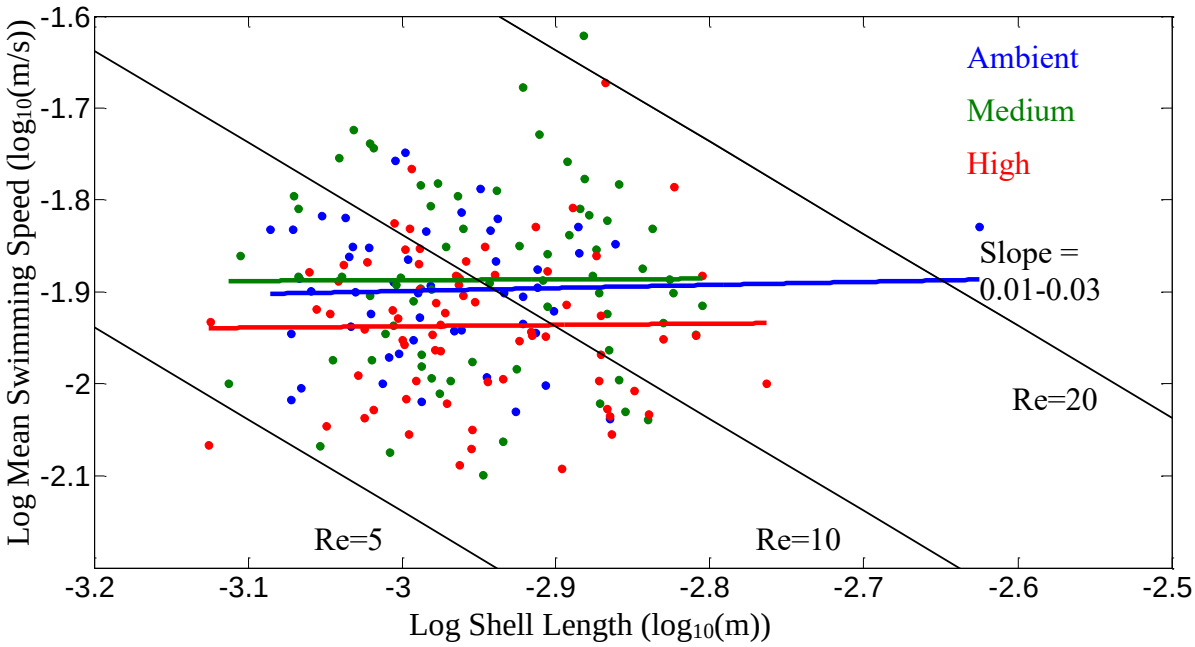

Supplementary Figure S2. The $\log_{10}$ mean swimming speed vs $\log_{10}$ shell length (points, colored according to treatment) along with a linear regression for each treatment (colored lines). The slopes of the linear regressions indicate the power scaling between swimming speed and shell length. Reynolds numbers (Re) 5, 10, and 20 are shown in black lines.

Supplemental Table S1. Carbonate chemistry parameters measured and calculated over the course of the four experiments for the three treatments: ambient, medium, and high, nominally targeting pCO_2 levels of 400, 800, and 1200 µatm, respectively. Water changes happened at weekly intervals, at which time dissolved inorganic carbon (DIC) and total alkalinity (TA) were measured. The TA/DIC measurements of ingoing pre-bubbled water entering the carboys are labelled "In" and the TA/DIC measurements of outgoing water leaving the carboys are labelled "Out". Mid-week measurements of pH were made between water changes, labelled "Mid." "Out" and "Mid" measurements shown are an average of the 2-3 carboys for each treatment, while "In" is a single measurement from the pre-bubbled holding tanks for each treatment. For the ingoing and outgoing water, DIC/TA measurements were used to calculate the values in the last three columns: pH, dissolved CO_2 (pCO_2), and aragonite saturation state (Ω_A). Mid-week measurements of pH were used with the nearest measurement of TA in time to calculate the pCO_2 and Ω_A values to estimate the carbonate chemistry between water changes.

Cruise	Treat	Day	Water Change	MEASURED			CALCULATED		
				DIC (µmol/kg)	TA (µmol/kg)	pH	pH	pCO_2 (µatm)	Ω_A
Apr '14	Ambient	0	In	2058	2216	---	8.03	390	1.76
		1	Mid	---	---	7.96	---	470	1.54
		3	Mid	---	---	7.97	---	450	1.57
		5	Mid	---	---	7.99	---	440	1.62
		7	Out	2093	2234	---	7.96	470	1.54
		7	In	2068	2216	---	8.01	420	1.68
		8	Mid	---	---	7.97	---	450	1.58
		10	Mid	---	---	7.96	---	460	1.54
		13	Mid	---	---	7.98	---	440	1.59
		14	Out	2082	2215	---	7.97	460	1.55
		26	Mid	---	---	8.03	---	390	1.77
		29	Mid	---	---	8.03	---	390	1.74
	Medium	0	In	2092	2214	---	7.94	500	1.45
		1	Mid	---	---	7.75	---	790	0.99
		3	Mid	---	---	7.77	---	760	1.02
		5	Mid	---	---	7.78	---	750	1.05
		7	Out	2175	2227	---	7.72	860	0.93
		7	In	2147	2217	---	7.78	740	1.05
		8	Mid	---	---	7.72	---	860	0.92
		10	Mid	---	---	7.70	---	910	0.88
		13	Mid	---	---	7.73	---	830	0.95
		14	Out	2166	2222	---	7.73	830	0.95
		26	Mid	---	---	7.79	---	710	1.09
		29	Mid	---	---	7.80	---	710	1.09
	High	0	In	2111	2215	---	7.88	570	1.31
		1	Mid	---	---	7.59	---	1180	0.69
		3	Mid	---	---	7.61	---	1110	0.73
		5	Mid	---	---	7.68	---	940	0.86
		7	Out	2210	2220	---	7.57	1230	0.67
		7	In	2184	2216	---	7.65	1010	0.80
		8	Mid	---	---	7.57	---	1240	0.67
		10	Mid	---	---	7.55	---	1280	0.65
		13	Mid	---	---	7.58	---	1220	0.68
		14	Out	2202	2219	---	7.60	1150	0.72
		26	Mid	---	---	7.58	---	1200	0.69
		29	Mid	---	---	7.60	---	1150	0.72
Aug '14	Ambient	0	In	2016	2176	---	8.04	379	1.77
		1	Mid	---	---	7.99	---	430	1.58

		3	Mid	---	---	7.92	---	510	1.38
		6	Mid	---	---	7.95	---	470	1.47
		7	Out	2052	2182	---	7.96	460	1.50
		7	In	2028	2183	---	8.03	390	1.73
		8	Mid	---	---	7.99	---	430	1..60
		11	Mid	---	---	7.99	---	430	1.60
		14	Out	2039	2185	---	8.00	414	1.65
	Medium	0	In	2103	2162	---	7.74	790	0.95
		1	Mid	---	---	7.71	---	840	0.90
		3	Mid	---	---	7.69	---	890	0.85
		6	Mid	---	---	7.72	---	840	0.92
		7	Out	2125	2194	---	7.78	750	1.04
		7	In	2104	2180	---	7.80	690	1.07
		8	Mid	---	---	7.70	---	870	0.89
		11	Mid	---	---	7.69	---	900	0.84
		14	Out	2085	2198	---	7.91	540	1.38
	High	0	In	2082	2177	---	7.86	590	1.22
		1	Mid	---	---	7.59	---	1150	0.69
		3	Mid	---	---	7.55	---	1260	0.63
		6	Mid	---	---	7.58	---	1190	0.67
		7	Out	2160	2186	---	7.63	1060	0.75
		7	In	2143	2186	---	7.69	910	0.85
		8	Mid	---	---	7.60	---	1120	0.71
		11	Mid	---	---	7.64	---	1030	0.77
		14	Out	2150	2198	---	7.70	880	0.89
Nov ‘14	Ambient	0	In	2062	2197	---	7.98	440	1.57
		6	Mid	---	---	8.07	---	360	1.89
		7	Out	2118	2233	---	7.93	520	1.42
		7	In	2066	2195	---	7.97	460	1.52
		8	Mid	---	---	8.01	---	410	1.65
		10	Mid	---	---	7.99	---	430	1.58
		14	Out	2065	2198	---	7.98	440	1.55
	Medium	0	In	2129	2197	---	7.78	730	1.03
		6	Mid	---	---	7.79	---	730	1.06
		7	Out	2234	2234	---	7.55	1320	0.64
		7	In	2142	2194	---	7.73	830	0.92
		8	Mid	---	---	7.73	---	830	0.92
		10	Mid	---	---	7.72	---	840	0.92
		14	Out	2154	2201	---	7.71	870	0.89
	High	0	In	2153	2196	---	7.70	890	0.86
		6	Mid	---	---	7.63	---	1080	0.76
		7	Out	2241	2239	---	7.54	1350	0.62
		7	In	2185	2191	---	7.57	1230	0.65
		8	Mid	---	---	7.58	---	1200	0.67
		10	Mid	---	---	7.57	---	1240	0.64
		14	Out	2205	2206	---	7.55	1290	0.63
Apr ‘15	Ambient	0	In	2081	2218	---	7.99	440	1.59
		7	Out	2082	2222	---	8.00	430	1.62
		7	In	2077	2212	---	7.98	440	1.58
		7	Mid	---	---	8.01	---	420	1.65
		11	Mid	---	---	7.99	---	430	1.61
		14	Out	2085	2222	---	7.99	440	1.60
		14	In	2108	2257	---	8.01	420	1.72

		16	Mid	---	---	8.02	---	410	1.73
		18	Mid	---	---	8.01	---	420	1.70
	Medium	0	In	2153	2229	---	7.81	700	1.10
		7	Out	2166	2222	---	7.74	820	0.95
		7	In	2147	2211	---	7.77	760	1.01
		7	Mid	---	---	7.79	---	720	1.06
		11	Mid	---	---	7.82	---	680	1.12
		14	Out	2143	2225	---	7.83	660	1.15
		14	In	2173	2253	---	7.82	680	1.14
		16	Mid	---	---	7.79	---	740	1.06
		18	Mid	---	---	7.78	---	750	1.05
	High	0	In	2191	2223	---	7.66	1000	0.80
		7	Out	2208	2221	---	7.59	1170	0.70
		7	In	2208	2209	---	7.55	1300	0.62
		7	Mid	---	---	7.64	---	1050	0.76
		11	Mid	---	---	7.63	---	1070	0.75
		14	Out	2201	2214	---	7.59	1190	0.70
		14	In	2198	2251	---	7.73	850	0.94
		16	Mid	---	---	7.59	---	1190	0.70
		18	Mid	---	---	7.59	---	1200	0.70

Chapter 3

Shell condition of three thecosome pteropod species (*Limacina retroversa*, *Limacina helicina*, and *Clio pyramidata*) from CO_2 exposure experiments and wild populations

Abstract

Thecosome pteropods are pelagic mollusks that form thin aragonite shells which are susceptible to dissolution due to ocean acidification. Ocean acidification and regional variability affect the aragonite saturation state (Ω_A), which determines the availability of ions for building and repairing shell as well as controlling the rate of dissolution. The condition of pteropod shells was examined across a range of Ω_A, both through elevated carbon dioxide (CO_2) experiments and across natural gradients of Ω_A over large spatial scales. *Limacina retroversa* were captured in the Gulf of Maine and kept in one of three CO_2 treatments (~400 µatm, 800 µatm, and 1200 µatm). The shells showed clear differences in condition between treatments after four days of exposure, turning less transparent in the elevated CO_2 treatments. Furthermore, calcification as estimated by calcein staining increased after two and three weeks in response to elevated CO_2. Scanning electron microscopy imaging revealed changes to the surface of the shells of *L. retroversa* that related to the Ω_A of the treatments. Across a Ω_A gradient in the North Pacific, *L. helicina* showed regional, depth, and size differences in shell condition. The regional variability in *L. helicina* shell condition did not appear to relate solely to Ω_A, since there was relatively high shell condition in the northernmost station where Ω_A was lowest. It is possible that food availability affected the condition *of L. helicina* shells, with lower shell condition in regions where chlorophyll fluorescence was lower. The pattern of shell condition across depths however did reveal a possible relationship between shell condition and Ω_A. The shells of smaller *L.*

helicina had slightly lower shell condition than the larger co-located individuals. *Clio pyramidata* shells were compared across stations in the Atlantic and Pacific at lower and higher latitudes; the shells did not differ significantly between stations, although the trends in shell condition were consistent with regional variability in Ω_A. Overall the findings suggest that at under-saturated ($\Omega_A<1$) conditions shell dissolution was prevalent in the wild, but at higher Ω_A (>1.5) the variability in shell condition was not particularly sensitive to Ω_A. There may have been other factors that affected shell condition such as food availability.

Introduction

Ocean acidification is caused by anthropogenic carbon dioxide (CO_2) emissions entering the ocean, where it lowers the pH and removes carbonate via acid-base reactions (e.g. Doney *et al.* 2009). By the end of the century, ocean acidification is expected to lower the surface ocean pH by 0.3 – 0.4 and the availability of carbonate (CO_3^{2-}) by 60% globally (Feely *et al.* 2004, Orr *et al.* 2005). With lower CO_3^{2-} concentrations, organisms that create calcium carbonate structures will be less capable of building and maintaining those structures, such as shells, otoliths, and coral skeletons (e.g. Fabry *et al.* 2008, Ries *et al.* 2009, Bednaršek *et al.* 2014b). The dynamics of formation and dissolution of the aragonite form of calcium carbonate are governed by the aragonite saturation state (Ω_A), the product of the concentrations of the aqueous calcium and carbonate ions divided by the apparent solubility product at a certain pressure, temperature, and salinity (Mucci 1983). Seawater conditions favor the precipitation of aragonite when the Ω_A is above one (super-saturated) and aragonite dissolution when the Ω_A is below one (under-saturated). The depth where the Ω_A passes the threshold $\Omega_A=1$ is known as the aragonite saturation horizon, and the Ω_A continues to decrease with depth. The vertical distribution of

dissolved inorganic carbon (DIC, which increases with inputs of dissolved CO_2) can also affect how Ω_A changes with depth. Waters that have high DIC and low buffering ability, or total alkalinity (TA), will have low Ω_A.

Shelled pteropods, or thecosomes, are holoplanktonic mollusks that live in the pelagic environments and form aragonite shells (e.g. Lalli and Gilmer 1989). This taxon can be found ubiquitously in open ocean and coastal environments (e.g. Bednaršek *et al.* 2017). They are ecologically important as they have many predators that span a wide range of sizes from other zooplankton to fish, seabirds, and bowhead whales (LeBrasseur 1966, Ackman *et al.* 1972, Conover and Lalli 1974, Levasseur *et al.* 1996, Pakhomov *et al.* 1996, Armstrong *et al.* 2005, Hunt *et al.* 2008, Karnovsky *et al.* 2008, Pomerleau *et al.* 2012, Sturdevant *et al.* 2013). Experiments have shown that live pteropods have impaired calcification and enhanced dissolution when exposed to lower Ω_A (Comeau *et al.* 2009, Comeau *et al.* 2010a, Lischka et al. 2011, Lischka and Riebesell 2012, Bednaršek *et al.* 2014b, Lischka and Riebesell 2016). Dissolution of shells after pteropods die can affect the sequestration of carbon to depth, since the shells of pteropods sink until they reach the ocean floor or dissolve in the water column (Byrne *et al.* 1984). The role of pteropods in the carbon cycle, which also includes the production of quick sinking fecal pellets, results in the removal of CO_2 from the atmosphere and surface ocean and the storage of carbon in the deep ocean (Lalli and Gilmer 1989).

The focus of this work is on pteropods in the Gulf of Maine (GOM), offshore North Atlantic, and North Pacific. The movement of water masses and the balance of primary production and respiration affect Ω_A, leading to regional and seasonal variability. On the continental shelf of the Northwest Atlantic, the GOM is particularly susceptible to ocean acidification due to its high DIC and low TA (Wang *et al.* 2013, Glendill *et al.* 2015,

Wanninkhof *et al.* 2015). During phytoplankton blooms, the high productivity will decrease the DIC and increase Ω_A, but after the termination of a bloom, respiration will increase the DIC and decrease Ω_A. The GOM has strong seasonal cycles because of high productivity and the subsequent remineralization of organic matter, which appears to cause deep basin waters to periodically drop to $\Omega_A<1$ (Wang *et al.* 2017). In the upper layer (0-60 m) of the GOM, net respiration and water column mixing in the fall and winter tends to decrease the Ω_A to the lowest annual values (Wang *et al.* 2017).

The large scale circulation of the global oceans leads to natural differences in the Ω_A between regions in the North Atlantic and North Pacific. Wild caught populations of pteropods could have differences in shell condition that reflect the spatial patterns of Ω_A. The deep water of the North Pacific has spent more than 1000 years since it last ventilated with the atmosphere (Matsumoto 2007). With age, the water increases its load of CO_2 from the remineralization of sinking organic material. The upwelling deep Pacific water and the higher capacity for dissolved CO_2 in cold water establish a gradient of decreasing Ω_A in more northerly waters. Unlike the Pacific, the Atlantic does have deep water formation sites and therefore the waters throughout the water column are relatively younger and lower in DIC in the Atlantic than the Pacific. This results in the Pacific having a lower Ω_A than the Atlantic at the same latitude and depth as well as a shallower aragonite saturation horizon (e.g. Feely *et al.* 2004).

The species examined in this study are *Limacina retroversa*, *Limacina helicina*, and *Clio pyramidata*. *Limacina retroversa* are abundant in subpolar waters of the North and South Atlantic (e.g. Chen and Bé 1964, Dadon 1990). Elevated CO_2 has been shown to affect shell appearance, metabolism, mortality, and locomotion of *L. retroversa* (Lischka and Riebesell 2012, Manno *et al.* 2012, Lischka and Riebesell 2016, Chapter 2). Additionally, under-saturated

conditions can delay the development of *L. retroversa* from egg to veliger larvae (Thabet *et al.* 2015). Seasonal changes in the shell condition of *L. retroversa* could also arise from acclimatization or developmental history.

Limacina helicina also undergoes changes in shell condition when exposed to enhanced CO_2 (Lischka et al. 2011, Lischka and Riebesell 2012, Bednaršek *et al.* 2014b). Shells of both *Limacina* species becoming darker and more opaque when viewed with standard light microscopes after exposure to elevated CO_2 (e.g. Almogi-Labin *et al.* 1986, Gerhardt *et al.* 2000, Lischka and Riebesell 2012, Wall-Palmer *et al.* 2013). Fine scale shell changes in surface roughness have been revealed with scanning electron microscopy (SEM) at lower Ω_A (Lischka *et al.* 2011, Bednaršek *et al.* 2012a, Bednaršek *et al.* 2014b, Peck *et al.* 2016). Wild caught *L. helicina* and *L. helicina antarctica* showed variability in shell appearance when examined with SEM that was consistent with a relationship between dissolution and Ω_A in coastal regions of the Southern Ocean (Bednaršek *et al.* 2012b, Johnson *et al.* 2016) and off the California coast (Bednaršek *et al.* 2014a, Bednaršek and Ohman 2015). In these regions, *L. helicina* shell dissolution was most pronounced when Ω_A decreased below approximately 1.2. However, pteropods in the open ocean have received relatively little attention.

Clio pyramidata is a cosmopolitan species (Maas *et al.* 2016). The shell of *C. pyramidata* does not coil like the shells of the *Limacina* pteropods, but is pointed. The inner layer of the shell is helical in *C. pyramidata* and crossed-lamellar in *Limacina* pteropods which could lead to differences in mechanical properties such as hardness and elasticity (Zhang *et al.* 2011, Teniswood *et al.* 2013, Li *et al.* 2015). Orr *et al.* (2005) examined the shells of *C. pyramidata* from the Southern Ocean and found pitting on the shell aperture after exposure for two days to under-saturated conditions.

In this study, both laboratory experiments and natural gradients in CO_2 were used to examine relationships between the Ω_A and shell condition in order to gain insight into how calcification and dissolution might be affected by ocean acidification. Pores are pits in the surface shell, or outer prismatic layer. Pores increase in frequency and/or size as shell dissolves. Fine-scale porosity on the shell surface can be used as a metric for shell condition, where a higher porosity is indicative of poorer condition (Roger *et al.* 2011). When dissolution is advanced, pores can become large patches of missing prismatic layer and reveal rough, disordered aragonite (Bednaršek *et al.* 2012a, Bednaršek *et al.* 2014b). Shell condition was also assessed by shell thickness for *C. pyramidata* and by transparency to light for *L. retroversa* and *L. helicina*. The following hypotheses were addressed: 1) *L. retroversa* shell condition will decline after exposure to elevated CO_2, 2) the shell condition of wild-caught *L. helicina* will decline in more northerly stations in the Pacific, corresponding with decreasing Ω_A, 3) *L. helicina* caught below the saturation horizon will have lower shell condition, and 4) the shell condition of *C. pyramidata* will correspond to differences in Ω_A between the North Atlantic and North Pacific.

Methods

Limacina retroversa under experimentally elevated CO_2

Limacina retroversa were collected in Reeve net tows (1-m diameter, 333µm mesh size) at depths of ca. 45-260 m in the Gulf of Maine near Provincetown, MA aboard the R/V *Tioga* during January 2014, April 2014, August 2014, November 2014, and April 2015 (Table 1, Figure 1). Further details on the collection, transportation, and experimental setup can be found in Chapter 2. To summarize, healthy *L. retroversa* were carefully removed from the plankton

samples and transported back to a cold room where they were randomly assigned to carboys (2-3 replicates per treatment) with pre-bubbled, 8ºC Gulf of Maine water (collected *in situ* at ca. 30 m depth via electric pump and 64 µm filter) at ambient, medium, or high CO_2 conditions (~400, 800, and 1200 µatm respectively). These target CO_2 concentrations were continuously bubbled throughout the experiment and used for pre-bubbling of water (at least 8 hours for equilibration) in 150 L barrels prior to entering the treatment carboys. The pteropods were fed an algal diet of *Rhodomonas lens* (1500-4000 cells/mL) and *Heterocapsa triquentra* (150-500 cells/mL). Water and pteropods were siphoned out of the carboys every week in order to remove the dead pteropods and replace the water with clean pre-bubbled water.

The DIC and TA were measured during water changes, both for the water leaving each carboy and the water entering the carboys. Total Alkalinity was measured using an Apollo SciTech alkalinity auto-titrator (AS-ALK2, Apollo SciTech, Newark, DE, USA), an Orion 3 Star pH meter, and a Ross combination pH electrode using the modified Gran titration method (Wang and Cai 2004). Dissolved Inorganic Carbon was analyzed with a DIC auto-analyzer (AS-C3, Apollo SciTech, Newark, DE, USA) via acidification and non-dispersive infrared CO_2 detection (LiCOR 7000: Wang and Cai 2004). The saturation state of aragonite, pCO_2, and pH were calculated from DIC and TA with the CO2SYS software (Pierrot *et al.* 2006), using constants K_1 and K_2 from Mehrbach *et al.* (1973) refitted by Dickson and Millero (1987), and the dissociation constant of $KHSO_4$ from Dickson (1990).

To preserve shells for transparency analysis, animals were placed in de-ionized (DI) water and then dried. Approximately ten shells from each treatment were analyzed after 4 days of exposure during four experiments, January 2014, August 2014, November 2014, and April 2015. The shells were weighed wet and after drying with a Cahn C-33 microbalance with a

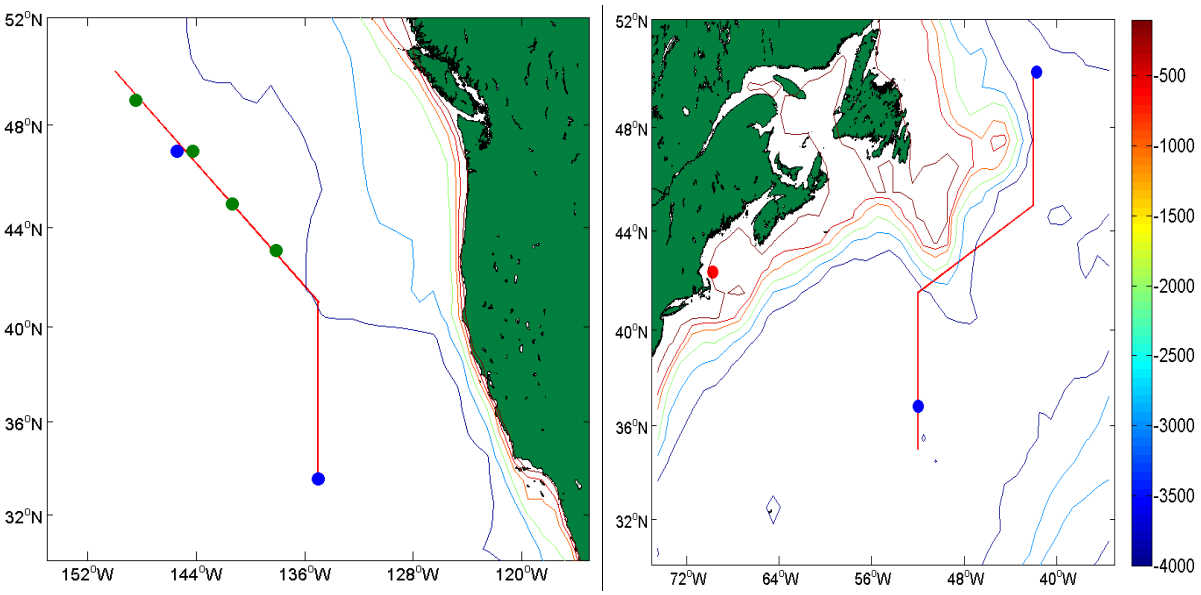

Figure 1. Study regions in the Northeast Pacific (left) and Northwest Atlantic (right). Blue dots are stations where *C. pyramidata* were collected and examined, green dots are stations where *L. helicina* were collected, and the red dot is the approximate location where *L. retroversa* were caught for experiments. The track lines of the Atlantic and Pacific off-shore cruises are shown with red lines. Bathymetry contours are shown at 100 m, 500 m, 1000 m, 2000 m, 3000 m, and 4000 m with the colors corresponding to the depth of the seafloor.

Table 1. Summary of each experiment with the days of pteropod collection (cruise dates), the exposure duration and sample size for a given test comparing the variables (Transparency, Calcein, Porosity, and Pore Size) between the treatments (Ambient, Medium, and High CO_2). Tests were performed with a one way ANOVA (F) or a one way Kruskal-Wallis ANOVA (H). Significance is denoted with: *p<0.05, **p<0.01, ***p<0.001, ^{NS} Not Significant.

Experiment	Cruise Dates	Exposure Duration	Sample Size Amb., Med., High	One-way ANOVA: F Kruskal-Wallis one-way ANOVA: H
January 2014	Jan 29 – Jan 30 2014	4 d	6, 8, 5	Transparency: H=6.9*
April 2014	25 Apr – 27 Apr 2014	7 d	4, 4, 5	Calcein: F=4.0^{NS}
		14 d	9, 5, 5	Calcein: F=11.0**
		21 d	9, 2, 7	Calcein: F=14.5***
August 2014	19 Aug 2014	4 d	7, 4, 6	Transparency: F=32***
November 2014	4 Nov – 6 Nov 2014	4 d	7, 8, 7	Transparency: F=30.3***
		7 d	4, 4, 3	Transparency: F= 138***, Porosity F=25***, Pore size: H=8.9***
April 2015	26 Apr – 27 Apr 2015	4 d	8, 8, 8	Transparency: H=9.0*

precision of 1 µg, then placed in 8.25% hypochlorite bleach for 24–48 hours to remove tissue, rinsed in DI water again, and dried. Using a light microscope, the now empty shells were photographed at 2.5X magnification for transparency and length measurements. Each shell was placed in a glass petri dish with the aperture facing up and the light from below and passing

through the shell. A photograph was taken through a microscope with white balance, contrast, and brightness values conserved across images.

In order to compare calcification activity between the treatments, calcein solutions of 50 mg L^{-1} in 0.2 µm filtered seawater were mixed in quart jars then bubbled with CO_2 gas at the target concentrations of the three treatments. During the April 2014 experiment, alive and active *L. retroversa* were collected on days 7, 14, and 21 from the treatment carboys and were placed in the calcein solutions with the same CO_2 conditions for one hour. The animals were then rinsed with DI water and the shells were imaged under a fluorescence and differential interference contrast microscope. Calcein stained shells were transported to the fluorescent microscope inside of a box to avoid the degradation of calcein by UV-light.

Shells that were analyzed with SEM were taken directly from the experiments on day 7 in November 2014 and placed in vials of 70% ethanol. For this analysis, four shells from the ambient treatment, four shells from the medium treatment, and three shells from the high treatment were used. The shells were prepared by first placing them in 50% ethanol for 10 minutes, then DI water for 10 minutes, next placed in 6% H_2O_2 for 15-20 minutes, then transferred to DI water for 10 minutes, then soaked in potassium hydroxide (KOH) for 2 hours, and then rinsed in DI water for 10 minutes. This method dissolves most of the periostracum (Bednaršek *et al.* 2016b). The periostracum is a thin organic covering that extends over the shell, which needs to be removed to clearly see the underlying shell structure. The shells were then moved to aluminum weighing boats with soft forceps to dry overnight. The dry shells were imaged with a light microscope before being carefully placed on aluminum SEM stubs with double sided carbon tape. The shells were coated in 10 nm of platinum using a sputter coater. Images were taken using a Zeiss Supra 40 NTS VP scanning electron microscope over the shell

of each *L. retroversa* at a magnification of 2500X for fine-scale measurements. At least 20 images were taken with a consistent progression from the aperture to the whorl. To determine the number of images needed for a good representation of the shell, the mean porosities of random subsets of images were compared to the mean of a full set of 40 images and the values converged reasonably well after 20 images or less. The consistent spacing between images and moving the electron beam from a zoomed out view helped to remove selection bias. The histograms of grayscale values among the pixels of an image were checked and adjusted (using brightness and contrast controls) to maintain consistency across images.

Wild-caught Limacina helicina and Clio pyramidata from open ocean stations

Individuals from the species *Clio pyramidata* and *Limacina helicina* were collected on two cruises in August and September of 2011 and 2012 from 33.5°N to 50°N at open ocean stations in both the Atlantic aboard the R/V *Oceanus* and Pacific with the R/V *New Horizon* (Figure 1). Part of the cruise tracks coincided with the CLIVAR transects A20 in the Atlantic and P17N in the Pacific. Plankton were caught with a Multiple Opening Closing Net and Environmental Sensing System (MOCNESS) with a 1 m^2 opening and nine nets of 150 µm mesh. The depth intervals of the nets were 0-25 m, 25-50 m, 50-100 m, 100-200 m, 200-400 m, 400-600 m, 600-800 m, and 800-1000 m (and one net integrating the whole 1000 m as the MOCNESS descended). The plankton samples were split using a box splitter, preserving ¼ of each sample in 70% ethanol, ½ in 95% ethanol, and ¼ in 5% buffered formalin. The 70% ethanol fraction was deemed the best preservation method for the analysis of shell condition (Bednaršek *et al.* 2012a). Some of the *C. pyramidata* individuals were caught in an obliquely hauled Reeve net with 333 µm mesh (1-m diameter) from 200 m depth to the surface. These individuals were

handpicked from a sorting tray and placed into 70% ethanol in glass vials. The rest of the *C. pyramidata* were taken from MOCNESS plankton samples preserved in 70% ethanol. The shell condition of *C. pyramidata* were compared at four stations, two in each the Pacific and Atlantic Oceans and at the northernmost and southernmost stations where the *C. pyramidata* were present in each ocean. *Clio pyramidata* were all caught in nets from 200 m to the surface from night tows. *Limacina helicina* were only caught in the North Pacific and the shell structure was examined across four stations mostly from daytime tows (and one nighttime tow). For *L. helicina*, shell condition across different depth ranges and shell lengths was also examined. Co-located water chemistry measurements were made from water collected by Niskin bottles at discrete depths and continuous hydrographic profile data was collected by a Conductivity, Temperature, and Depth sensor (CTD) and fluorometer (Wet Labs ECO-AFL) on casts to 3000 m depth. Water from the Niskin bottles was collected in 250 mL borosilicate glass bottles, poisoned with 100 µL of saturated mercuric chloride, and then capped with a greased stopper for later analysis of TA and DIC, which were measured by the same method as was described above.

Preparation for SEM and transparency images for *L. helicina* was performed in the same manner as for *L. retroversa*. Only shells with tissues inside were used for SEM analyses in order to avoid dead individuals. At least 20 images of the shells were taken in order to accurately represent each shell's surface. *Clio pyramidata* were prepared by a different method, described in Bednaršek *et al.* (2012a). The shells were first imaged under the light microscope to measure the length and width of each specimen. Width was a measurement of the line across the widest part of the *C. pyramidata* shell, which occurs at the aperture and length was measured from the caudal to rostral tips. To chemically clean and dehydrate the *C. pyramidata* shells, they were carefully moved to 50% ethanol for 2-3 minutes, then DI water for 3-5 minutes, next two soaks

in 6% H_2O_2 for 15-20 minutes each, then rinsed twice in DI water for 2-3 minutes each, then transferred for two 50% methanol soaks for 5 minutes each, next they were placed in 85% methanol for 10 minutes, next placed into 2,2-dimethyoxypropane (DMP) for two 15-20 minutes soaks, then a 1:1 mixture of DMP and hexamethyldisilizane (HMDS) for 10 minutes, then a soak in HMDS for 20-25 minutes, and finally placed a last soak in HMDS until the solution had evaporated from the ceramic wells, usually overnight. Next, the dry shells were mounted on aluminum stubs. The shells were oxygen plasma etched for between 10 and 30 minutes to remove the periostracum. The *C. pyramidata* shells were coated with between 5 and 8 nm of platinum, and then imaged with a Zeiss Supra 40 NTS VP scanning electron microscope at a magnification that was slightly higher (2740 to 2860 X) than the *Limacina spp.* images for fine-scale measurements. The teloconch (adult shell) is the majority of the shell, whereas the protoconch is the caudal tip, a small bulb that was initially the larval shell (Van der Spool 1969). Fine-scale shell properties were measured on approximately 30 images of surface teloconch and 5 images of protoconch per individual. To measure thickness of *C. pyramidata*, SEM images were taken of the apertures by tilting the stub platform to 70°.

Image Analysis

Images were analyzed in MATLAB to calculate various shell metrics. For transparency, the shells of *L. retroversa* and *L. helicina* were identified against the brighter background using the same protocol as described in Chapter 2. Calcein intensity of *L. retroversa* shells was measured by thresholding the fluorescing shell from the darker background and then calculating the mean grayscale values of the shells from 0 (dark) to 1 (bright). Measurements of the dimensions of shells of all three species were made manually on images in MATLAB. The

length of the shells of *L. helicina* that were less than 1 mm (range: 0.22-0.70 mm) were designated as small and individuals that were larger than 1 mm (range: 1.07-2.09 mm) were considered large. These size classes correspond to juveniles and sub-adults (Bednašek *et al.* 2014a). For *C. pyramidata,* shell thickness was measured by making ten manual measurements on each SEM image and averaging 5-9 images from the central region of the aperture (Figure 2a, b). The thickness measurements were divided by the sine of 70º (0.940) because 70º was the limit of the SEM platform's tilt and the face of the shell aperture was approximately parallel with the platform. Porosity and mean pore size were calculated separately for the teloconch and protoconch (Figure 2c) regions of *C. pyramidata* shells.

In order to calculate porosity and pore size, the pores needed to be differentiated from the intact shell. To do this, the images were converted to black and white using a threshold value that was in between the darkness of pores and the brightness of shell (Figure 3). The threshold was determined by manual examination of grayscale values within images using a subset of randomly chosen images for each species (36 *L. helicina*, 26 *L. retroversa*, and 24 *C. pyramidata*). The darkest pixel that was intact shell and the brightest pixel that was part of a pore were found by manual inspection. The midpoint between the average darkest shell and brightest pore values across these sets of images was used for thresholding between black and white. For *L. helicina* and *L. retroversa* the threshold was 60.5 (out of 255), and for *C. pyramidata* it was 63.5 (each pixel value is an integer). With a binary image, the proportion of black pixels determined porosity, and the porosities of all of the images of individual's shell were then averaged. After thresholding, each pore had an area determined by the number of neighboring black pixels. The areas of all of the pores were averaged for each image, and then the mean pore size for an

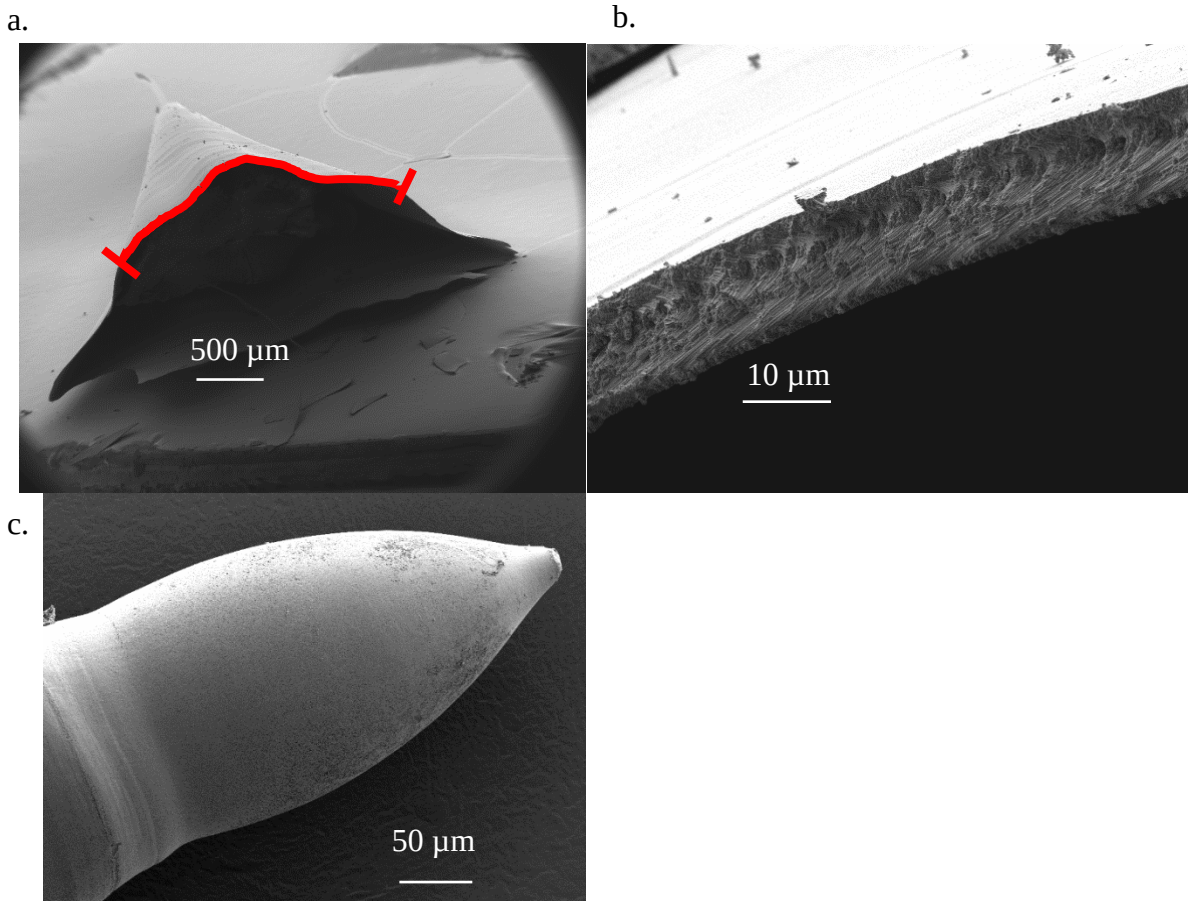

Figure 2 Aperture and protoconch regions of *C. pyramidata* shells. a. SEM image of the aperture of a *C. pyramidata* shell with the red line indicating which part is the central region used for analyzing thickness, b. a close up of the central aperture on which thickness measurements were made, and c. the protoconch region of a *C. pyramidata* shell.

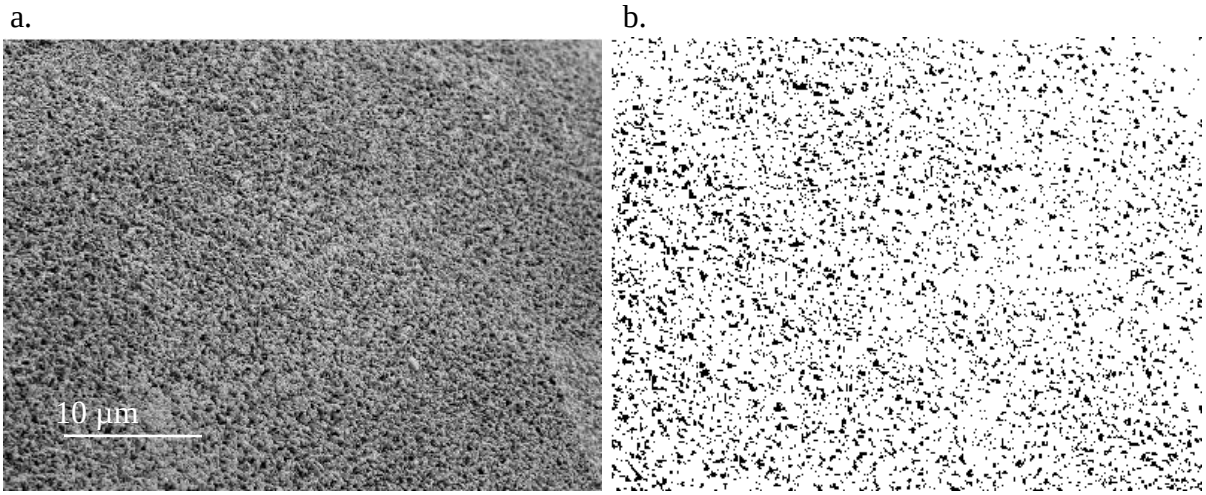

Figure 3 Converting a SEM image to black and white; a. the original SEM image of *L. helicina* taken at 2500 X magnification, b. the binarized black and white image after thresholding.

individual was taken as an average from the images' mean pore sizes and then converted from pixels to μm^2.

Statistics

For the *L. retroversa* laboratory experiments, differences in the Ω_A between treatments measured at day 0 and 7 were compared for each of the experiments using one-way Analysis of Variance (ANOVA) and the Holm-Sidak pairwise method for significant results or Kruskal-Wallis one-way ANOVA on ranks and Dunn's pairwise method if normality or equal variance of the data was not satisfied using the software package SigmaPlot 11. Changes to the shells (transparency, calcein intensity, porosity, and pore size) of *L. retroversa* were compared across treatments using ANOVA. Seasonal differences in *L. retroversa* transparency and dry weight were also tested with ANOVA. For *L. helicina,* an Analysis of Covariance (ANCOVA) was used to test how each of the shell metrics (transparency, porosity, and mean pore size) were related to the covariates (station, depth range, and shell length). Station and depth were categorical covariates and shell length was continuous. Two sample t-tests or the nonparametric Mann-Whitney U test were used to compare the shell condition of two samples of *L. helicina*, either between different nets or size classes. The porosity, mean pore size, thickness, and length/width ratios of *C. pyramidata* were compared across stations using ANOVA and the Holm-Sidak/Dunn's method for pairwise comparison.

Results

Limacina retroversa under experimentally elevated CO_2

The Ω_A values in the first week were significantly different between treatments in every experiment and were associated with differences in shell transparency measured at day four (Table 2). In January 2014 and April 2015, pairwise comparison showed that the Ω_A of every treatment was significantly different from the rest (Holm-Sidak $p<0.05$), while in November 2014, the ambient treatment was significantly different from both the medium and high treatment, but the medium and high treatments were not significantly different (Holm-Sidak $p<0.05$). The April 2014 and August 2014 only had a significant difference between the Ω_A of the ambient and high treatment (Dunn's method $p<0.05$). Since the calcein binding was measured in April 2014 on days 7, 14, and 21, the chemistry in the latter part of this experiment was also important. The Ω_A at days 14, 26, and 29 had significantly distinct values for ambient (1.55-1.77), medium (0.95-1.09), and high treatments (0.69-0.72, one-way ANOVA $p<0.001$, Holm-Sidak $p<0.05$). The full comprehensive set of carbonate chemistry measurements, including mid-week pH measurements, for April 2014, August 2014, November 2014, and April

Table 2. The dissolved CO_2 (pCO_2), pH, and aragonite saturation state (Ω_A) in the first week of the experiments. Values are averaged between water entering the carboy at the initiation (day 0) of the experiment and water leaving the treatment carboys at day 7. Total Alkalinity (TA) and Dissolved Inorganic Carbon (DIC) were directly measured and used for calculating the other parameters. The values are reported as the mean ± standard deviation.

Experiment	**Treatment**	**pCO_2 (ppm)**	**pH**	**Ω_A**
Jan 2014	Ambient	430±30	8.00±0.03	1.62±0.09
	Medium	720±50	7.80±0.03	1.06±0.06
	High	930±130	7.70±0.06	0.87±0.10
April 2014	Ambient	430±50	8.00±0.04	1.65±0.13
	Medium	680±190	7.83±0.11	1.19±0.26
	High	900±330	7.73±0.16	0.99±0.32
Aug 2014	Ambient	420±50	8.00±0.04	1.64±0.14
	Medium	770±120	7.76±0.07	1.00±0.16
	High	830±230	7.74±0.12	0.98±0.23
Nov 2014	Ambient	490±50	7.95±0.04	1.47±0.11
	Medium	1080±310	7.64±0.10	0.78±0.16
	High	1290±150	7.56±0.05	0.64±0.06
April 2015	Ambient	440±10	7.99±0.01	1.61±0.02
	Medium	760±90	7.77±0.05	1.03±0.10
	High	1090±140	7.63±0.05	0.75±0.08

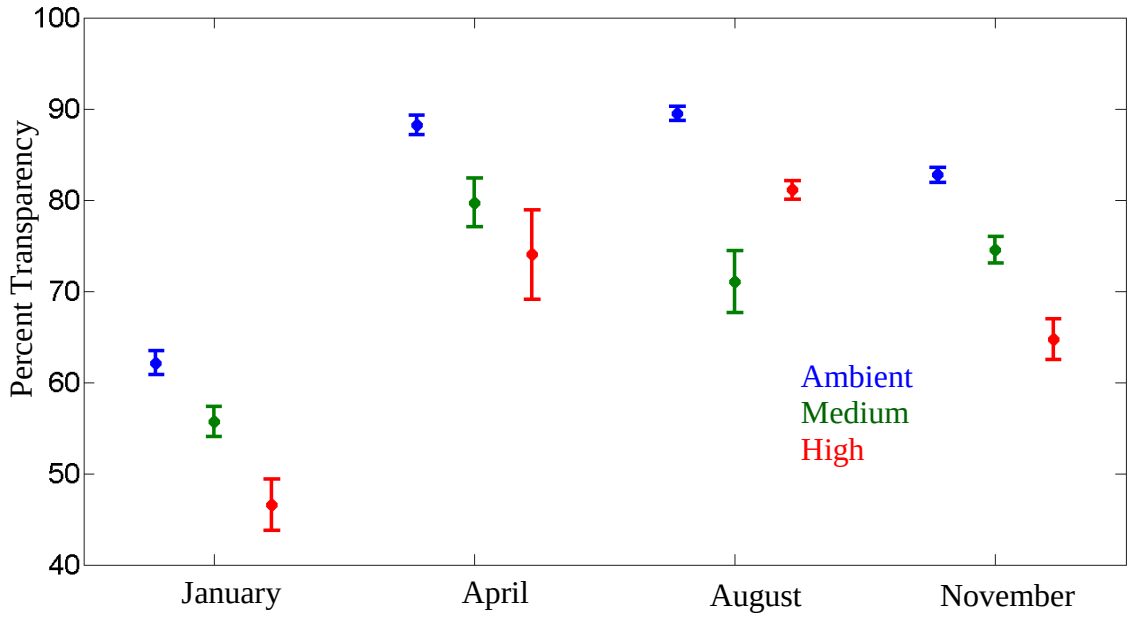

Figure 4. The percent transparency from day 4 of the experiments during different seasons (January 2014, April 2015, August 2014, and November 2014). Blue is the ambient, green is the medium, and red is the high treatment. Error bars show one standard error (S.E.)

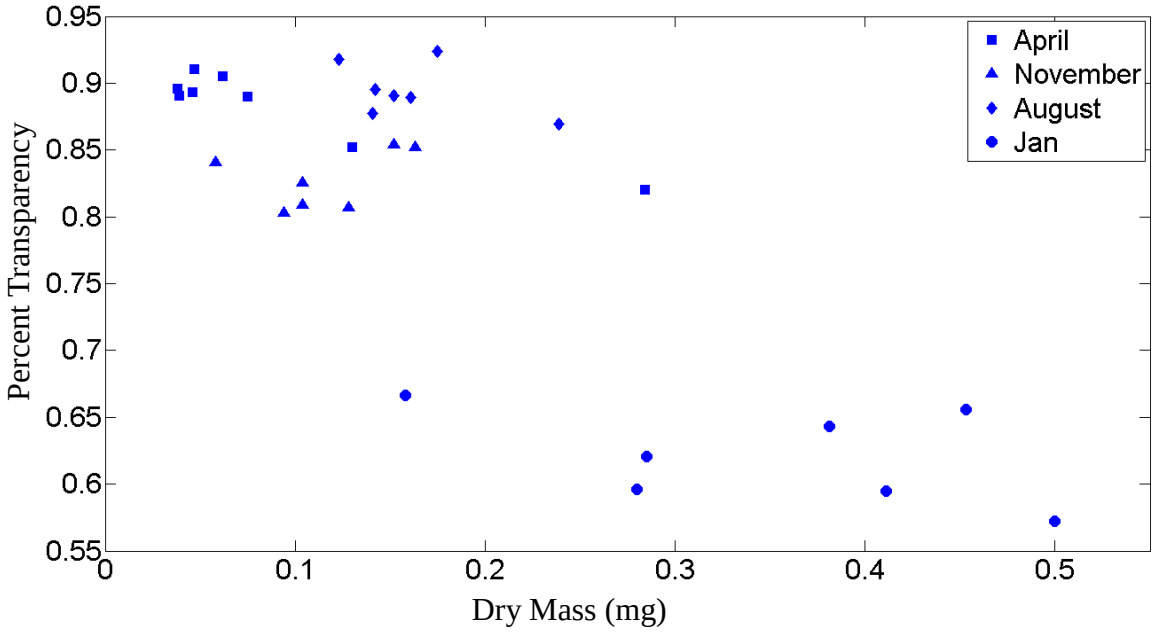

Figure 5. The percent transparency of *L. retroversa* shells vs dry mass from the ambient treatment from day four of the experiments in January 2014, August 2014, November 2014, and April 2015.

2015 experiments can be found in the supplementary material (Table S1) of Chapter 2.

By day four, significant differences were observed between the transparency of *L. retroversa* shells in each treatment for every experiment (Table 1, Figure 4). In August and

November 2014, every treatment was significantly different from each other (one-way ANOVA $p<0.001$, Holm-Sidak $p<0.001$), whereas in January 2014 and April 2015, only the ambient and high treatments were significantly different (Kruskal-Wallis one way ANOVA $p=0.032$ and $p=0.11$ respectively, Dunn's method $p<0.05$). In August 2014, the medium shells were the least transparent of the treatments, while for the other experiments the high treatment was observed to have the least transparent shells.

Differences in the shell transparency observed between the *L. retroversa* CO_2 exposure experiments might reflect seasonal differences in shell condition when they were caught. The ambient shells from January 2014 and November 2014 had significantly different transparency from each other and from all the other experiments (one way ANOVA $p<0.001$, Holm Sidak $p<0.05$). In January 2014 the transparency of the ambient shells was greatly reduced by more than 20% compared to November 2014 and the other experiments, which was as large of a difference as the treatment effect. The dry mass also varied between the experiments (Kruskal-Wallis one way ANOVA, $H=64.6$, $p<0.001$). The shells were largest in January 2014 (0.33±0.15 mg; ±standard deviation), followed by August 2014 (0.14±0.04 mg), November 2014 (0.09±0.04 mg), and April 2015 (0.07±0.06 mg). Although transparency generally appeared to decline as shells increased in mass, mass did not explain all of the patterns in transparency. There were transparency differences between the experiments that were not a function of mass that were apparent when plotting transparency versus dry mass (Figure 5). The transparencies of these shells were significantly affected by experiment but not dry mass (two way ANOVA, $F=22.4$, $p<0.001$, $F=1.6$, $p=0.2204$, respectively). The medium and high shells from January 2014 were also significantly less transparent than the medium and high treatments from other experiments, but the only significant pairwise difference was between the medium treatments of January 2014

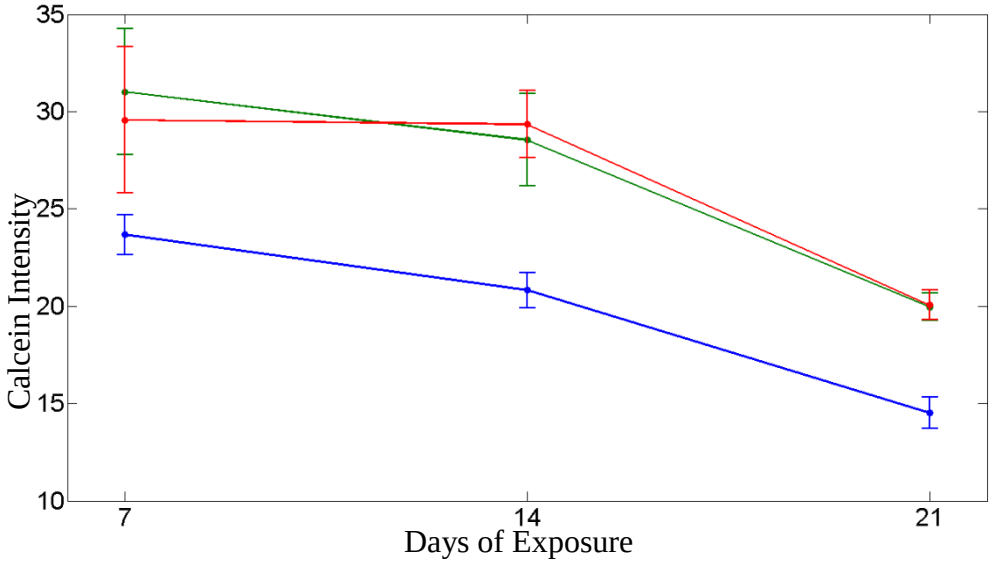

Figure 6. Calcein intensity for the April 2014 experiment, shown at days 7, 14, and 21. Blue is the ambient treatment, green is the medium, and red is the high treatment. Error bars show one standard error (S.E.)

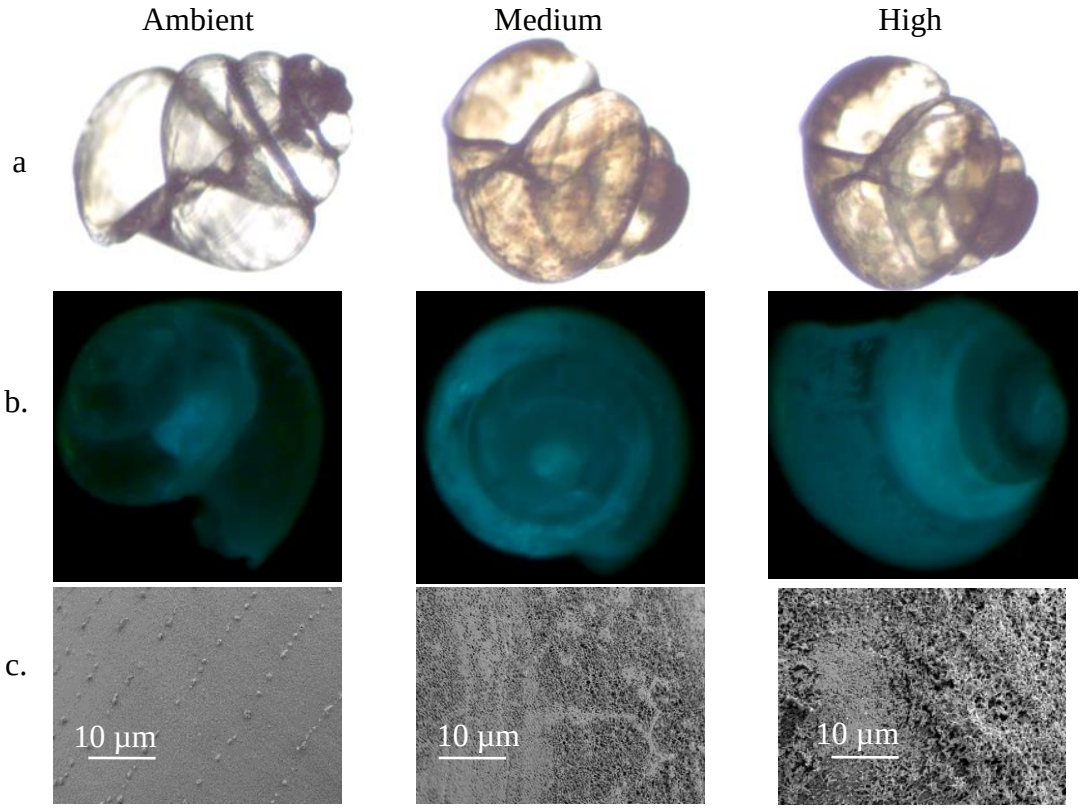

Figure 7. Representative images of transparency, calcein stained shells, and SEM images from each of the treatments (from left to right: ambient, medium, and high). a. Light microscopy images used for transparency after 7 days of exposure in November 2014 experiment, b. fluorescent microscopy images used for calcein intensity from April 2014 day 21, and c. SEM images used for porosity and pore size from November 2014 day 7.

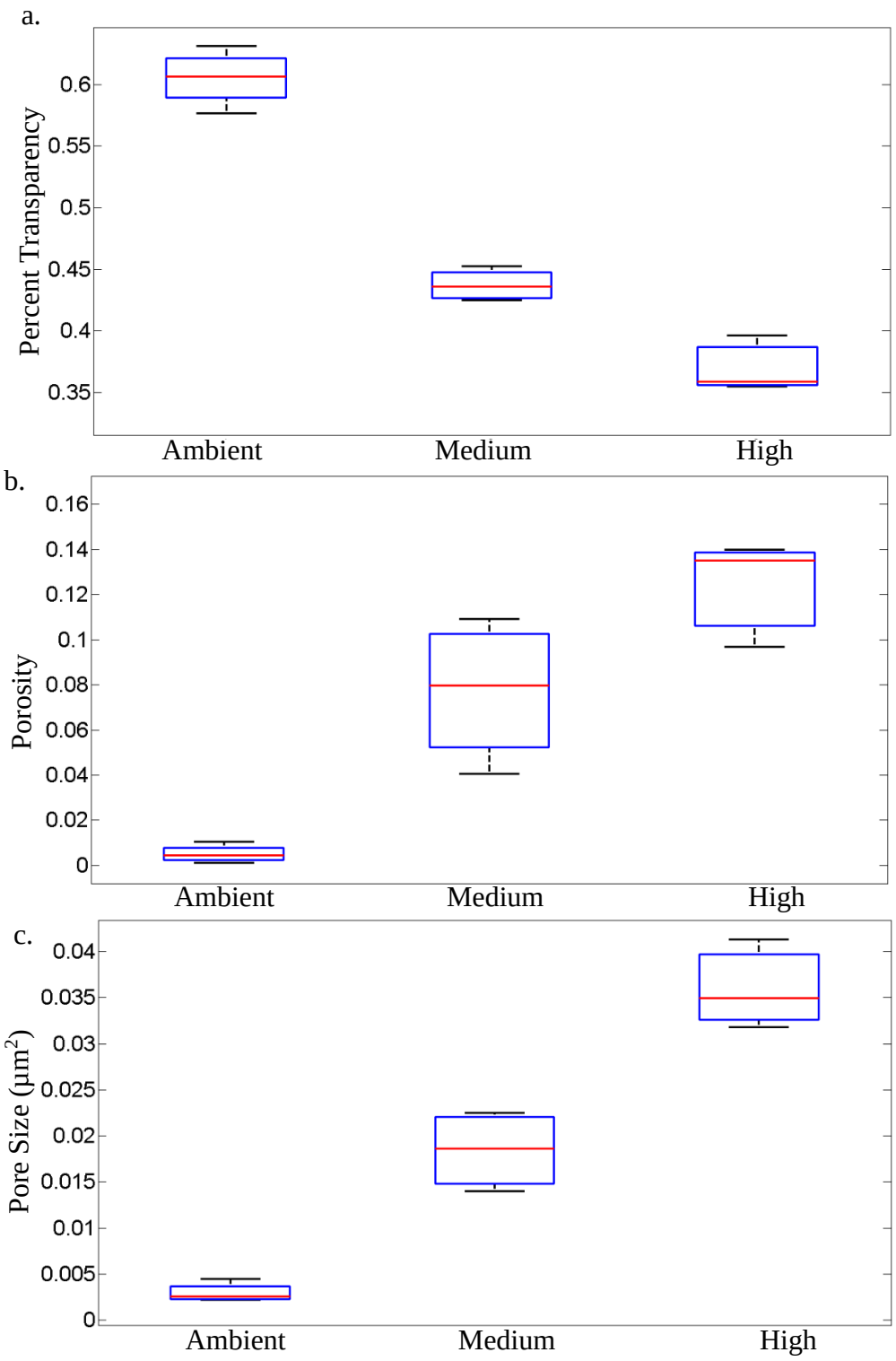

Figure 8. Shell condition of *L. retroversa* from day 7 of the November 2014 experiment. a. Mean transparency (from light microscopy) b. mean porosity, and c. mean pore size (from SEM). Box plots show the median (red), 25 and 75 quartiles (blue), and maximum and minimum (black whiskers).

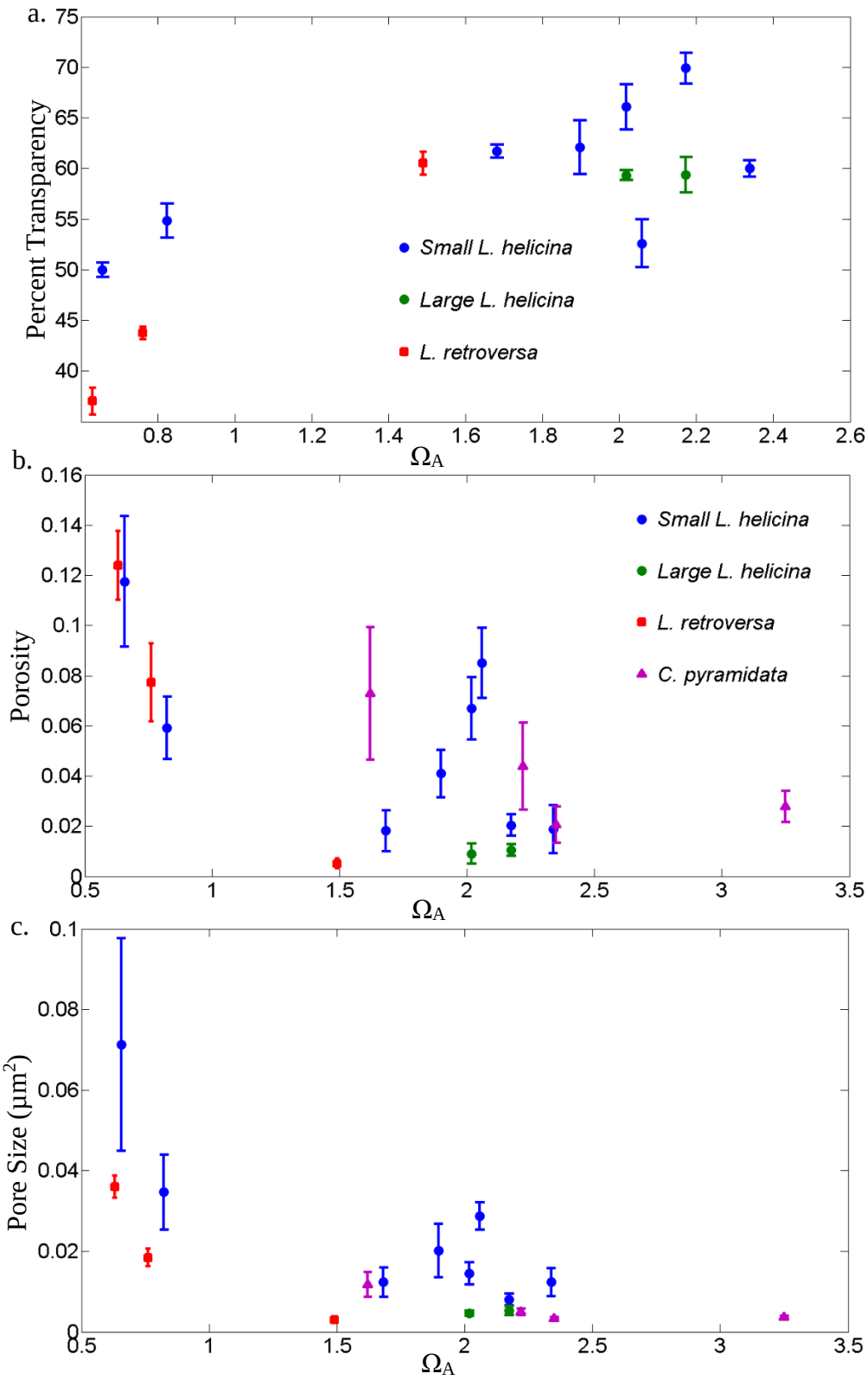

Figure 9. Shell condition metrics vs aragonite saturation state (Ω_A) for multiple pteropod species a. transparency vs. Ω_A, b. porosity vs Ω_A, and c. mean pore size vs Ω_A. Error bars show one S.E.

and April 2015 (Holm-Sidak, $p<0.05$) and the high treatments between January 2014 and August 2014 (Dunn's method, $p<0.05$).

Calcein intensity values of *L. retroversa* shells were significantly different between the treatments for weeks two and three of the April 2014 experiment (Figure 6, Figure 7b). The medium and high treatments had greater calcein fluorescence than the ambient treatment at all time points. The location of the calcein fluorescence in the enhanced CO_2 treatments was not limited to the growing edge, but rather covered most of the shell (Figure 7b). An overall decrease in calcein intensity was measured within every treatment after longer exposure durations.

Light microscopy (transparency) and SEM (porosity and pore size) based measurements both revealed significant changes in shell condition by day 7 of the November 2014 experiment after exposure to elevated CO_2. The transparency, porosity, and pore size had significant differences between the *L. retroversa* shells of each treatment (Figure 7a, c, Figure 8). The transparency was significantly lower and the porosity was significantly higher in the elevated CO_2 treatments with each treatment significantly different from the others (Holm-Sidak, $p<0.05$). Pore size was significantly larger in the high treatment compared to the ambient (Dunn's method, $p<0.05$), but was not significantly different between the medium treatment and the other treatments. The light microscopy and SEM based measurements on the shells of *L. retroversa* exposed to experimentally elevated CO_2 were well correlated. The shell metrics (transparency, porosity, and pore size) were plotted against Ω_A and showed a pronounced decrease in transparency, and increases in porosity and pore size under elevated CO_2 (Figure 9).

Limacina helicina from the North Pacific

The shells of wild-caught *L. helicina* were examined between 43°N and 49°N in the open Pacific Ocean. Along a latitudinal gradient, Ω_A decreased by approximately 0.66 in the sub-surface layer (25-50 m) from the southernmost to northernmost station (Figure 10, Table 3). The Ω_A also decreased with depth, such that *L. helicina* caught below 200 m were exposed to the lowest *in situ* Ω_A conditions. The peaks in measured chlorophyll-a fluorescence showed that 43°N had the most chlorophyll-a, suggestive of more phytoplankton biomass, and 45°N had the least chlorophyll-a (Figure 11). At station 47°N, the night CTD cast had higher fluorescence than the day CTD cast. Station 49°N had intermediate levels of fluorescence. Furthermore, the surface fluorescence values at 49°N, 47°N during the night, and 43°N were considerably higher than 47°N during the day and 45°N.

A net by net comparison of the porosity small sized (≤0.7 mm) *L. helicina* showed interesting regional, depth, and day/night patterns (Figure 12). At station 49°N, the shells had generally low porosity in the only net examined, 25-50 m. Porosity of *L. helicina* shells was highest in the 25-50 m net at station 47°N during the day. Examining the shells at this station during both day and night tows in the upper 50 m revealed that the 25-50 m day net was significantly different from the others, including the night tow net from 25-50 m (Kruskal-Wallis, $H=19.74$, $p<0.001$, Dunn's method, $p<0.05$). This was the only station where a night tow was examined and compared to a day tow. The deep nets of station 47°N, 200-400 m and 400-600 m, were combined due to low sample size (4 and 3 respectively) and non-significant differences between the porosity of those shells (two-sample t-test, $t=-2.22$, $p=0.077$). In these deep nets, the *L. helicina* porosity was substantially elevated in association with under-saturated Ω_A. Station 45°N had high porosity with large variance in the one net analyzed, 25-50 m. At

station 43°N, shells were tested in the 25-50 m and 50-100 m depth nets, and although the latter had higher porosity the difference was not significant (two-sample t-test, t=1.64, p=0.126).

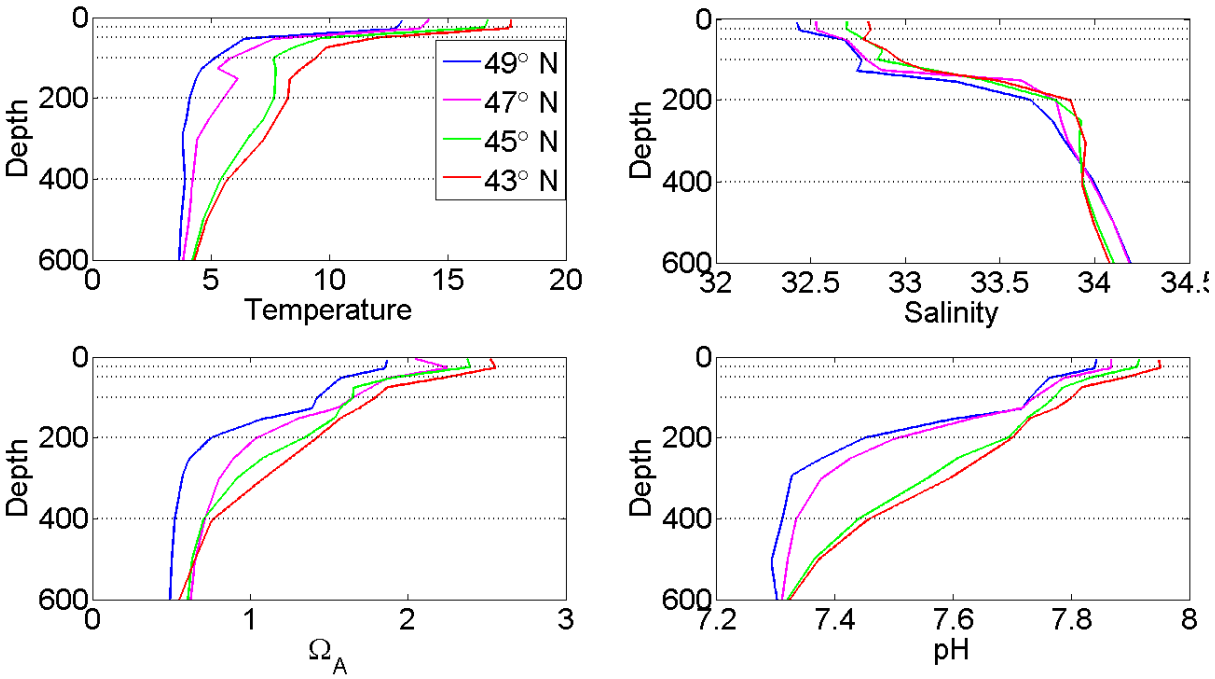

Figure 10. Vertical profiles of temperature, salinity, aragonite saturation state, and pH in the North Pacific where *L. helicina* were caught. The stations and latitudes are: Station 49ºN (blue), Station 47ºN (purple), Station 45ºN (green), and Station 43ºN (red). The aragonite saturation horizons were at these approximate depths for each station: 49ºN (160 m), 47ºN (210 m), 45ºN (270 m), 43ºN (320 m). Dashed lines show the depth intervals for the nets.

Table 3. The aragonite saturation state (Ω_A), temperature, and salinity for each latitude (station) and depth ranges of the nets where *L. helicina* were examined.

Latitude	Depth (m)	Ω_A	Temperature	Salinity
49	25-50	1.68	9.0	32.6
47	0-25	2.17	13.9	32.5
47	25-50	2.02	10.1	32.8
47	200-600	0.74	4.3	33.9
45	25-50	2.06	11.9	32.8
43	25-50	2.34	13.8	32.8
43	50-100	1.90	10.0	32.9

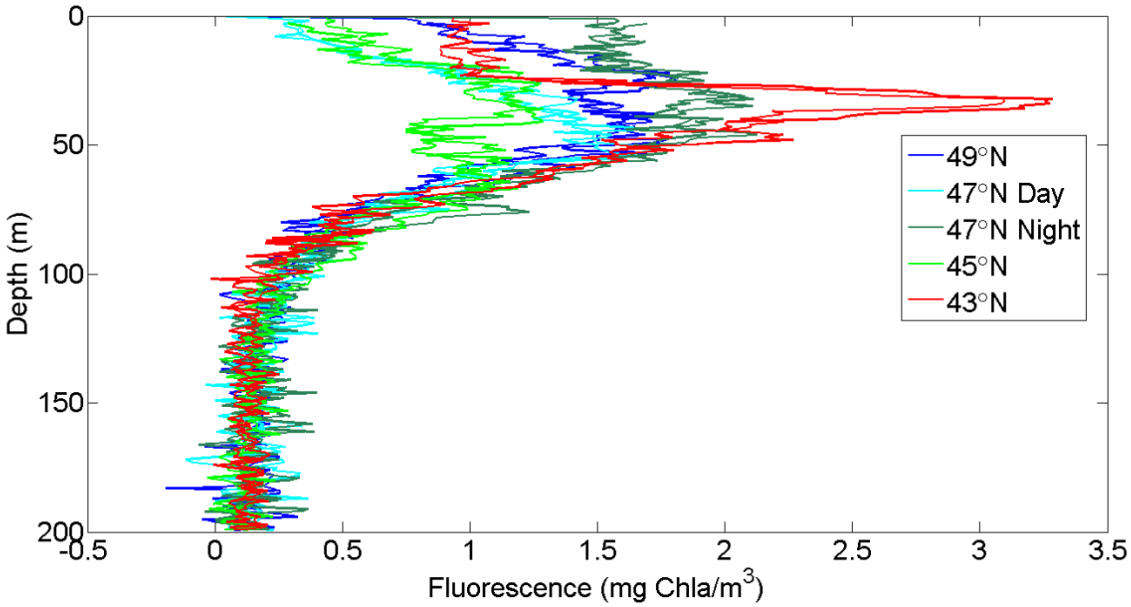

Figure 11. Fluorescence vs depth at the stations where *L. helicina* were caught. There are two lines for each CTD casts showing the upwards and downwards data of the casts. At station 47ºN, the day and night CTD casts are shown.

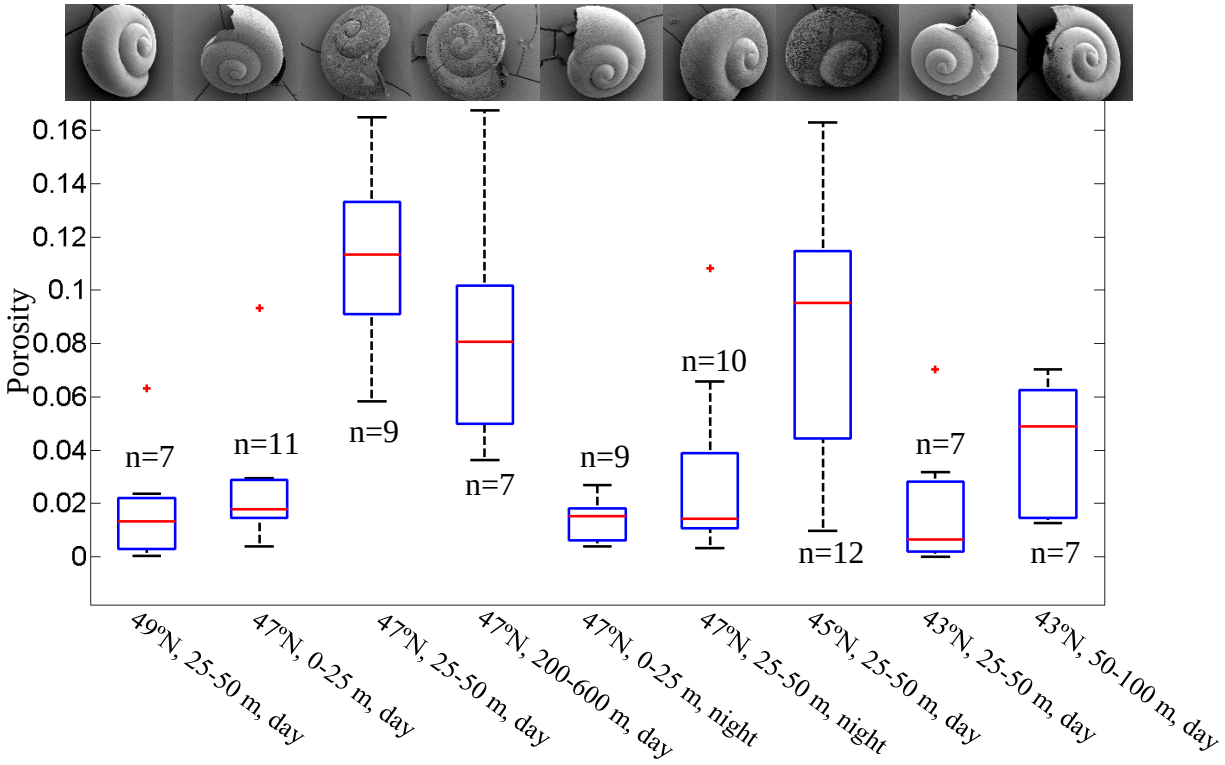

Figure 12. The porosity of wild-caught *L. helicina* in the North Pacific from each of the nets, only showing small (≤0.7 mm) shells. The labels indicate the latitude, net depth range, and whether the tow was conducted during the day or night. Box plots show the median (red line), 25 and 75 quartiles (blue), maximum and minimum (black whiskers), and outliers (red crosses). The sample size and a representative SEM image of a whole shell are shown above or below each of the box plots.

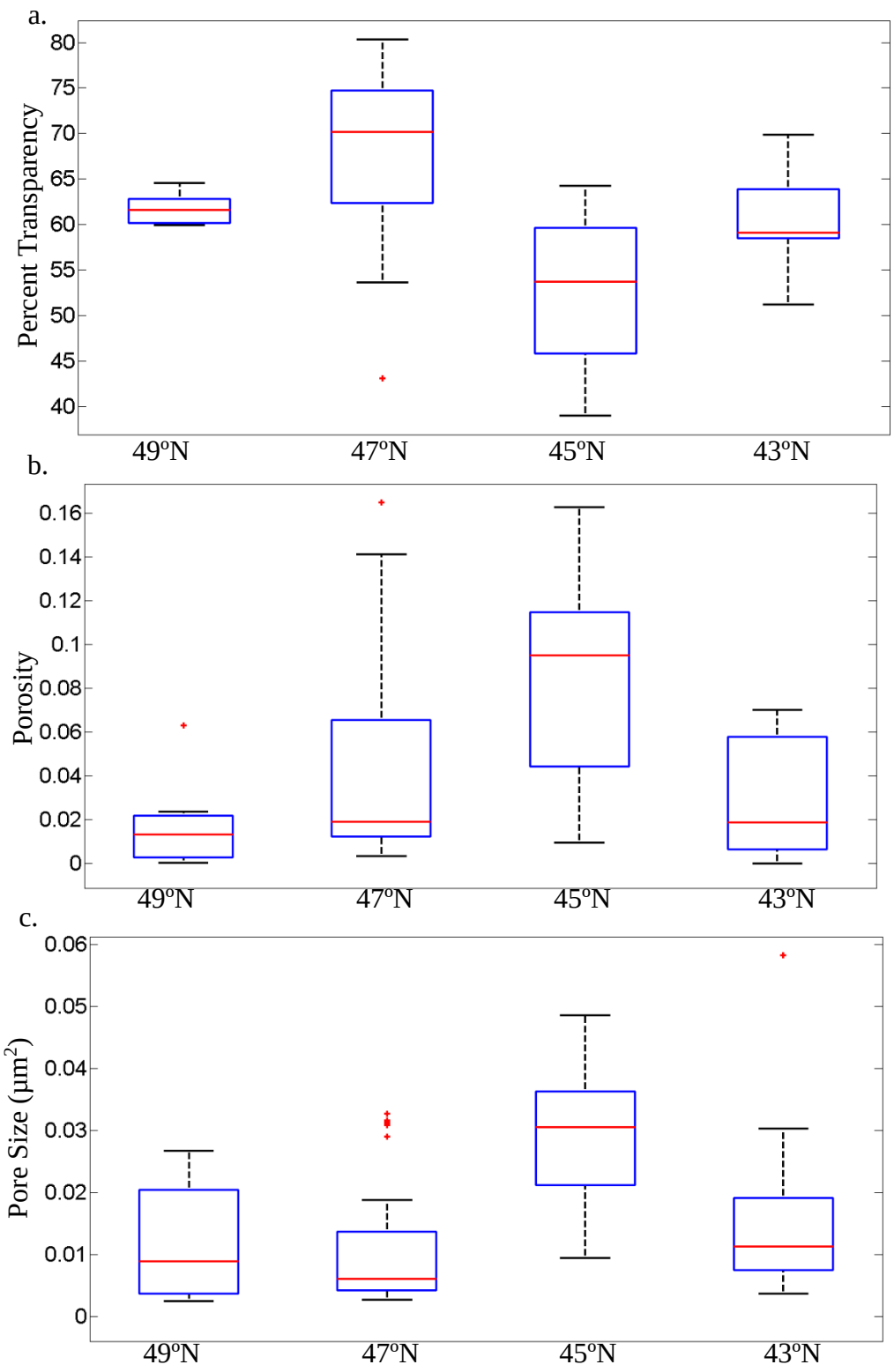

Figure 13. The shell condition of wild-caught small *L. helicina* (≤0.7 mm) across different stations from the upper 100 m a. Percent transparency vs. station, b. porosity vs. station, and c. mean pore size vs. station. Box plots show the median (red line), 25 and 75 quartiles (blue), maximum and minimum (black whiskers), and outliers (red crosses).

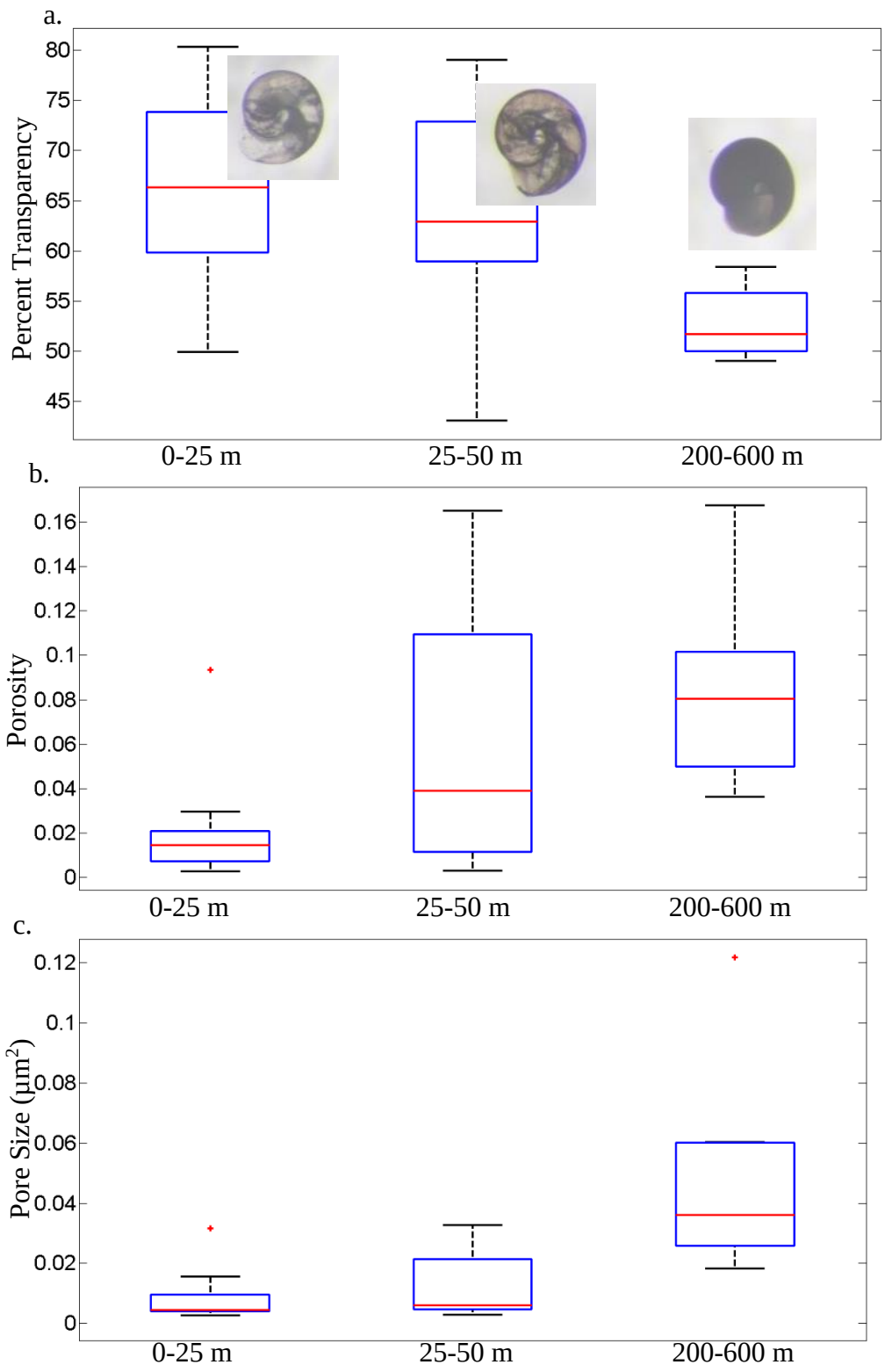

Figure 14. The shell condition of wild-caught small *L. helicina* (≤0.7 mm) across different depths from station 47ºN a. Percent transparency vs. depth range with representative light microscopy pictures for each depth range, b. porosity vs. depth range, and c. mean pore size vs. depth range. Box plots show the median (red line), 25 and 75 quartiles (blue), maximum and minimum (black whiskers), and outliers (red crosses).

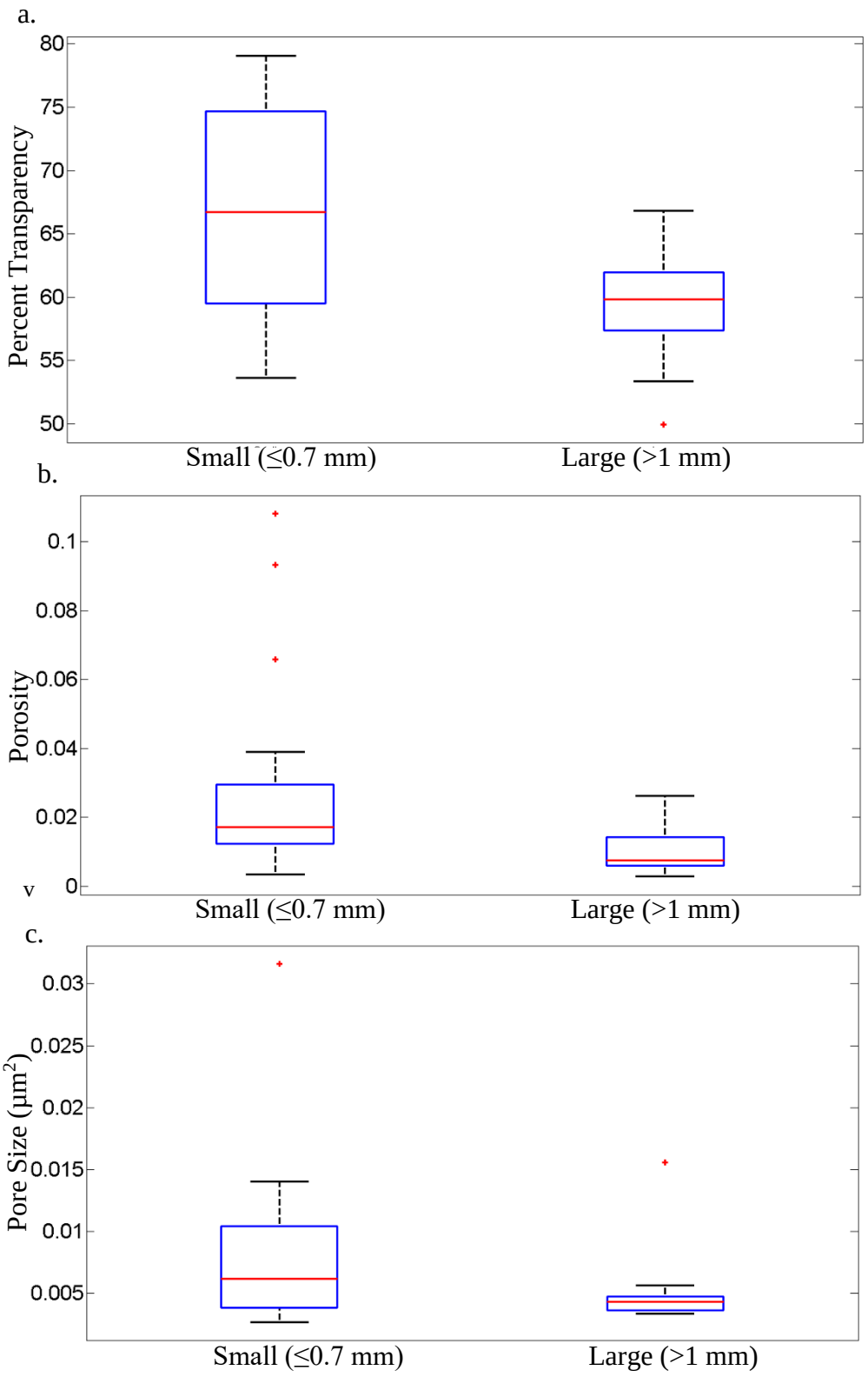

Figure 15. A comparison of shell condition between two size classes of wild-caught *L. helicina*, both sets of specimens were caught at station 47°N in the day net from 0-25 m and the night net from 25-50 m, a. percent transparency vs. size class, b. porosity vs. size class, and c. mean pore size vs. size class. Box plots show the median (red line), 25 and 75 quartiles (blue), maximum and minimum (black whiskers), and outliers (red crosses).

To disentangle the possible effects of station, depth, and size on the shell condition of *L. helicina*, ANCOVA tests were used. Significant relationships were found between the transparency, porosity and pore size of *L. helicina* shells and the station (Table 4). Porosity was elevated at the two intermediate latitude stations (45°N and 47°N) and lower at the northernmost and southernmost stations (Figure 13a). At station 45°N, the transparency was lower and pore size was higher than the other stations, indicating overall lower shell quality (Figure 13b, c). Significant relationships were also observed between transparency, porosity, and pore size of the shells and the depth range (Table 4). The transparency decreased significantly in deeper nets, while the porosity and pore size increased significantly (Figure 14). Shell size had a significant negative relationship with both porosity and transparency, but not with pore size (Table 4).

At station 47°N the small (≤0.7 mm) and large (>1 mm) individuals were compared from the 0-25 m net from the day tow and the 25-50 m net from the night tow, and in these nets the small individuals had similar porosity (Mann-Whitney U, T=103, p=0.647) and the large individuals had similar porosity (Mann-Whitney U, T=19, p=0.80). Although neither group (large or small) of specimens had particularly high porosity, the large individuals were significantly less porous and less transparent than the small individuals (porosity: Mann-Whitney U, T=144, p=0.003, transparency: two-sample t-test, t=3.28, p=0.003, Figure 15a, c). The size classes did not have significant differences in pore size (Mann-Whitney U, T=184, p=0.128, Figure 15b).

The shell condition metrics (transparency, porosity, and pore size) were plotted against the Ω_A for large and small *L. helicina* (Figure 9). For the range of Ω_A between ca. 1.7 and 2.4, shell condition varied for the small *L. helicina* without a clear relationship to Ω_A (Figure 9). In the deep nets, where the average Ω_A was 0.83 and 0.66, the shells had elevated porosity, large

pores, and decreased transparency, which all indicated a lower shell condition. Large individuals were not found in these deep nets. The large *L. helicina* showed little variability in shell condition and were in overall good condition with low porosity and small pore sizes in the range of Ω_A between ca. 2 and 2.2.

Table 4. Results from the ANCOVA (transparency, porosity, and pore size) with covariates: station, depth, and size. The R^2 values show the fit of the model and the intercept shows the base value. For the discrete covariates of station and depth, the parameter estimates for station (top) and depth range (bottom) are shown in the plots for transparency, porosity, and pore size. Since size is a continuous variable there is one coefficient that is listed in parentheses in the table. The p values for each covariate are listed in the right hand column.

Response Variable	R^2	Intercept	Covariates	P-value
Transparency	0.41	0.59	Station	<0.001
			Depth	<0.001
			Size (-0.22)	0.004
Porosity	0.41	0.053	Station	<0.001
			Depth	<0.001
			Size (-0.009)	0.021
Pore Size	0.46	0.027	Station	0.007
			Depth	<0.001
			Size (-0.0015)	0.030

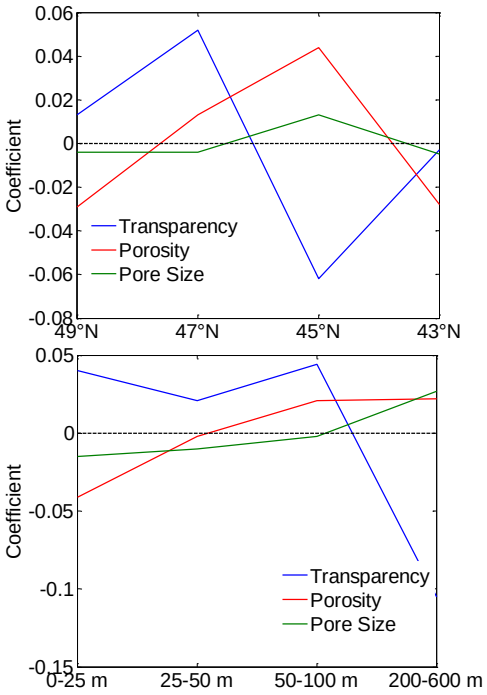

Clio pyramidata from the North Atlantic and North Pacific

The Atlantic stations where *C. pyramidata* were caught had higher average Ω_A in the upper 200 m than in the Pacific (Table 5, Figure 16). At 50ºN in the Atlantic and 37°N in the Pacific, the Ω_A profiles were similar from the surface to ca. 150 m, but then Ω_A decreased more with depth at the Pacific station than at the Atlantic station. For both oceans, the more northerly stations had a lower Ω_A than the southerly stations. The saturation horizon was around 2000 m or

deeper at both Atlantic stations, whereas the southernmost and northernmost Pacific stations with *C. pyramidata* present had saturation horizons at 350 and 240 m respectively. The Ω_A of the two Pacific stations were about equal by ca. 500 m depth. The maxima in Ω_A at the most northerly stations of the Atlantic and Pacific were at 15 m and 27 m respectively, and could have been due to subsurface primary productivity since both stations had peaks in fluorescence and dissolved oxygen at around 40 m. The more northerly stations were cooler and fresher than the more southern ones, and the Atlantic had higher salinity than the Pacific. At 50ºN in the Atlantic, the relatively small vertical temperature gradient and fresher surface water might be due to proximity to Atlantic deep water formation and freshwater inputs.

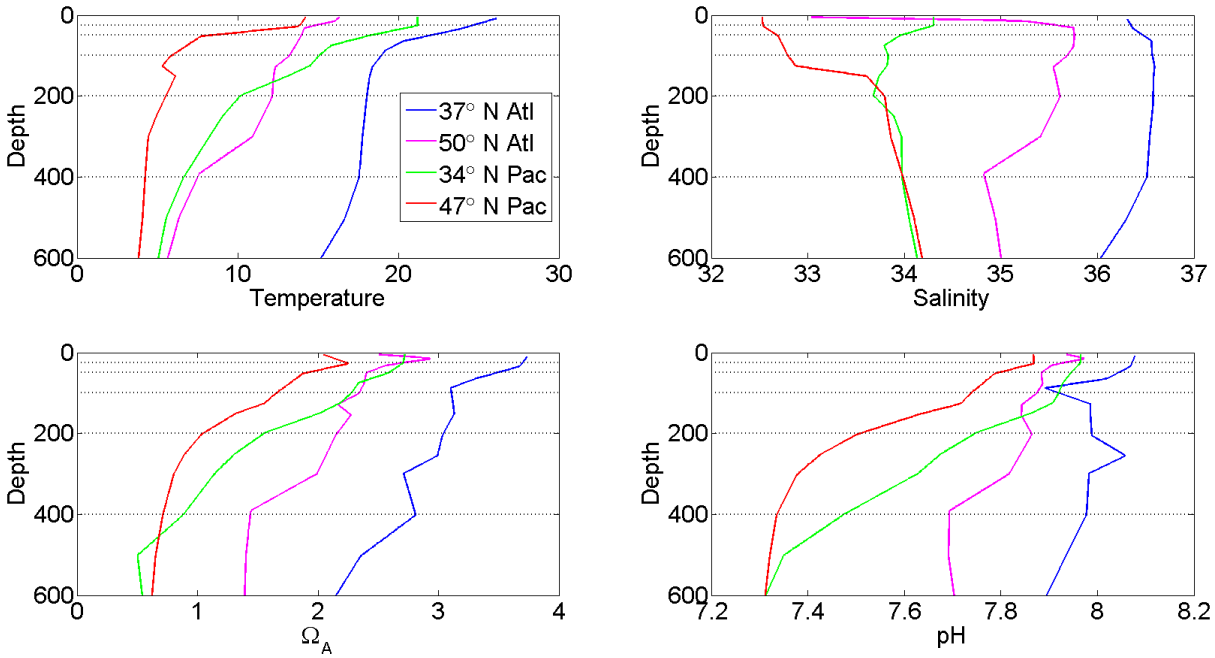

Figure 16. Vertical profiles of temperature, salinity, aragonite saturation state (Ω_A), and pH at the Atlantic and Pacific stations where *C. pyramidata* were caught. Dashed lines show the depth intervals for the nets.

Table 5. The aragonite saturation state (Ω_A), temperature, and salinity and depth of the saturation horizon (SH) for each latitude (station) where *C. pyramidata* were examined in the Atlantic or Pacific ocean basins. The aragonite saturation state, temperature, salinity values were averaged from 0-200 m.

Lat	Basin	Ω_A	Temperature	Salinity	Depth of SH (m)
37	Atlantic	3.25	20.0	36.5	1970
50	Atlantic	2.35	13.2	35.6	2450
34	Pacific	2.22	15.4	33.9	350
47	Pacific	1.62	7.5	33.0	210

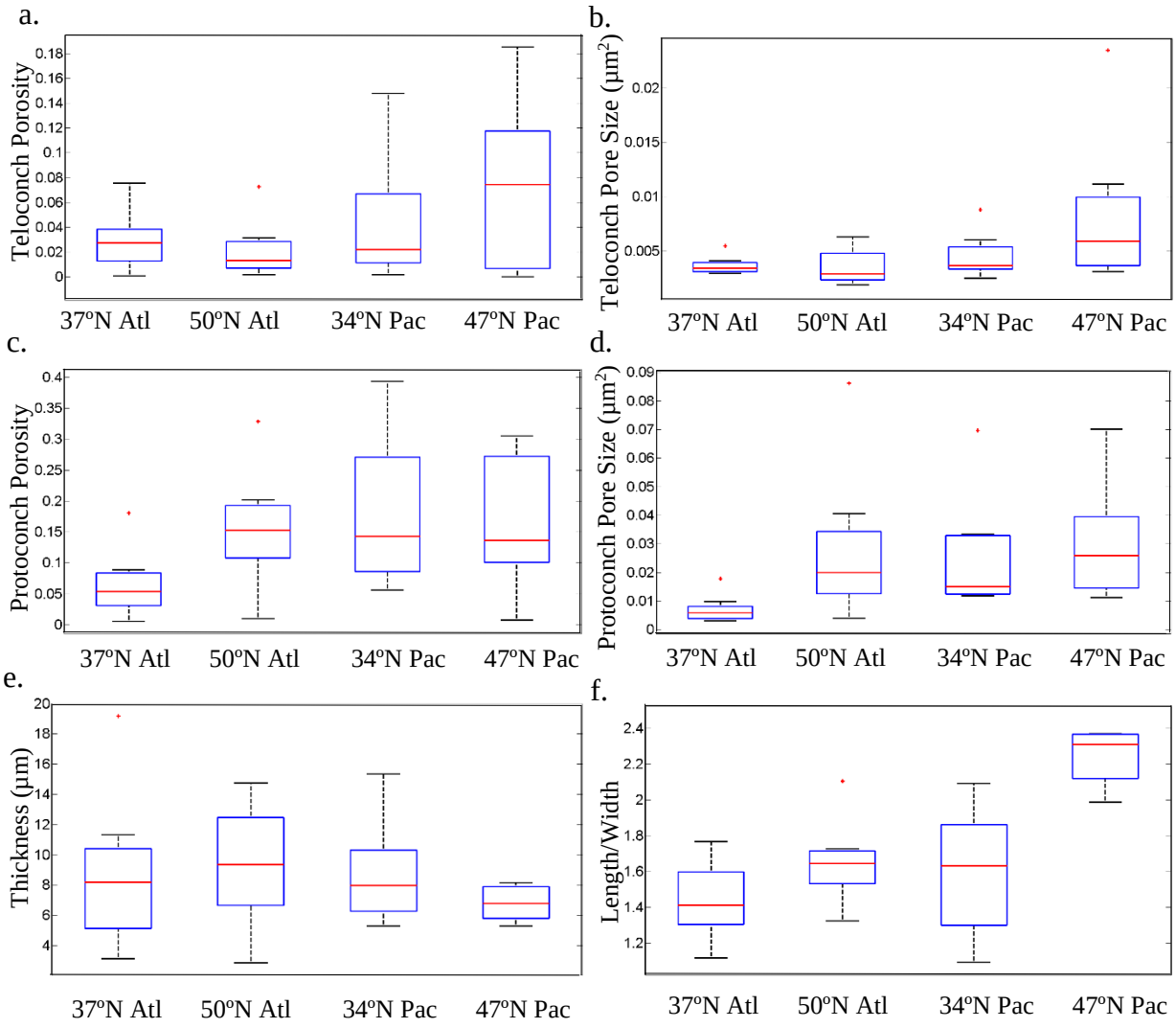

Figure 17. Morphological and shell condition measurements of wild caught *C. pyramidata* a. teloconch porosity, b. teloconch pore size, c. protoconch porosity, d. protoconch pore size, e. the average thickness of the aperture, and f. the length/width ratio of the shells. Abbreviations are Atl for Atlantic and Pac for Pacific.

The teloconch porosity and pore size did not have significant differences when compared across the Atlantic and Pacific stations (Kruskal-Wallis ANOVA, porosity H=2.5, p=0.48, pore size H=6.3, p=0.10, Figure 17a, b). The teloconch porosity and pore size where the highest at 47°N in the Pacific, but with high variability. The protoconch pore size was significantly different between stations, with the smallest pores at Atlantic station 37°N and the largest pores at Pacific station 47°N (Kruskal-Wallis ANOVA, H=9.9, p=0.019, Figure 17c). Protoconch

porosity did not have significant regional differences (one-way ANOVA, F=2.3, p=0.10, Figure 17d). Differences in the shell thickness were also not significant (one-way ANOVA F=0.50, p=0.69, Figure 17e). The *C. pyramidata* at the Pacific station 47°N had a significantly different length:width ratio from the other stations, likely indicative of a different forma (one-way ANOVA F=13.5, p<0.001, Figure 16f).

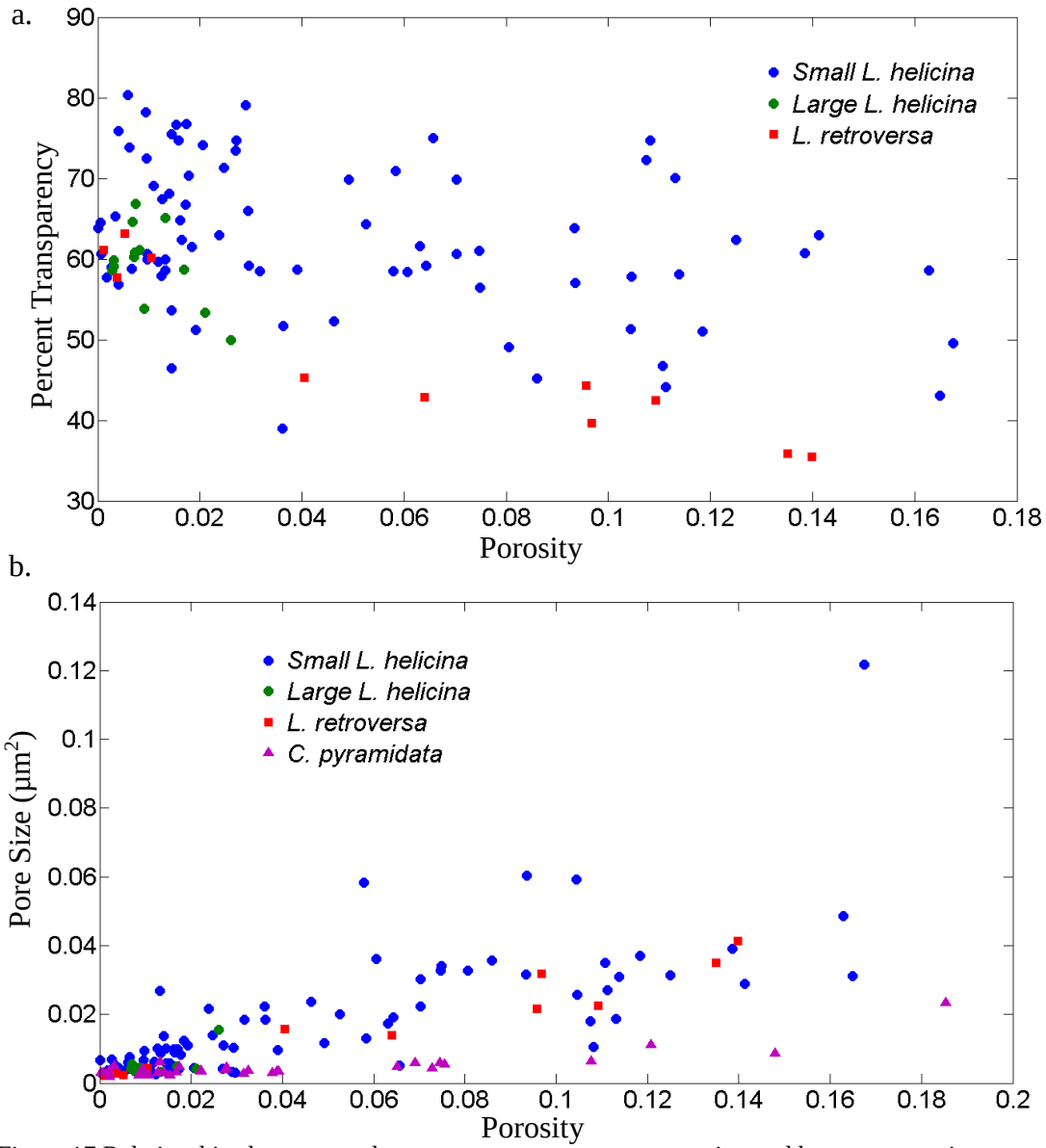

Figure 17 Relationships between a. the percent transparency vs. porosity, and b. mean pore size vs. porosity for multiple species of pteropod: *L. helicina* (small≤0.7 mm, large>1 mm), *L. retroversa*, and *C. pyramidata*.

Comparison of Multiple Species

Overall, transparency and Ω_A were positively correlated for the *Limacina spp.* (Figure 9a, R^2=0.296, p<0.001), while the porosity and pore size were negatively correlated to Ω_A for all of the species (Figure 9b, porosity: R^2=0.123, p<0.001, Figure 9c, pore size: R^2=0.245, p<0.001). The shells of both *Limacina* species had lower condition in under-saturated conditions, with similar porosity values. *Limacina retroversa* had lower transparency and smaller pore size than the wild *L. helicina* at similar Ω_A, when Ω_A<1. At intermediate Ω_A (ca. 1.6 to 3.3) some dissolution was evident on the shells of wild caught *L. helicina* and *C. pyramidata*. While the shells of *C. pyramidata* had a general decreasing trend in shell condition as Ω_A declined, *L. helicina* had the lowest shell condition at Ω_A=2–2.1 and better shell condition at lower and higher Ω_A. *Limacina retroversa* from the ambient treatment of the laboratory experiment had lower porosity than the other species when Ω_A was ca. 1.5, which could be indicating that the wild-caught *L. helicina* and *C. pyramidata* experience greater Ω_A variability and possibly lower Ω_A values than was observed for the exact depths (<200 m) where they were collected and therefore had lower shell condition at higher apparent Ω_A values than *L. retroversa*.

Patterns in shell condition were fairly consistent regardless if transparency, porosity, or pore size was being compared since these metrics were significantly correlated. Significant negative correlations were observed between the shell transparency and the porosity of *L. helicina* and *L. retroversa* shells (Figure 18a, R^2=0.167, p<0.001). The relationship between porosity and transparency differed between the larger and smaller *L. helicina* with the smaller individuals having a higher shell transparency at a given porosity. Mean pore size and porosity was positively correlated for all of the species (Figure 18b, R^2=0.484, p<0.001). *Clio pyramidata* generally had smaller pores (on the teloconch) at a given porosity value than the *Limacina* species.

Discussion

Limacina retroversa under experimentally elevated CO_2

Quantitative measurements of shell condition are important tools for comparing pteropod shells in the context of ocean acidification. The change in appearance of *L. retroversa* shells seen in these experiments has been measured in other studies using the LDX (Lischka and Riebesell 2012, Manno *et al.* 2012). The transparency method described in this study has the benefit of being less subjective and more continuous than the LDX. Even with small sample sizes (3–4), the porosity, pore size, and transparency between of *L. retroversa* exposed to ambient, medium, and high CO_2 for 7 days were significantly different between each of the treatments. The degree of under-saturation appeared to be important for the shell condition of *L. retroversa*. The medium treatment was under-saturated with respect to aragonite (0.76) at day 7 in November 2014 and had significant differences in shell condition from the high treatment which had lower Ω_A (0.63). Measuring porosity from SEM images was also used by Roger *et al.* (2011) on two tropical species of pteropod to compare historical and present (1963-2009) samples; that was the first and only study other than this one to do so. The porosity and pore size metrics are less time consuming and more objective than classifying regions of dissolution (types I, II, and III), a method used in other shell dissolution studies (Bednaršek *et al.* 2012a, Bednaršek *et al.* 2012b, Bednaršek *et al.* 2014a, Bednaršek *et al.* 2014b, Bednaršek and Ohman 2015). Since the category type I dissolution is defined as an increase in the density of pores, porosity is a good approach for capturing this type of dissolution, however more advanced dissolution (type II and III) may be better correlated to pore size. Both metrics can underestimate the porosity and pore size when dissolution covers large regions of the shell because the electron beam illuminates parts of the

underlying, damaged aragonite, and for this reason even when the prismatic layer is completely removed the porosity will not reach one. Despite sometimes failing to identify the absolute porosity or pore size, these are useful metrics for comparing shell condition.

The seasonal differences in the transparency of *L. retroversa* after four days of exposure to the ambient CO_2 concentrations seemed to relate to seasonal variability in the *in situ* Ω_A and animal size. The shells from the ambient treatments of January and November experiments had lower transparency than April and August, with the average transparency from the January experiment being particularly low. The average transparency of ambient shells from January was actually lower than the average shell transparency after exposure to elevated CO_2 for four days in the other experiments. Differences in the dry mass of the *L. retroversa* showed that January individuals were the largest followed by those from November. It is possible that thicker shells are less transparent, while still being in good condition (i.e. not dissolved). This is supported by the finding that larger *L. helicina* had significantly darker shells than the smaller ones, despite also having lower porosity and pore size, indicative of good shell condition. However, differences in transparency in the ambient treatments between experiments were probably not caused by differences in size alone. The different experiments had a significant relationship with shell transparency in the ambient treatment while dry mass did not. The *in situ* Ω_A could explain patterns in seasonal transparency. In January, the Ω_A in the upper 60 m of the Gulf of Maine was about 0.32 lower than average (annual average=1.86), and in November Ω_A was slightly below average (0.04 lower), while in August and April the Ω_A was about average, which could explain why ambient shells were less transparent when collected in January and November (Wang *et al.* 2017).

The magnitudes of differences in shell transparency between the ambient, medium, and high CO_2 treatments across the seasonal experiments were compared to determine whether there was seasonality in the sensitivity of shell condition to elevated CO_2. The differences in transparency between treatments were mostly similar across experiments, indicating that there was not seasonality in the sensitivity of shell condition to changes in carbonate chemistry. A slightly different response to elevated CO_2 was observed in August 2014, when there was a larger reduction in transparency between the ambient and medium treatments than between the ambient and high treatments. Differences in the carbonate chemistry of the treatments could be affecting the relative effects of the treatments. In August 2014, the high treatment did not achieve the target level of CO_2, but rather ~800 µatm, and had a similar saturation state as the medium treatment (Ω_A=1). The significantly lower transparency of the medium treatment compared to the high treatment was likely spurious. In November 2014, the medium treatment was very under-saturated (Ω_A=0.78) and the high treatment had a lower saturation state (Ω_A=0.64) than the other experiments. Still, the transparency in November 2014 was significantly different between all the treatments. Differences in the Ω_A between the treatments in each experiment were not consistent, which create some uncertainty about seasonality in the sensitivity of shells to elevated CO_2. With improved control of the carbonate chemistry, future experiments could re-test this seasonal response to determine if there might be critical periods of sensitivity to changes in CO_2 that relate to *in situ* conditions or the developmental state of the animals.

Repair calcification may be a response to increased dissolution under low Ω_A, but since shell condition still declined it is likely that dissolution was outpacing any repair calcification in the elevated CO_2 treatments. Greater calcein fluorescence was observed on the *L. retroversa*

shells from both the medium and high CO_2 treatments, which was contrary to the expectation that calcification would be greatest in the ambient treatment. In some studies, calcein binds to the leading edge (Comeau *et al.* 2009, Thabet *et al.* 2015) while in other studies, including this one, calcein covers many parts of the shell, possibly showing that individuals perform repair calcification in response to elevated CO_2 (Lischka *et al.* 2011). There could have been differences in the developmental state of the specimens that could account for these different observations or shell extension could be periodic and may not have been occurring during the one hour exposures to calcein solutions. Calcein binds to calcium, so it also attaches to muscle and other animal tissue. Although some calcein was seen inside the animal tissue, it was not as evident as the fluorescent shells. Fluorescing tissues were most apparent in the ambient treatment due to the reduced fluorescence from the shells.

Limacina helicina from the North Pacific

Limacina helicina shell condition had significant differences across regions, depths, and sizes. The hypothesis that the shell condition would decrease at more northerly stations was not borne out by the results. The shell condition was lower at the intermediate two stations such that the monotonic latitudinal gradients in Ω_A and temperature fail to account for the spatial pattern in *L. helicina* shell condition. The regional differences in shell condition could be explained by forma differences (McGowan 1963), differences in vertical migratory behavior (Comeau *et al.* 2012a, Bednaršek and Ohman 2015), differences in food availability (Siebel *et al.* 2012), or the presence of fine scale temporal and/or spatial processes. With the small *L. helicina*, it was not possible to identify which forma they belonged to, but the large specimens at station 47ºN had pronounced ridges and ratios of height to width, which indicated that they were Type A

(Height/Diameter this study 1.08±0.08 S.D., n=7, McGowan 1963: type A~1, type B~0.8). In McGowan (1963) the more southern stations had forma type B, followed by a mixed population, and then type A in the north. The forma may have different vertical distributions even when they occupy the same water column. McGowan (1963) observed evidence of diel vertical migration (DVM) between 200 m (day) and 60 m (night) for forma type B, but did not see a DVM for forma type A. Whether differences in the structure of shells of forma or differences in the migratory behavior and therefore the Ω_A experienced by the organisms are leading to regional variability in the shell condition of *L. helicina* could be addressed by future work.

Calcification requires energy and demands more as Ω_A decreases (e.g. Cohen and Holcomb 2009). In regions with less primary productivity, pteropods might not have enough food, which can lead to metabolic suppression and reduced calcification (Seibel *et al.* 2012). Food availability might be particularly important for how well pteropods can cope with environmental stressors like ocean acidification (Bednaršek *et al.* 2016a). The fluorescence profiles at each of the stations supported the idea that differences in food availability that might have caused differences in shell condition. The station (45ºN) with the poorest shell condition also had the lowest fluorescence values. Furthermore, the significant differences in shell condition between day and night in the 25-50 m net at station 47ºN coincided with differences in the fluorescence between day and night CTD casts. The MOCNESS tows during the day and night at 47ºN were about 10 km apart and 11 hours apart. The suggestion of fine scale variability in shell condition and food availability presents a problem for trying to discern larger regional differences. Fine scale variability might be caused by the patchiness of plankton and the movement of the ship (e.g. Wiebe 1970). More sampling effort with greater spatial coverage and larger sample sizes may be needed to adequately compare the shell condition across regions.

Smaller juvenile *L. helicina* might be more sensitive to ocean acidification than larger individuals. Where larger *L. helicina* were caught and examined, the porosity was lower than the smaller size class. Transparency was deemed to not be an appropriate metric for comparing individuals of different size classes due to differences that might arise due to shell thickness. Larger individuals might have better shell condition because they have larger energy budgets that can be allocated towards shell maintenance (Lischka and Riebesell 2016). Early life stages are often the most susceptible to ocean acidification and other environmental stressors (e.g. Kurihara *et al.* 2008, Kroeker *et al.* 2010, Bednaršek *et al.* 2014b). Other studies have found that development of pteropods after hatching from eggs is delayed by elevated CO_2 (Thabet *et al.* 2015) and that at a high CO_2 concentration (1700 µatm) larval pteropods do not start forming shell (Comeau *et al.* 2010b).

A significant relationship was observed between shell condition and the depth at which *L. helicina* were caught, indicating that there could be vertical structure in the *L. helicina* populations that might cause groups of individuals to experience different amounts of dissolution. Unfortunately, I cannot determine the history of these individuals before they were caught. For the shells found below 200 m there is uncertainty as to whether the *L. helicina* were actually alive when they were caught. To try to avoid dead *L. helicina* only shells with tissues inside were used. The *L. helicina* found in the deep nets had dissolution comparable to that of the live *L. retroversa* from high CO_2 treatment which had a similar Ω_A as what was measured at 200-600 m deep North Pacific. Most studies on wild-caught pteropod dissolution integrate the vertical environment (Bednaršek 2012a, Bednaršek 2014a). Bednaršek and Ohman (2015) is the only other study of wild-caught pteropod shell quality to use a discrete depth sampling, and they

also found that shell condition of *L. helicina* was worse in deeper waters, particularly near the saturation horizon.

Wild-caught Clio pyramidata from North Atlantic and North Pacific stations

Clio pyramidata is a strong migrator, residing at daytime depths of 240-460 m and at nighttime depths of 50-100 m (Atlantic: Sargasso Sea, Wormuth 1981). In this study, nighttime tows (0-200 m) were used to examine *C. pyramidata* shell condition, at which time the individuals were expected to be in the shallow phase of their DVM. Patterns in the vertical distribution of *C. pyramidata* were observed from the depth stratified MOCNESS sampling (not shown). During the day, *C. pyramidata* was migrating down to 400 m deep in the North Pacific, and a large part of the population migrated down to 600 m deep with some individuals still being found in the 600-1000 m nets in the North Atlantic. These differences in DVM behavior between oceans might have reduced differences in regional shell condition by exposing *C. pyramidata* to similar Ω_A conditions across stations due to their deeper daytime positions in the Atlantic. Individual variability in shell condition could arise from differences in DVM within the *C. pyramidata* population at each location. With *L. helicina* there were vertical differences in the shell condition and this could also be tested using *C. pyramidata* caught at different daytime depths within a station.

While most of the *C. pyramidata* shell condition metrics did not have significant regional differences, there was a significant difference in the protoconch pore size between stations. The shells of *C. pyramidata* at 47ºN in the Pacific had the largest protoconch pore sizes and shells at 37ºN in the Pacific had smallest protoconch pore sizes. There were non-significant trends for teloconch shell condition with the northernmost Pacific station having higher porosity, larger

pore size, and thinner shells. There was also lower variability in the shell thickness at 47ºN in the Pacific suggesting that there were fewer individuals with thick shells than there were at the other stations. Taken together, there could be real differences in the shell condition of *C. pyramidata* between the North Atlantic and North Pacific, especially the lower shell condition observed in the northernmost station in the Pacific. However, larger sample sizes may be needed to find significant relationships due to the high variability in shell condition within stations.

Clio pyramidata may be well adapted to low Ω_A because it has relatively deep migrations. Having thicker protective periostracum or engaging in repair calcification could help to counteract the effects of living in more corrosive water (Lischka *et al.* 2011, Peck *et al.* 2016). The protoconch of *C. pyramidata* appears to have experienced higher dissolution than the teloconch. In contrast, the shells of *L. helicina* did not have different extents of dissolution on the innermost whorl, which was the larval shell. Incomplete periostracum removal before SEM analysis on some samples showed that the periostracum did in fact extend over the protoconch. The protoconch region may not be actively maintained by adult *C. pyramidata* and therefore have higher porosity and larger pore size than the teloconch.

Comparison of Multiple Species

The correlation between porosity, pore size, and transparency indicates a strong link between these metrics in the *Limacina* species. These relationships can be used for less resource intensive measurements on *Limacina* shells and could facilitate more surveys of shell dissolution in other ocean regions with the ability to predict fine-scale changes by measuring transparency with a light microscope. The transparency of *C. pyramidata* was not measured in this study, but if the internal tissue was digested by bleach, then transparency could be measured. The

transparency of *C. pyramidata* would likely differ from the *Limacina spp.* due to differences in shell structure and thickness. Additional metrics of shell condition, notably including thickness, could be provided by micro-computed tomography (micro-CT) scanning, which provides high resolution 3D information on pteropod shells, but is even more costly and time consuming (Howes *et al.* 2017).

The comparison of shell structure across the three species of pteropod showed comparable porosity and pore sizes. In general, shell condition decreased as Ω_A decreased, but was probably under the influence of other factors as well. The wild-caught *C. pyramidata* shells had decreasing shell condition as Ω_A decreased from ca. 3.3 to 1.6, but the differences were not large enough to be significant. *Limacina helicina* had lower shell condition in under-saturated conditions (Ω_A=0.83 and 0.66) and around Ω_A=2. *Limacina helicina* caught in the California Current Ecosystem had the most pronounced dissolution at Ω_A from 1 to 1.4, but some specimens had detectible shell dissolution where Ω_A was greater than 2 (Bednaršek and Ohman 2015). Other species of pteropod have been studied in the context of ocean acidification including *Cavolinia inflexa*, *Creseis acicula*, and *Diacavolinia longirostris* (Comeau *et al.* 2010b, Roger *et al.* 2011, Comeau *et al.* 2012b). The porosity on the species in this study were similar, while Roger *et al.* (2011) found inter-species differences with *C. acicula* having smaller pores than *D. longirostris*, and evidence that porosity can be increased and shell thickness decreased in these species due to saturation state changing from ca. 3.9 to 3.6.

Every pteropod species will probably have a slightly different response to ocean acidification, but there were not obvious species-specific differences in the shells of these three species at similar Ω_A. The species in this study, *L. helicina*, *L. retroversa*, and *C. pyramidata*, are found in polar or subpolar waters, experience some of the lowest Ω_A of any pteropod species,

and may have adaptations to cope with these conditions. The Ω_A in the environment as well as the rate that Ω_A is changing from historic values may be important for determining the shell condition of pteropods. Measurements of shell condition spanning more regions and species are needed to develop a better understanding of the sensitivity of pteropod shells to Ω_A and other environmental factors.

Chapter 4

Variability in the abundance, distribution, and habitat use of *Limacina retroversa* in the Gulf of Maine

Abstract

Pteropods are calcifying zooplankton that are found throughout the world's oceans, are important parts of food webs and biogeochemical cycles, and are considered sentinel species for the effects of ocean acidification. In this study, a multi-decadal time series (1977-2015) of the pteropod *Limacina retroversa* in the Gulf of Maine (GOM) was used to characterize the habitat (temperature, salinity, bottom depth) and examine inter-annual patterns in the abundance and distribution of *L. retroversa*. The annual abundance anomalies of *L. retroversa* in spring and fall were examined in order to determine whether there had been a long-term decline or range shift of the population and were also compared to inter-annual patterns in temperature, salinity, water mass composition, and climate oscillations. The springtime habitat of *L. retroversa* was characterized by lower salinities and lower temperatures than the overall available conditions. In the fall, the *L. retroversa* were associated with shallow and nearshore habitats. There was not a decline of *L. retroversa* over the course of the time series. In the spring, the multi-year cycles in abundance were most correlated to annual anomalies in temperature and salinity, while in the fall the abundance anomalies were significantly correlated to two regional climate oscillations, the Atlantic Multidecadal Oscillation (AMO) and the North Atlantic Oscillation (NAO) with a two year lag. Continued monitoring of *L. retroversa* in the GOM is important for determining how climate change and natural variability affect this taxon.

Introduction

Shelled pteropods (Order: Thecosomata) are a group of zooplankton that form aragonite shells. They are found in all of the world's oceans and are prey for fish, whales, seabirds, and other zooplankton (LeBrasseur 1966, Ackman *et al.* 1972, Conover and Lalli 1974, Levasseur *et al.* 1996, Pakhomov *et al.* 1996, Armstrong *et al.* 2005, Hunt *et al.* 2008, Karnovsky *et al.* 2008, Pomerleau *et al.* 2012, Sturdevant *et al.* 2013). Thecosomes are suspension feeding omnivores and contribute to the biological carbon pump through feces, pseudofeces, and mortality and to the carbonate pump via sinking of the shells (Byrne *et al.* 1984, Lalli and Gilmer 1989, Accornero *et al.* 2003). Shelled pteropods have been receiving increased attention in the last ten years in the context of ocean acidification, which is expected to cause dissolution of the shells (e.g. Comeau *et al.* 2009, Lischka and Riebesell 2012, Bednaršek *et al.* 2017).

Generally, what is known about the responses of pteropods to varied physical conditions comes from laboratory experiments that aim to predict the effects of climate change, which is concurrently affecting several aspects of marine habitats. As a calcifying taxon, the calcification and dissolution of pteropod shells is affected by the decreasing availability of carbonate caused by ocean acidification (Comeau et al. 2009, Comeau et al. 2010a, Lischka et al. 2011, Lischka and Riebesell 2012, Bednaršek et al. 2014b). Ocean acidification also has the potential to affect the metabolism, mortality, and locomotion of pteropods (Lischka and Riebesell 2012, Manno *et al.* 2012, Lischka and Riebesell 2016, Chapter 2). Additionally, changes in temperature and salinity might affect the fitness of pteropods. The warming of the surface ocean has occurred at a global average of about 0.7°C over the past 100 years (Gruber 2011). When combined with changes in dissolved CO_2 (pCO_2), changes in temperature can synergistically affect pteropod metabolism, mortality, and calcification (Comeau *et al.* 2010a, Lischka *et al.* 2011, Lischka and

Riebesell 2012, Lischka and Riebesell 2016). Salinity might be affected by climate change differently in certain regions of the world's oceans, with coastal regions particularly affected by changes in precipitation. The salinity of polar and subpolar marine habitats are also being affected by the melting of polar ice (Greene *et al.* 2013). Freshening and ocean acidification might affect the survival and swimming ability of pteropods, as was observed for the species *Limacina retroversa* (Manno *et al.* 2012). Other possible synergistic stressors that may affect wild pteropod populations in the future include deoxygenation, changing food availability, and stratification (Bednaršek *et al.* 2016a). Environmental effects on pteropods fitness could manifest in population scale changes.

Long-term time series of pteropods are a way to directly address whether abundances have already been declining in response to climate change. So far, the directional trends in pteropod abundances have been mixed. In the Northeast Atlantic and North Sea, *Limacina* pteropods decreased in abundance from 1958-2010, had habitat reduction, and a poleward distribution shift (Beare *et al.* 2013, Beaugrand *et al.* 2013). In the Northwest Atlantic, from Nova Scotia to Iceland, there was no significant change in the abundance of *Limacina spp.* between 1958 and 2006 (Head and Pepin 2010). Neither Georges Bank (1977-2004) nor the Mid-Atlantic Bight (1977-2009) showed declines in the abundance of shelled pteropods (Kane 2007, Kane 2011a). In the Pacific, shelled pteropods populations experienced an increase off southern California between 1951 and 2008 (Ohman *et al.* 2009). Two taxa of pteropods, the shelled *Clio pyramidata* and the shell-less *Clione limacina,* showed increases off Vancouver Island from 1979-2010 while the abundance of *Limacina helicina* declined over that time period (Mackas and Galbraith 2011). Pteropods (*L. helicina antarctica, C. pyramidata, Clione antarctica, Spongiobranchaea australis*) from near the Antarctic Peninsula did not have

significant directional trends over a 16 year dataset (Loeb and Santora 2013). For the years of 1967-2003 in the Mediterranean Sea, the assemblage of pteropods had increased in abundance (Howes *et al.* 2015).

The Gulf of Maine (GOM) has a long history of oceanographic research and is part of the Northeast Shelf Large Marine Ecosystem (NES LME), a region that is regularly surveyed by the Northeast Fisheries Science Center (NEFSC) of the National Marine Fisheries Service. Since 1977, NEFSC has been conducting approximately four cruises per year to sample hydrographic properties and zooplankton using nets as part of the Marine Resource Monitoring, Assessment, and Prediction (MARMAP: 1977-1987) and Ecosystem Monitoring (EcoMon: 1988-present) programs. This provides valuable data for the analysis of long-term trends of zooplankton taxa, like shelled pteropods, in the context of environmental change and climate forcing (Kane 2007, Kane 2011a, Morse *et al.* 2017).

The hydrography in the GOM can change from year to year depending on the water masses brought into the region which can be affected by climate oscillations and in turn affect different zooplankton taxa. The surface currents in the semi-enclosed GOM generally follow a cyclonic circulation. Deep water enters through the Northeast Channel, and also leaves at the Northeast Channel as well as the Great South Channel (Townsend *et al.* 2010). The structure of the water column is important for the mixing of nutrients to the surface. Scotian Shelf Water (SSW) is cold, low salinity, and low density surface water. Warm Slope Water (WSW) is an intermediate water mass that is relatively warm and salty. The deepest water is Labrador Slope Water (LSW), which is fresher, cooler, and carries less nutrients than WSW (Townsend *et al.* 2015). There is inter-annual variability in the composition and mixing of these water masses that may relate to climate indices including the North Atlantic Oscillation (NAO), Arctic Oscillation

(AO), and Atlantic Multidecadal Oscillation (AMO, Mountain 2012, Nye *et al.* 2014). Climate oscillations can have ecological consequences, such as regime shifts in GOM zooplankton between the relative abundance of adult *Calanus finmarchicus* and the smaller bodied copepods, like *Centropages* and *Oithona* (Greene *et al.* 2003, Greene and Pershing 2007, Greene *et al.* 2013). Climate oscillations affect the regional temperature, salinity, precipitation, wind speeds, and nutrient supply, and these bottom up factors affect plankton and therefore higher trophic levels such as fish, turtles, and whales (Greene *et al.* 2013, Nye *et al.* 2014).

Despite being the subject of study in the early twentieth century, there is much that is not known about the habitat use and population variability of *L. retroversa* (Bigelow 1924, Hsiao 1939, Redfield 1939). *Limacina retroversa* in the GOM have a lifespan of about 6 months, taking about 1 month to become a juvenile and 3 months to reach reproductive age (Thabet *et al.* 2015). Hsiao (1939) found that reproduction occurs year round for adults, which are larger than 0.85 mm in length, but peaks in May. The vertical distribution of *L. retroversa* in the GOM is mostly restricted to the upper 50 m (Bigelow 1924, Wang *et al.* 2017). Furthermore, *L. retroversa* were associated with surface layers in the Great South Channel (Gallager *et al.* 1996). *Limacina retroversa* can form dense swarms and are the numerically dominant shelled pteropod species in the GOM (Bigelow 1924). Bigelow (1924) only found a few examples of other species, *Limacina helicina*, *Diacria trispinosa*, and *Heliconoides inflatus* (formerly *Limacina inflata*), in 10 years of net sampling. Two conflicting hypotheses have been given, either that *L. retroversa* is a permanent resident of the GOM that sustains its population by local reproduction (Bigelow 1924) or that it is a transient species whose population is sustained by immigration from an offshore population (Redfield 1939). Like other zooplankton species, there might be population connectivity between *L. retroversa* in the GOM and adjacent regions, like the Scotian

Shelf, Georges Bank, and the Mid-Atlantic Bight (Kane 2007, Pershing *et al.* 2010, Kane 2011a, Morse *et al.* 2017).

In this study, the spring and fall habitat use by *L. retroversa* in the GOM was examined using time series data from 1977 to 2015. Annual abundances and distributions of *L. retroversa* were considered in the context of climate change and natural climate cycles. The following questions were addressed: 1) what are the temperature and salinity ranges, bottom depths, and proximities to the coast characteristic of *L. retroversa* habitat, 2) has *L. retroversa* declined in the GOM over the time series, 3) are multi-year cycles of *L. retroversa* abundances related to climate oscillations and their effects on the GOM, and 4) has the distribution of *L. retroversa* shifted northward over the time series in response to regional warming?

Methods

Study Region and Sampling

The ecosystem monitoring surveys (EcoMon/MARMAP) were conducted by the NEFSC using seasonal cruises (2-6 per year) to provide observations of zooplankton density, temperature, and salinity. These survey programs have been conducted for nearly 40 years. Zooplankton were collected on the surveys with obliquely towed Bongo nets with 333 μm mesh size and 61 cm diameter (area: 0.292 m^2), towed to 200 m depth or within 5 m of the bottom where bottom depth was less than 200 m. On the net was a Conductivity, Temperature, and Depth sensor (CTD) for recording depth, temperature, and salinity. The timing and exact locations of sampling varied between the years, but generally followed a random stratified sampling design. Observations in the spring months (March-April-May) were combined and the fall months (September-October-November) were combined because surveys in these seasonal

windows had the greatest spatial coverage of sampling within the GOM region (Figure 1). It is important that the spatial coverage is consistent between years in order to avoid inter-annual biases. Also, by analyzing the spring and fall time periods separately some understanding of the seasonality in the GOM can be gained. A total of 966 spring time net tows (with hydrography measurements) and 1753 fall time net tows from 1977-2015 were used to characterize the habitat of *L. retroversa* and inter-annual changes in abundance and distribution. Within the GOM, a sub-region was defined as the Cape Cod and Massachusetts Bay region (CCMB) from the latitudes of Chatham (41.65°N) to Cape Ann (42.65°N) and from the shoreline to the 100 m bathymetric contour (Figure 1). The 100 m bathymetric contour offshore of Massachusetts Bay roughly describes the position of the Western Maine Coastal Current (Geyer *et al.* 2004, Pettigrew *et al.* 2005). The CCMB acts like a trap for nutrients and fosters high productivity (Salisbury *et al.* 2009). This specific sub-region was identified as having particularly high *L. retroversa* abundance in both the spring and fall. Within the CCMB there were 70 net tows taken in the spring and 227 net tows in the fall over the time series that were used to characterize *L. retroversa* habitat within the sub-region to determine whether the patterns of seasonal habitat use differed from the whole of the GOM.

Zooplankton densities were reported as number per m^2 as well as number per m^3. Number per m^2 was chosen to best represent *L. retroversa* densities because the vertical habitat (ca. 0-50 m) of *L. retroversa* is less than the maximum sampling depth of the nets (200 m). The taxonomic resolution to which the shelled pteropods were identified varied within and between years from the level of suborder, genera, to species. Counts of Thecosomata, *Limacina spp.*, and *L. retroversa* were combined, assuming that these all represented *L. retroversa*. *Limacina retroversa* was the only limacinid pteropod reported at the species level over the time series,

which largely corresponds to information reported by Bigelow (1924). Cavoliniid pteropod species were nearly absent in the dataset, with the exception of one tow where *Creseis* spp. were caught (out of 7056), and also cavoliniid have very different shell morphologies from *L retroversa*, so would be easily differentiated during sample enumeration.

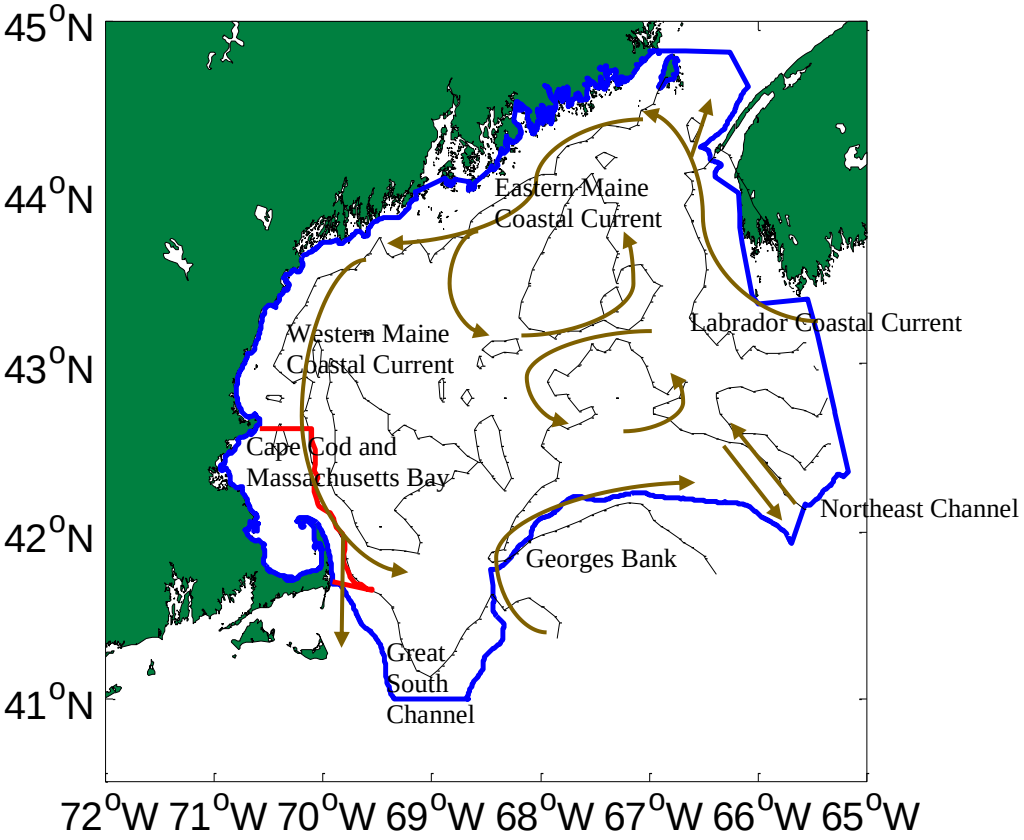

Figure 1. The study region in the Gulf of Maine. The boundaries of the Gulf of Maine are shown with the blue line, the Cape Cod and Massachusetts Bay region is shown with a red line, and the 100 m and 200 m bathymetric contour are shown with black lines. Gold arrows show the general circulation, adapted from Pettigrew *et al.* (2005).

Temperature and salinity values were binned at 1 m intervals from the surface to 50 m depth or to just off the bottom in regions shallower than 50 m, and then averaged. The bottom depth, latitude, and longitude were also recorded for each net tow. Distance to shore for each tow was calculated as the minimum distance to a coastal point defined using the full resolution Global Self-consistent, Hierarchical, High-resolution geography (GSHH) database (Wessel and Smith 1996).

Spatial distribution

Weighted means that combined data from all years were used to examine the habitat use of *L. retroversa* and were compared between seasons and regions. Weighted means were calculated for temperature, salinity, bottom depth, and distance to shore for the fall and spring seasons and for the GOM and CCMB. To calculate a weighted mean, the environmental value of interest for each net tow was multiplied by the *L. retroversa* density in that tow, these terms were summed for all the tows within a season/region, and then divided by the sum of the *L. retroversa* densities across all tows. The difference between the seasons/regions was calculated between the two weighted means. To assess statistical significance, a randomization test was used, which uses random permutations to assign the tows to either season/region and then calculates the difference of the weighted means between the seasons/regions from the arbitrary assignment. After 100,000 randomly generated permutations had each produced arbitrary differences, the proportion of these random absolute value differences that were larger than the actual absolute value difference between weighted means for a season/region was set as the test statistic (p). A difference between seasons and regions was significant if $p<0.05$.

Within a region and season, the association between whether and how many *L. retroversa* were caught with environmental conditions (i.e. temperature, salinity, and bottom depth) was examined in two steps: 1) the associations between the presence and absence of *L. retroversa* and environmental conditions, and 2) the associations between *L. retroversa* density only in those locations where *L. retroversa* were present and environmental conditions. This method addressed the fact that the data were heavily zero inflated. These tests combined data from all years to examine the habitat use of *L. retroversa* in the spring and fall and in the GOM and CCMB. A

multiple linear regression test with a logistic response term (presence/absence of *L. retroversa*) was used for each season and region with the regressors being temperature, salinity, bottom depth, year-day, and area filtered. The relationship between year-day and *L. retroversa* presence was used to control for possible distribution changes over the temporal sampling window of three months. Non-randomness in the spatial distribution of pteropods would affect the way in which the probability of presence varies with area filtered (m^2). To account for the patchiness of *L. retroversa*, area filtered raised to the power c was used as a regressor. The parameter c was then estimated by the method of maximum likelihood. To determine the relationship between the density of pteropods caught and the environmental conditions, another multiple linear regression test was used. The log-10 of the density of *L. retroversa* (#/m^2) only in net tows where they were present was tested with the regressors being temperature, salinity, bottom depth, and year-day, and using separate tests for spring and fall as well as for the GOM and CCMB. The year-day was used again to control for changes within a season that could relate to the timing of population growth, mortality, immigration, and emigration.

The plankton data and CTD data were in different databases, making it necessary to match the two records. While much of the data had little or no time or location differences between CTD and net tow records, 5 km and 48 hours were used as matching criteria to allow for small discrepancies in time and/or location, but reject larger ones. Data was excluded from spatial analysis if temperature and salinity data were missing from a net tow based on the matching criteria. Approximately 30% of the temperatures and salinities could not be matched to net tows either due to CTD malfunction or record keeping error. Most of the tows that could not be matched occurred between 1977 and 1994.

Inter-annual patterns

Annual anomalies of *L. retroversa* density, temperature, and salinity were calculated in the GOM as the annual mean for the spring or fall months minus the mean of the time series divided by the standard deviation of the time series. For this analysis, all of the net tows within the GOM for the spring or fall in a given year were combined if the spatial coverage was deemed adequate. Certain years were excluded based on insufficient sampling. To determine whether the coverage of sampling was sufficient within a given year, the region was divided into three sectors: east of Penobscot Bay (68.92°W, East), the western region north of Cape Ann (42.65°N, Northwest), and the western region south of Cape Ann (Southwest). If a year had more than 50% of sampling in the Southwest or less than 10% of samples coming from any of the three regions, then that year was excluded. The average percentage (±standard deviation) of the samples coming from each region after excluding years was: East (58±9%), Northwest (18±4%), and Southwest (24±8%). For spring *L. retroversa* anomalies, the years removed from inter-annual analyses were 1980, 1981, 1984, 1989, 1990, 1991, 1992, 2000, 2003, and 2013. In the fall, the years removed were 1989, 1990, 1991, 1992, 1993, 1997, and 2005. The time series of temperature and salinity had additional years omitted (spring: 1977, 1982, 1983, 1985, 1986, 1987, 1988, and 1993; fall: 1981, 1982, 1983, 1984, and 1988) based on the same criteria, but for the spatial coverage of the hydrography data.

A variety of climate indices were considered from 1977 until 2015 using values provided by the NEFSC. The annual NAO was taken as a wintertime average of December through March (Hurrell 1995) and the AO values were also taken as wintertime averages of December through March. The AMO value was an average of all the monthly values for a given year. The proportions of Labrador Slope Water (LSW), Warm Slope Water (WSW), and Scotian Shelf

Water (SSW) were calculated from average interpolated temperature and salinity values from 150-200 m in the deep basins of the GOM using the method described in Mountain (2012). This method uses a three point mixing triangle of temperature-salinity values of source waters to determine the proportional mixing of LSW, WSW, and SSW of water sampled from 150-200 m.

Long-term trends in spring and fall *L. retroversa* density, temperature, and salinity were examined using linear regression over the years. Correlations between the time series were evaluated with Pearson Correlation Coefficients. Since climate indices have been observed to have lagged effects on conditions in the GOM, the three climate indices were also tested for correlations with the other time series using lags of one and two years (Townsend *et al.* 2010, Greene *et al.* 2013).

Changes in the spring and fall habitat of *L. retroversa* in the GOM over time was assessed using the mean temperature, salinity, latitude, longitude, bottom depth, and distance to the coast weighted by *L. retroversa* density for each year. Long-term changes in these values were tested using linear regression. The maximum and minimum values where *L. retroversa* were present in the spring and fall were also tested to see if the bounds of *L. retroversa* habitat were changing over the time series.

Results

Spatial Distribution

Limacina retroversa were on average more abundant in the spring than the fall and were present in about half of all tows (spring=51%, fall=47%, Figure 2). The mean spring *L. retroversa* density in the GOM was 2860±540 (±standard error) per m^2, while in the fall the mean density was 1230±160 per m^2 ($t=3.61$, $p<0.001$). Between seasons, there were significant

differences in the mean weighted bottom depths, distances to shore, and temperatures (Table 1). In the fall the pteropods were more concentrated in shallow and nearshore waters in the Gulf of

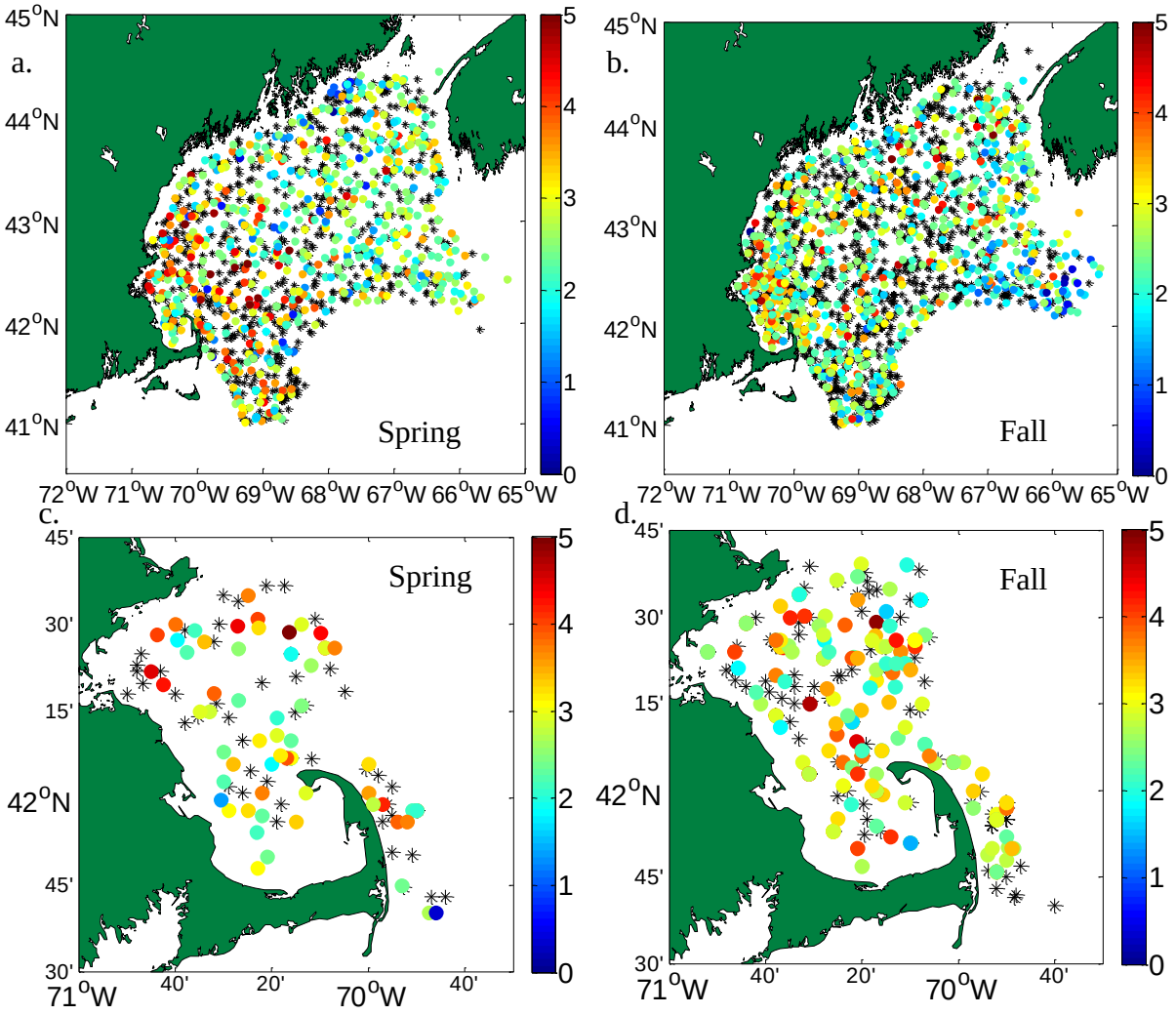

Figure 2. The location and density of *L. retroversa* net samples 1977–2015 colored by log density (# per m^2) and no catch represented with a black asterisk in a. the GOM spring, b. the GOM fall, c. CCMB spring, and d. CCMB fall.

Table 1. The mean bottom depth, distance to coast, temperature, and salinity weighted by the density of pteropods in the spring and fall ± weighted standard deviation. Differences between seasons were tested with a randomization test, and significance is indicated as * p<0.05, ** p<0.001, *** p<0.0001.

Region	Weighted Variable	Spring Mean	Fall Mean
GOM	Bottom depth (m)	162±52	134±65*
	Distance to Coast (km)	70±35	47±35**
	Temperature (ºC)	5.9±1.5	10.6±1.6***
	Salinity	32.44±0.44	32.57±0.64
CCMB	Bottom depth (m)	87±27	65.3±20*
	Distance to Coast (km)	22±10	18±10
	Temperature (ºC)	4.8±0.7	10.5±0.9***
	Salinity	32.00±0.42	31.95±0.29

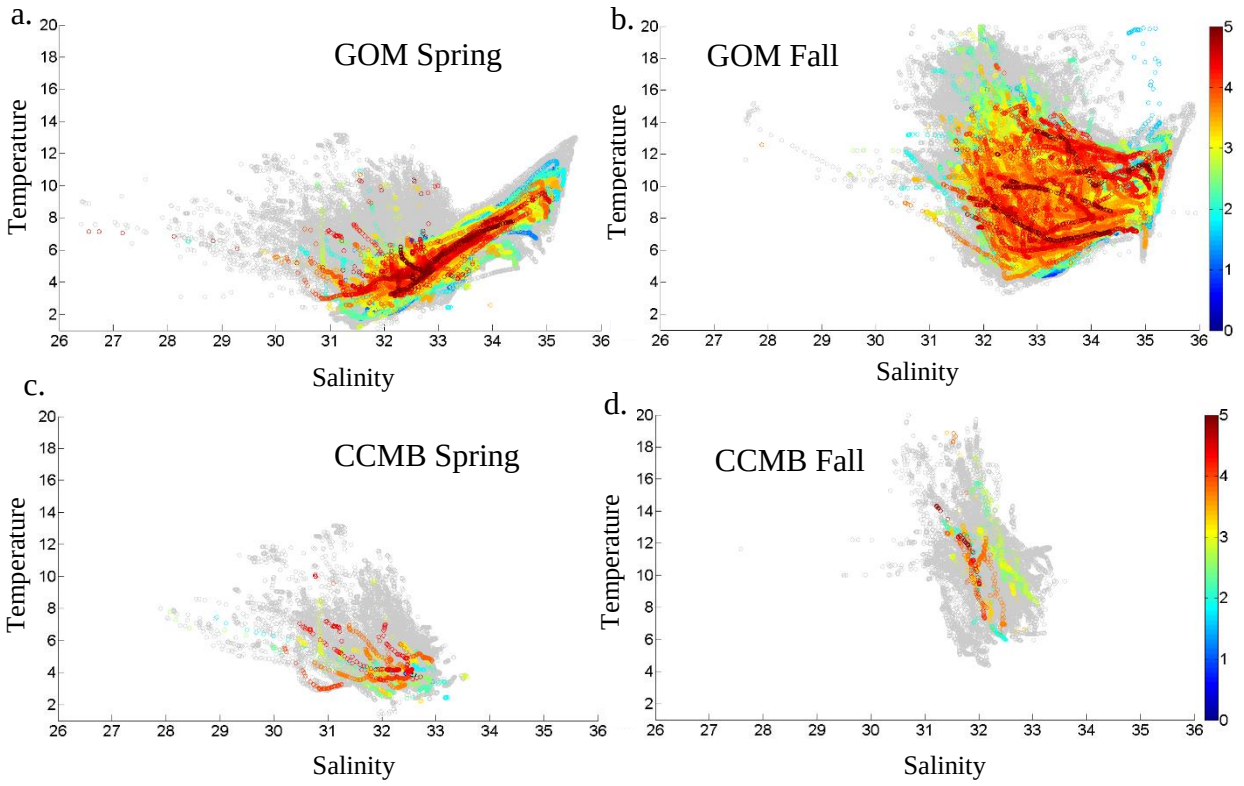

Figure 3. The temperature and salinity plots of all casts from 1977–2015 (light gray) and tows containing pteropods (colored according to the log density # per m^2). a. Spring in the GOM, b. fall in the GOM, c. spring off Cape Cod and in Massachusetts Bay, and d. fall off Cape Cod and in Massachusetts Bay

Maine (GOM, Figure 2). The salinities at which they were found were not significantly different between seasons. In the Cape Cod and Massachusetts Bay region (CCMB), more pteropods were caught on average in the spring (4050±1510 per m^2, t=0.58, p=0.56) and fall (2780±570 per m^2, t=3.20, p=0.0014) than in the whole GOM region. *Limacina retroversa* were caught in nearly two-thirds of all tows (spring 64%, fall 65%) in the CCMB.

In the spring in the GOM and CCMB, *L. retroversa* were generally found in water columns with weaker thermal gradients where the surface temperature did not exceed 8°C (Figures 3a, c). Multiple linear regression tests revealed a significant negative relationship between *L. retroversa* presence in the spring and temperature in both the GOM and CCMB (Table 2). However, the density of *L. retroversa* in the GOM was significantly positively correlated to springtime temperature in nets where *L. retroversa* were caught, in contrast to the negative correlation

between *L. retroversa* presence and temperature (Figure 4a). Overall, *L. retroversa* were associated with low salinity water in the spring. In places where *L. retroversa* were present in the GOM during the spring, significantly more *L. retroversa* were collected in waters with the mean salinity in the upper 50 m less than or equal to 33 than above 33 (≤33: 6600±1200 per m^2, >33: 370±90 per m^2, t=2.17, p=0.0306, Figure 4b). In the CCMB, higher springtime abundances of *L. retroversa* were found when the mean salinity in the upper 50 m was less than or equal to 33, but the differences were not significant (≤33: 7000±2600 per m^2, >33: 480±250 per m^2, t=0.896, p=0.375). Multivariate statistics also indicated that there was a negative correlation between the spring densities of *L. retroversa* and salinities in the tows where they were caught for both regions (Table 3). In the CCMB there was a positive relationship between *L. retroversa* density and bottom depth.

Table 2. Results for the linear regression model of the binary presence-absence of *L. retroversa* with regressors: temperature, salinity, bottom depth, year day, and area filtered. The area filtered is raised to the power c, where c is the value which minimizes the deviance of the model. The equation for the model is shown above the table. The deviances (sample sizes) of each model from top to bottom were 1284 (966), 2316 (1753), 59.65 (70), and 285.7 (227). Significance is indicated by * p<0.05, ** p<0.001, *** p<0.0001.

$$\log\frac{\rho}{1-\rho} = \beta_0 + \beta_1 X_1 + \beta_2 X_2 + \beta_3 X_3 + \beta_4 X_4 + \beta_5 X_5^c$$

Region	Season	Intercept β_0	Temp β_1	Salinity β_2	Bottom depth β_3	Year Day β_4	Area Filtered β_5	c
GOM	Spring	0.0769	-0.366***	0.0559	-0.0010	0.0018	-5.1e-08	2.8
	Fall	-0.218	0.0404	-0.185	-0.0005	0.0210***	-0.0477***	0.7
CCMB	Spring	28.4	-1.77**	-0.751	0.0286	0.0322	-0.0014	1.45
	Fall	36.9*	-0.105	-1.11*	0.0095	0.0006	-1.2e-12	6.6

Table 3. Results for the linear regression model of the log-normal response of *L. retroversa* density with regressors: temperature, salinity, bottom depth, and year day. The data only include the tows where pteropods were caught. The equation of the model is shown above the table. The adjusted R^2 fits (sample sizes) from top to bottom were 0.0756 (488), 0.0437 (825), 0.295 (45), and 0.0531 (148). Significance is indicated by * p<0.05, ** p<0.001, *** p<0.0001.

$$\log\mu = \beta_0 + \beta_1 X_1 + \beta_2 X_2 + \beta_3 X_3 + \beta_4 X_4$$

Region	Season	Intercept β_0	Temp β_1	Salinity β_2	Bottom depth β_3	Year Day β_4
GOM	Spring	12.6***	0.116*	-0.305**	-0.00052	0.0049
	Fall	0.533	0.0321	0.0697	-0.0025***	0.0028
CCMB	Spring	22.8**	0.157	-0.628*	0.0114*	0.00045
	Fall	19.1**	0.0247	-0.560**	0.00667*	0.0075

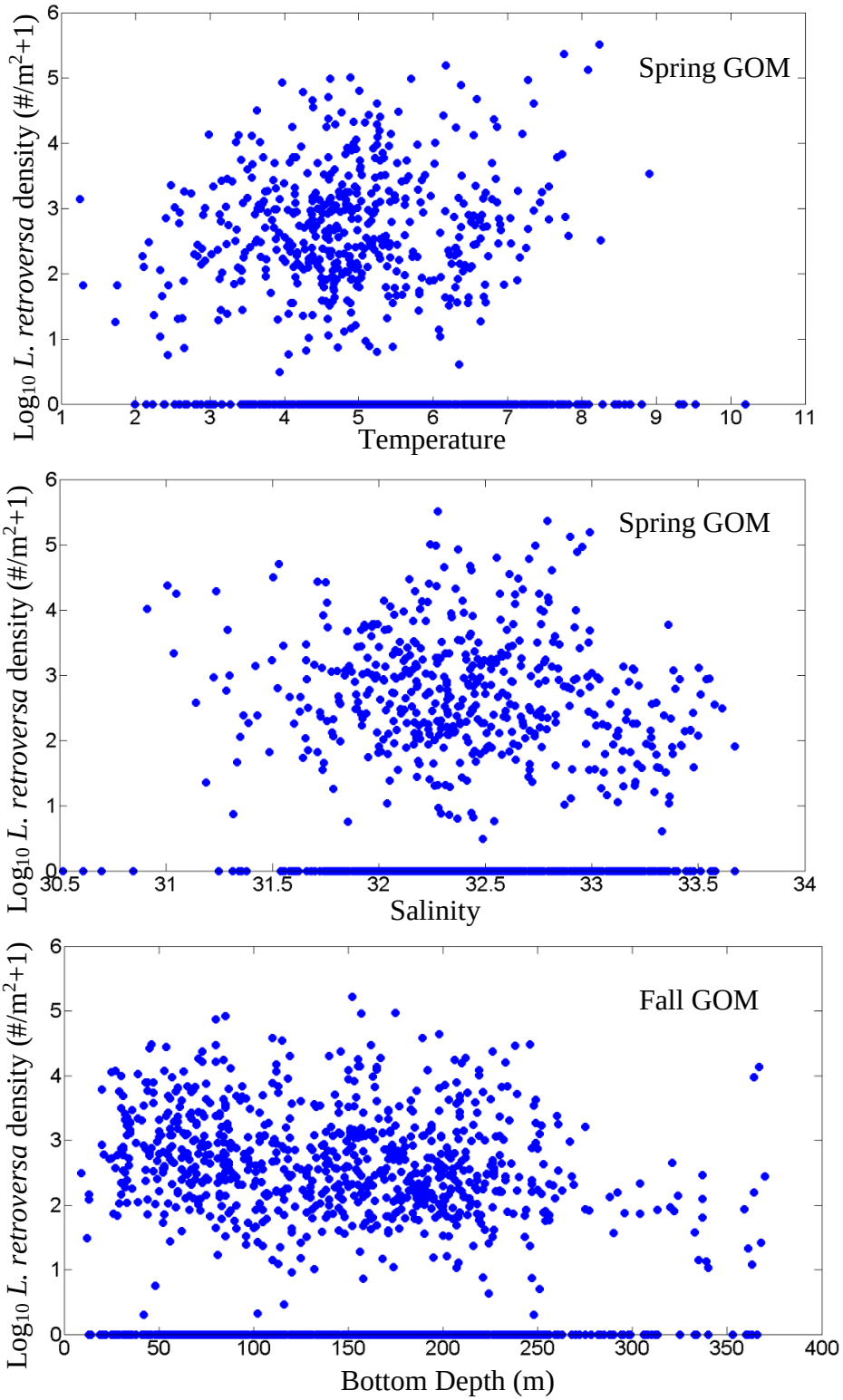

Figure 4 Plots of important relationships between *L. retroversa* and hydrography or bathymetry in the Gulf of Maine (GOM) a. Log *L. retroversa* density (# per m^2) vs. mean temperature in the upper 50 m in the spring, b. Log *L. retroversa* density vs. mean salinity in the upper 50 m in the spring, c. Log *L. retroversa* density vs. bottom depth in the fall.

In the fall, the mean weighted temperature for *L. retroversa* in the GOM was significantly lower (10.6±1.6ºC) than the available fall temperatures (11.0±1.4ºC, p=0.037). *Limacina retroversa* were less common at locations with the warmest fall surface temperatures in the GOM and CCMB (Figure 3b, 3d). Multivariate statistics indicated that there was not a significant relationship between fall *L. retroversa* presence or density (only where *L. retroversa* were caught) and temperature in either region (Table 2, 3). In the CCMB, *L. retroversa* were found at significantly lower salinities (31.95±0.29) than the average available fall conditions (32.13±0.33, p=0.012). *Limacina retroversa* presence in the fall was significantly negatively correlated with salinity in the CCMB, but not the GOM (Table 2). The fall density of *L. retroversa* (only where *L. retroversa* were caught) had a significantly negative correlation with salinity in the CCMB (Table 3). In locations in the GOM where *L. retroversa* were caught during the fall, *L. retroversa* density was negatively significantly correlated with bottom depth, indicating that abundances were greater in shallower regions, while in the CCMB the density of *L. retroversa* was significantly positively correlated with bottom depth, indicating that abundances were greater in deeper regions (Table 3). In the GOM, *L. retroversa* reached the greatest densities in bottom depths of around 80-175 m (Figure 4c), whereas the mean bottom depth of the CCMB was only about 60 m.

Inter-annual Patterns

Pteropod abundance anomalies showed cycles of high and low years, lasting between 6 and 13 years in each phase (Figure 5a, b). A directional linear change was not obvious; statistical analysis of linear trends in the inter-annual *L. retroversa* density anomalies revealed a slight significant increase in the fall densities (R^2=0.146, p=0.031) and no change in the spring densities (R^2=0.029, p=0.38). Between 1995 and 2000 there were above average densities of *L.*

retroversa in both the spring and fall. The spring *L. retroversa* densities were below average from 2002-2014, whereas in the fall *L. retroversa* densities were above average from 2009-2014. The spring *L. retroversa* abundance anomalies had a significant positive correlation to the fall *L. retroversa* abundance anomalies of the year before (R=0.447, p=0.048), but the correlation was not significant within the same year (Table 4).

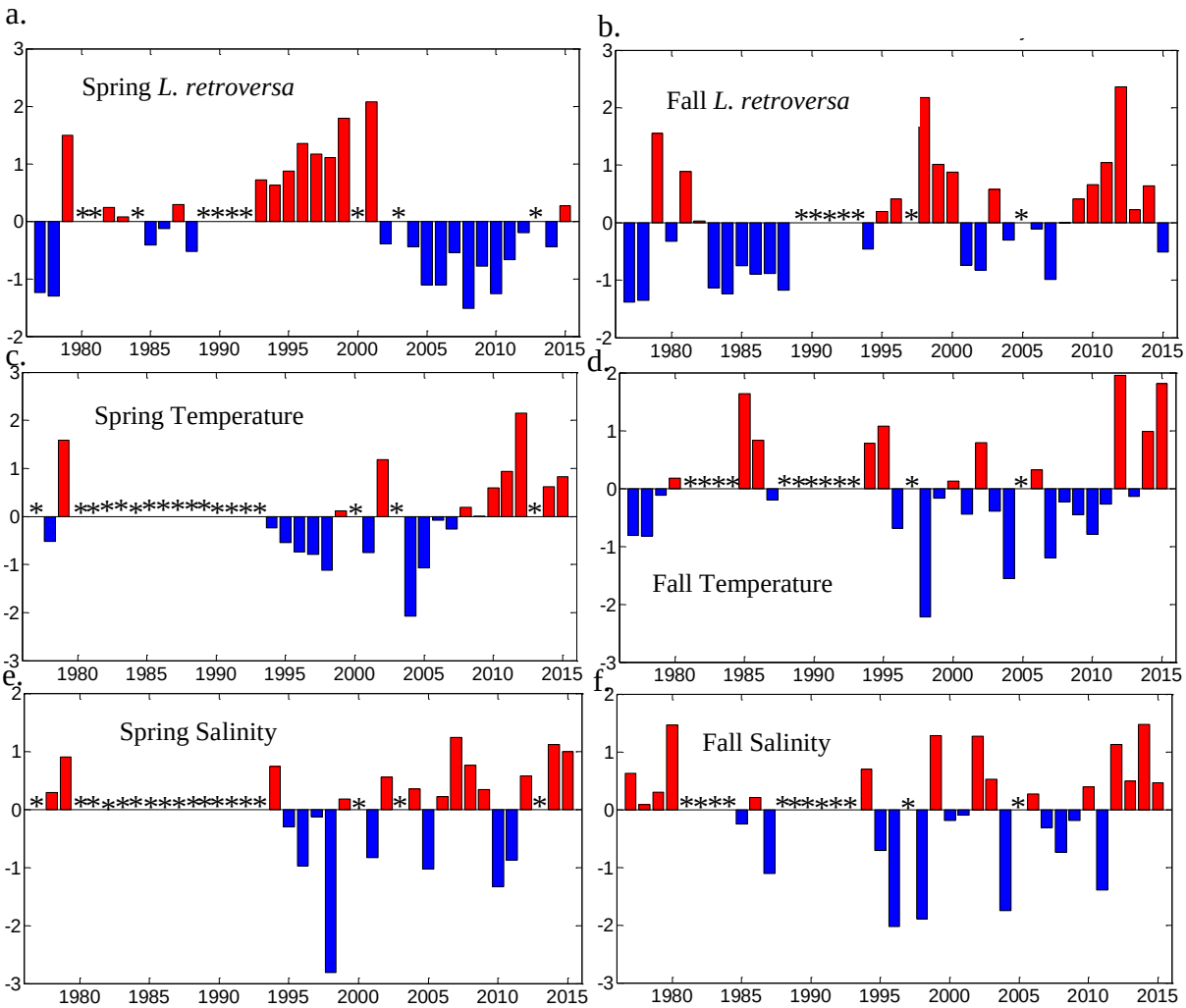

Figure 5. Annual abundance, temperature, and salinity anomalies of in the Gulf of Maine. a. Spring log abundance anomaly, b. fall log abundance anomaly in the GOM, c. spring temperature anomaly in the GOM, d. fall temperature anomaly in the GOM, e. spring salinity anomaly in the GOM, f. fall salinity anomaly in the GOM. An asterisk indicates that there was no anomaly calculated for this year due to insufficient data.

Temperature and salinity did not have significant long-term linear changes over the time series either for spring (p=0.38, p=0.80 respectively, Figure 5c, e) or fall (p=0.60, p=0.98 respectively, Figure 5d, f). The large gaps in data in the years before 1994 could affect the ability

to discern patterns in temperature or salinity. After 1994, the temperature in the spring was predominantly below average until 2010, and then from 2010 until 2015 the spring was anomalously warm. In the fall, temperatures were lowest in 1998, and then generally increased throughout the time series. The patterns in salinity are less clear, with strong reversals from fresher to more saline conditions in both seasons. The salinities from 1995 to 1998 were anomalously low, particularly 1998 in the spring.

Table 4. The Pearson Correlation Coefficients between annual time series of *L. retroversa* abundance, temperature, salinity, water mass composition, and climate indices. The spring correlations are in the upper right section of the table, and the fall conditions are in the lower left region. Significance is indicated by * p<0.05, ** p<0.001, *** p<0.0001 and is highlighted in yellow.

Spring / Fall	*L. retro.*	Temp	Sal	SSW	LSW	WSW	NAO	AO	AMO
L. retro.	0.306	-0.105	-0.199	-0.0721	-0.057	0.0904	0.0519	0.0737	-0.097
Temp	0.0292	0.652**	0.392	0.0512	-0.432	0.430	0.110	0.199	-0.122
Sal	-0.077	0.521**	0.564*	-0.010	-0.003	0.0071	0.495*	0.560**	-0.468*
SSW	-0.313	-0.005	0.216		-0.339*	-0.158	0.418**	0.333*	-0.365*
LSW	-0.062	-0.550**	-0.174			-0.88***	-0.146	-0.164	0.031
WSW	0.167	0.524**	0.107				-0.062	0.001	0.155
NAO	-0.145	0.447*	0.252					0.87***	-0.174
AO	0.0931	0.397*	0.117						-0.135
AMO	0.494**	-0.289	-0.144						

The climate indices NAO and AO were highly synchronous (Figure 6a, b, Table 4). In 1996, 2001, 2010, and 2013, there were strong reversals of the NAO and AO to the negative phase. The AMO switched from a negative phase to a positive phase in about 1995 (Figure 6c). The NAO and AO correlated positively with temperature and salinity. These correlations were significant between NAO/AO and spring salinity as well as NAO/AO and fall temperature. The spring *L. retroversa* density was significantly negatively correlated to the AMO with a 2 year lag. The fall *L. retroversa* density had a positive correlation to AMO. The AMO had a significantly negative correlation with spring salinity and was generally negatively correlated with NAO/AO, but non-significantly. However, the AMO had a significantly negative relationship with NAO when NAO was lagged by two years (R=-0.42, p=0.007).

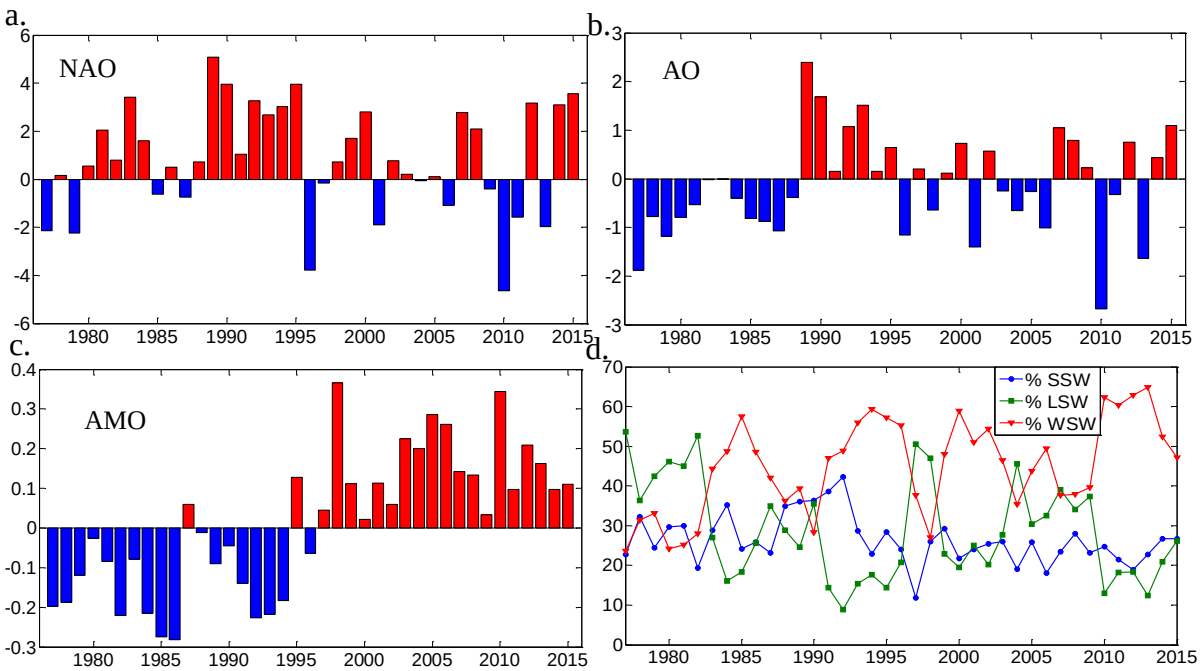

Figure 6. Annual climate indices and Gulf of Maine water mass composition from 1977-2015 showing a) the wintertime NAO index (December-March), b) the wintertime AO index, c) the annual average of monthly AMO, and d) The relative contributions of LSW, WSW, and SSW water masses to the average properties from 150-200 m depth in the GOM

Table 5. The Pearson Correlation Coefficients between lagged climate indices and the annual time series of *L. retroversa* abundance, temperature, salinity, water mass composition time series. The climate indices time series have lags of one year (-1) and two years (-2). Significance is indicated by * p<0.05, ** p<0.001, *** p<0.0001 and is highlighted in yellow.

	Spring *L. retro.*	Spring Temp	Spring Sal	Fall *L. retro.*	Fall Temp	Fall Sal	SSW	LSW	WSW
NAO-1	0.317	-0.268	0.030	-0.131	0.077	-0.215	0.331*	-0.277	0.111
AO-1	0.252	-0.284	-0.073	0.067	-0.028	-0.125	0.234	-0.240	0.123
AMO-1	-0.218	-0.045	0.007	0.345	-0.251	-0.032	-0.276	-0.011	0.159
NAO-2	0.007	-0.267	0.146	-0.540**	0.137	0.028	0.150	-0.310	0.245
AO-2	0.001	-0.354	-0.015	-0.311	-0.116	-0.091	0.207	-0.383*	0.291
AMO-2	-0.418*	0.355	0.359	0.323	0.010	0.207	-0.370*	0.006	0.194

All of the climate indices (with no lags) had significant correlations with the proportion of Scotian Shelf Water (SSW, Figure 6d). The Labrador Slope Water (LSW) and Warm Slope Water (WSW) generally corresponded to climate indices with 2 year lags, though the only significant correlation was positively between LSW and AO (Table 5). Two trends emerged from the water mass composition compared to the density of *L. retroversa*, first that there seemed to be more *L. retroversa* on the mixing line between WSW and SSW, and second that there

appeared to be greater densities of *L. retroversa* when the slope waters were proportionally more abundant than SSW (Figure 7). For the annual statistics, there were not significant relationships between the *L. retroversa* anomalies and the water mass composition in either season.

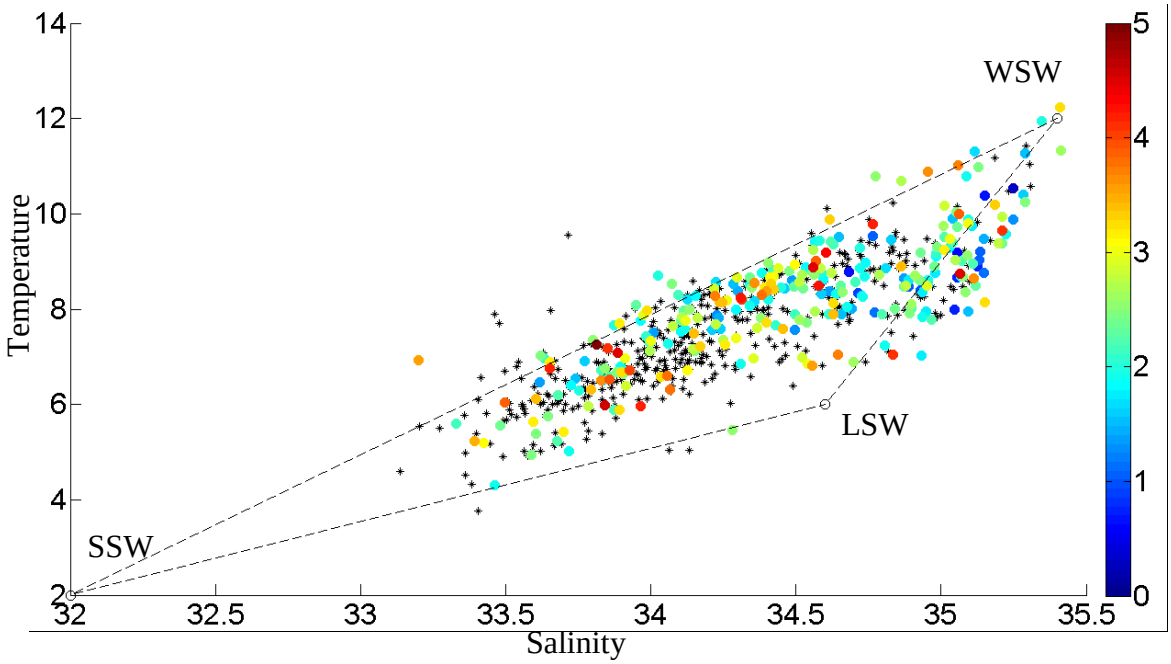

Figure 7. Temperature and salinity averages from 150-200 m from 1977-2015 colored by the log-10 *Limacina* density (# per m^2). Black asterisks show tows where no *L. retroversa* were caught. The black circles show characteristic temperatures and salinities of the end-member water masses in the GOM (Mountain 2012) and are connected by dashed lines. The proportion of water that is SSW, WSW, and LSW is calculated from each point using the geometry of the 3 point mixing triangle.

Annual weighted values of temperature, salinity, latitude, longitude, bottom depth, and distance to coast were compared over the time series using linear regression in order to evaluate whether the habitat of *L. retroversa* was changing over time. The weighted salinity by *L. retroversa* density and weighted temperature for each year did not have a significant change over the time series in either season. In the spring, no changes were evident in the distribution (latitude, longitude, bottom depth) of *L. retroversa*. In the fall, there was a slight but significant increase in the mean latitude (R^2=0.18, p=0.018), along with the minimum (R^2=0.13, p=0.045) and maximum latitude (R^2=0.24, p=0.005) at which *L. retroversa* was found within a year (Figure 8a), although this seemed to be largely affected by the years 1981and 1983, and when

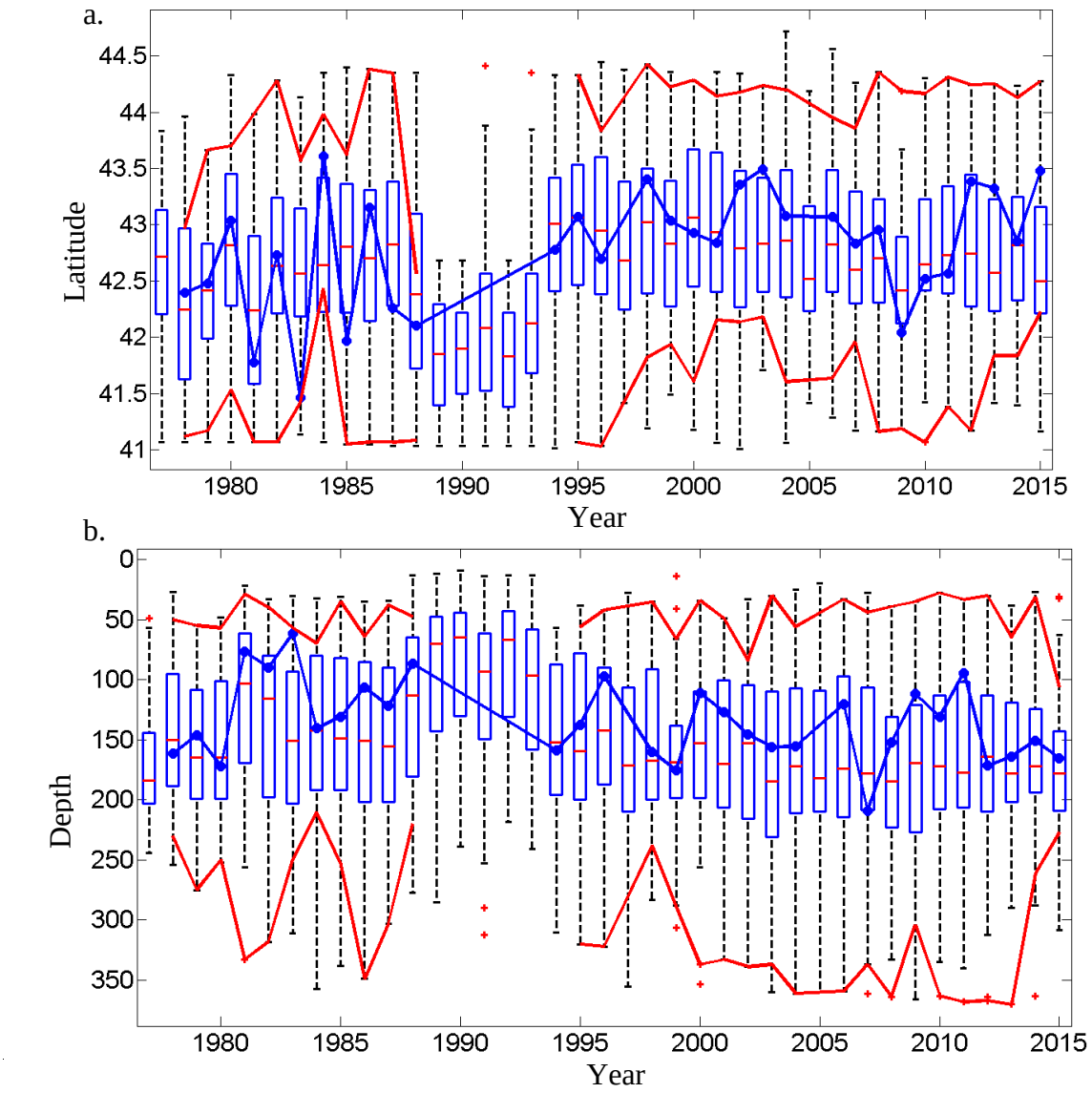

Figure 8a. Fall weighted mean latitude vs year (blue line), minimum and maximum latitudes (red lines) where *L. retroversa* were found within each year, and the sampled latitudes in each year in the box plots in the background b. Fall weighted mean bottom depth vs year (blue line), minimum and maximum (red lines), and the sampled bottom depths in each year in the box plots in the background. The box plots show the median (red line), 25th and 75th quartiles (blue lines), maximum and minimum (whiskers), and outliers (red crosses) of the total sampling effort within a year.

they were removed, the trend was no longer significant (mean latitude, R^2=0.089, p=0.12). There was a nearly significant change in the weighted mean bottom depth towards deeper waters (R^2=0.12, p=0.056), and a significant change in the maximum depth (R^2=0.0233, p=0.006) at which they were found (Figure 8b), but the trends were again not apparent when the years 1981 and 1983 were removed. In 1981, sampling seemed to be skewed towards the south and in

shallower waters. In 1983, despite good coverage of sampling, *L. retroversa* were only caught in two southern net tows, one in Massachusetts Bay and the other near the Great South Channel.

Discussion

Associations of L. retroversa with temperature, salinity, and depth

Limacina retroversa were abundant in the Gulf of Maine, particularly in the spring. The peak *L. retroversa* density (320,000 per m^2) over the time series was comparable to the peak densities in the Norwegian Sea (~300,000 per m^2, Bathmann *et al.* 1991, Noji *et al.* 1997) and more than an order of magnitude greater than the peak densities on the Patagonian continental shelf (6,800-13,600 per m^2, Dadon 1990). The highest densities of *L. retroversa* in the GOM were found in the CCMB sub-region. The CCMB may have such high abundances due to advection or population growth, or a combination of the two. This region has high regenerated nutrients and high productivity (Salisbury *et al.* 2009), and therefore it is likely to have high food (phytoplankton and small zooplankton) availability for *L. retroversa*.

In the GOM during fall, *L. retroversa* had higher densities in shallower water, with the highest density nets coming from bottom depths of around 80-175 m. In the CCMB, there was a significant positive relationship between *L. retroversa* density and bottom depth for both seasons. However, pteropods were capable of reaching densities greater than 100 per m^2 in waters as shallow as 10 m. Among the different pteropod species, *L. retroversa* was the most associated with the continental shelf in the South Atlantic (Dadon and Masello 1999). Since the multiple linear regression models were accounting for changes in temperature and salinity, the relationship between *L. retroversa* and bottom depth needs another explanation and could be investigated further. Possible ways that bottom depth might be affecting the distribution of *L.*

retroversa is through the interaction between bathymetry and patterns in advection or food availability.

Limacina retroversa is a subpolar species that favors cool waters (e.g. Chan and Bé 1964). Bigelow (1924) proposed that 18°C is an environmental barrier for *L. retroversa*, and that the optimum temperature was between 7°C and 12°C in the GOM. *Limacina retroversa* was present in the fall where the average water temperature in the upper 50 m was as warm as 15.8°C. In this study, the average upper 50 m temperature and salinity were used, while in Bigelow (1924) only the surface properties were measured. In the spring, the weighted mean temperature was 5.9±1.5°C, and *L. retroversa* were less common in the warmer water columns of GOM or CCMB. However, the effect of increased temperature on *L. retroversa* populations was mixed, since there was a positive relationship between springtime *L. retroversa* density and temperature in nets where *L. retroversa* were caught that contrasted the negative relationship between *L. retroversa* presence and temperature. In the fall, the mean weighted temperature of *L. retroversa* was significantly cooler than the available conditions, however temperature was not a significant factor in the fall presence or density multivariate models.

Significant negative relationships between *L. retroversa* abundance and salinity were reoccurring over seasons and regions: in the GOM and CCMB in the spring, and just the CCMB during fall. The weighted average salinities of *L. retroversa* were around 32.5 in the GOM and slightly lower, 32, in the CCMB during both seasons. In the spring, there was an apparent decline in *L. retroversa* catch after salinity exceeded 33. Other studies elsewhere have estimated that the optimum salinities for *L. retroversa* to be somewhat higher, >33.5 (Dadon 1990) and 34.5-35 (Chen and Bé 1964). In the GOM, Redfield (1939) stated that *L. retroversa* was found in proximity to a subsurface saline pool around a salinity of 33. Bigelow (1924) also found that *L.*

retroversa were associated with more saline conditions, and reported that they disappeared when the surface salinity was below 31.5. Salinities fresher than 31.5 were common in the spring and in during both seasons in the CCMB, and pteropods were present and abundant at these low salinities. Differences between these earlier studies of *L. retroversa* in the GOM and this one could be due to methodological differences, for example in this study an average salinity between 0-50 m was used rather than the surface value as well as the technological advancements in measuring salinity. The results of this habitat analysis were more consistent with the salinity associations of *L. retroversa* observed in more recent studies. *Limacina retroversa* in the Great South Channel were found in low salinity water between 32 and 32.4 (Gallager *et al.* 1996). In the Mid-Atlantic Bight, *L. retroversa* occupied a wide range of salinities (~31-35, Vecchione and Grant 1983), and similarly *L. retroversa* in the GOM were occupying waters where salinity ranged from approximately 31 to 34.

Limacina retroversa are likely non-migratory or have small diel vertical migrations. Knowing the exact depths at which *L. retroversa* were living would be useful for isolating the environmental conditions experienced by the pteropods. The vertical habitat of pteropods in the Gulf of Maine was assumed to be within the upper 50 m because of evidence from literature and MOCNESS sampling in the GOM (Bigelow 1924, Gallager *et al.* 1996, Wang *et al.* 2017). The surveys of *L. retroversa* were carried out with net tows that integrated to 200 m depth or less where bottom depths were shallower, therefore the tows did not provide any information concerning the depths at which the *L. retroversa* were living. Bigelow (1924) found that *L. retroversa* in the GOM was most concentrated between 20-25 m, but occasionally found at 80 m. Wang *et al.* (2017) found most *L. retroversa* to be living between the surface and 50 m. Chan and Bé (1964) found greater abundances of *L. retroversa* in the upper 10 m during the night

indicating that they were migrating. In the Norwegian Sea, large *L. retroversa* migrated between 50 and 25 m (Noji *et al.* 1997). Larger diel vertical migrations have been reported for *L. retroversa* of up to 200 m depth (Beckmann *et al.* 1987), although in this case the *L. retroversa* were in a cold core eddy and may have been migrating to stay within a certain layer in their preferred temperature range. In another study of *L. retroversa* vertical behavior in a cold core eddy, *L. retroversa* was suggested to have a reverse DVM, residing at 150 m during the night and returning to about 50 m during the day (Wormuth 1985). In the GOM and Mid-Atlantic Bight, *L. retroversa* may avoid strong density gradients, which might keep it concentrated near to the surface (Vecchione and Grant 1983, Gallager *et al.* 1996). If *L. retroversa* reside outside of the assumed depth range of 0 to 50 m or if they only associate with certain temperatures and salinities within this depth range, then the description of the *L. retroversa* habitat use in the GOM could be inaccurate. Temperatures and salinities could be different from what was reported if *L. retroversa* were migrating into deeper water, and furthermore any DVM would be accompanied by fluctuating conditions that were not considered in this examination of habitat use. Using an active acoustic system on the zooplankton surveys in the GOM might provide more precise information on the depth of the pteropods, which would be useful for improving the characterization of the temperatures and salinities in the habitat of *L. retroversa*.

The statistical analyses of habitat use suffer from certain limitations and possible sources of uncertainty, including some involved in the use of linear regressions. While linear relationships are good for avoiding the overfitting of data, some real relationships might be better fit with other non-linear equations. Future work with the habitat use of pteropods should consider using other non-linear modeling approaches. An advantage to non-linear modeling would be to identify intermediate environmental values that are optimal for *L. retroversa* presence or

abundance, since linear models will only reveal if there is a habitat bias towards low or high values.

Limitations to the use of the EcoMon/MARMAP dataset include a lack of size data for *L. retroversa* and the possibility that enumeration of *L. retroversa* was flawed due to poor preservation of the shells. The size and age structure of the *L. retroversa* over space and time would be useful for interpreting seasonal distribution patterns. With a net size of 333 µm many of the ~100 µm long veliger larvae will have been missed (Thabet *et al.* 2015). The preserved zooplankton samples from the surveys have been kept in storage, therefore it could be possible to sort the contents and measure *L. retroversa* lengths in order to gain understanding of the seasonal development of the population. There is concern that the shells of pteropods might dissolve in buffered formalin, which was the preservation method for the plankton samples. Without shells, pteropods could be unidentifiable in the samples. Rather than a complete loss of pteropod shells in a sample, there might be size selectivity with the shells of smaller individuals disappearing first. If there are many pteropods in the sample, the dissolution of some of the shells could buffer the rest of the sample. It might not be possible to discern between not catching any *L. retroversa* and only catching a few which then dissolved. If there is bias in the data, it is hopefully slight and constant. In the present study, the maximum density of *L. retroversa* in the GOM was as high as the largest value reported across other regions and there was a wide range of density values, suggesting that the preservation method was adequate for the enumeration of pteropods. This dataset has also been used by other studies to measure trends in pteropod populations in the NES LME (Kane *et al.* 2007, Kane *et al.* 2011a, Morse *et al.* 2017). Storing zooplankton samples in ethanol would alleviate this concern about the disappearance of pteropod shells. Furthermore,

ethanol preserved samples can be used for shell condition analysis between past and present pteropod population (Roger *et al.* 2011).

The timing of the cruises compared to the reproduction and growth of cohorts could be important both for assessing habitat use and examining inter-annual patterns. In most years the sampling was done over about 15 days of the 3 month time window. The maximum difference between the average sampling days for each of the years within the spring and fall sampling periods was about a month, but usually there was just a difference of no more than 10 days. The peak of reproduction of *L. retroversa* in the GOM was expected to be in the spring and the timing of the subsequent growth of this cohort to a catchable size (by 333 µm mesh) could have caused the spring to be more sensitive to the sampling year day than the fall. However the opposite was observed in the multiple regression models; the year day had a significant positive relationship between the fall presence of *L. retroversa* and sampling year day, such that *L. retroversa* were more common in the net tows of November than in September, but not in the spring. Neither season showed a significant relationship between density of *L. retroversa* (where *L. retroversa* were present) and year day. It therefore could be that in the fall, the *L. retroversa* were more common due to some dispersion of the population rather than an increase in numbers. The effects of collection timing on pteropods abundance and distribution was further complicated by inter-annual differences phenology, such as the timing of the spring bloom, which were not accounted for in the analyses. Using satellite based sensing, it might be possible to relate changes in the *L. retroversa* population to the timing of the spring or fall blooms.

Inter-annual changes in the L. retroversa population in the Gulf of Maine

Overall, there was no evidence of a decline in pteropod abundance that might be expected if climate change, including ocean acidification, was presently affecting the regional *L. retroversa* population. Instead, there was a slight but significant increase in the fall pteropod densities in the GOM over the time series and no significant directional change to the spring pteropod densities. Similarly, long-term changes were not seen for *Limacina spp.* to the Northeast of the GOM, which spanned a region from the Scotian Shelf, past Newfoundland, all the way to 25°W 65°N (Head and Pepin 2010). Also, pteropods on Georges Bank or Mid-Atlantic Bight did not exhibit long-term directional changes (Kane 2007, Kane 2011a). Near the Antarctic Peninsula the pteropod species did not show significant declines (Loeb and Santora 2013) and in the Mediterranean there was also no evidence of declining pteropods (Howes *et al.* 2015). Only in the North Sea and Northeast Pacific was there evidence of *Limacina spp.* declining (Mackas and Galbraith 2011, Beare *et al.* 2013, Beaugrand *et al.* 2013). These studies have shown that there has been regional variability in the abundances trends of pteropods over time, and currently there are not clear results that pteropod populations are declining at the global scale.

Recent years have been particularly warm in the GOM, yet the pteropod population did not appear to be negatively impacted. The mean global sea surface temperature has increased by about 0.7°C over the past 100 years (Gruber 2011). There was not a significant long-term trend in the GOM temperatures in spring and fall from 1977 to 2015, but this could be affected by missing data in many years. The surface temperature in the GOM has been reportedly increasing over the past 50 years (O'Brien *et al.* 2013). Considering the available habitat in the GOM, pteropods seemed to be mostly absent from the warmest surface waters in the spatial analysis, but relationships between the inter-annual abundance and temperature anomalies were not

significant. Although the population did not have an observable decline in response to warming, if the GOM continues to warm it might elicit a response in the *L. retroversa* population.

Associations between *L. retroversa* and temperature or salinity could manifest via effects on growth, reproduction, and survival. For instance, temperatures had a significant effect on the mortality of *L. retroversa* when elevated from 2°C to 7°C (Lischka and Riebesell 2012). In the GOM during spring, fewer pteropods were found where surface temperatures reached 7°C, but in the fall *L. retroversa* are often found at this temperature. Manno *et al.* (2012) found that low salinity and low pH had a combined effect of increasing the mortality of *L. retroversa*. They also found that low pH and salinity both affected shell condition, but that pH had a stronger effect. The study by Manno *et al.* (2012) may put a lower limit to the tolerance of *L. retroversa* at a salinity of 28, which was lower than what was usually found in the GOM. Seasonal acclimatization and regional adaptation may lead to differences in the environmental tolerances of a pteropod species.

Salinity affects seawater density, which in turn could affect water column stratification and the food supply for pteropods (Geyer *et al.* 2004, Townsend *et al.* 2010). There was a negative correlation between the springtime *L. retroversa* abundance anomaly and salinity which was not significant, but could be real since the habitat analysis also showed a significantly negative association between *L. retroversa* and salinity. In the fall, there was an indirect link between *L. retroversa* and salinity through the AMO and the 2 year lagged NAO, with positive relationships between abundance anomalies and the phases of these climate oscillations that bring low salinity water into the GOM. After NAO was lagged by 2 years, there was a significant negative relationship between AMO and NAO. Kane (2011b) found that a two year lag was appropriate for NAO and that no lag was necessary for AMO when examining a time series of

the phytoplankton abundance in the GOM. The salinity in the GOM is largely driven by the strength of the Labrador Current and its position along the continental margin relative to the position of the Gulf Stream, and is influenced by climate oscillations (Greene and Pershing 2007, Nye *et al.* 2014, Townsend *et al.* 2015). The cool Labrador Current brings fresher water into the GOM, accounting for about half of the freshwater input, with rivers contributing the other half (Townsend *et al.* 2010). Greene *et al.* (2013) hypothesized that fresher conditions in the Gulf of Maine would promote stratification and extend the phytoplankton growing season in the fall, which in turn would be beneficial for the feeding of many zooplankton species. The extent to which stratification and mixing is beneficial or detrimental to the pteropod population may depend on the timing of these processes. Fresher conditions appeared to be advantageous to the *L. retroversa* population in both the spring and the fall, with a stronger direct link during the spring and a climate driven response in the fall. The nature of the relationships between *L. retroversa*, salinity, stratification, and primary production should be investigated further.

Greene *et al.* (2013) found that some freshening events were not tied to the NAO and AO, but instead could have been related to an increased melting of Arctic sea ice, which created freshwater pulses. Such pulses are evident in the time series. A freshwater pulse reached the GOM in 1991 (Greene *et al.* 2013) and although there was a gap in the dataset for the whole GOM region, in the CCMB these years were characterized by low salinity and anomalously high abundances of *L. retroversa* (supplemental material, Figure S1). Another large pulse of freshwater arrived in the GOM 1998 and during this time there were again high *L. retroversa* densities. Unlike 1991, this freshwater pulse could be accounted for by an especially low NAO two years before.

Limacina retroversa abundance anomalies did not show strong inter-annual correlations with water mass composition. The NAO and AO seemed to influence the slope waters with a lag of 2 years and with no lag for the SSW. During a positive phase of NAO and AO, the Gulf Stream shifts northwards and WSW displaces LSW near the continental slope bringing warmer and more saline water through the Northeast Channel, while during a negative phase of NAO and AO the LSW is more prominent adjacent to the continental shelf and extends further south (e.g. Greene *et al.* 2013). Mountain (2012) proposed that the relationship between LSW and NAO (with a 2 year lag) becomes weaker after 1995, but that is not evident in this time series. The AMO did not seem to relate strongly to the slope water composition with the exception of having a significant negative relationship with SSW. Although there were not clear correlations between *L. retroversa* abundances and the water masses that move into the GOM, the water masses can alter conditions in the GOM and affect the growth of the *L. retroversa* population or affect the advection of *L. retroversa* into the GOM.

A range shift was observed for the fall *L. retroversa* with a significant northward movement over the years, however the results may have been an artifact caused by the data in two years with atypical and limited sampling. Beare *et al.* (2013) found that the distribution of *Limacina spp.* in the North Sea was moving northward as well as contracting. Nye *et al*. (2009) found that fish stocks were migrating north only in the Mid-Atlantic and South-Atlantic Bight. In the Gulf of Maine there was not such a poleward shift, but instead a distributional shift of fish taxa towards deeper water. Similarly, there was a nearly significant shift towards deeper water in the fall time series, but again could be an artifact caused by the same two anomalous years. Unlike nekton, pteropods have limited directed swimming, and changes to the distribution may be largely controlled by circulation or by changes in reproduction and mortality.

Changes in one taxon could be associated with changes to other members of the zooplankton community with impacts on higher trophic levels, including commercially harvested species (Pershing *et al.* 2010, Greene *et al.* 2013). *Limacina retroversa* in the Northwest Atlantic have shown strong positive correlations to the small and medium bodied copepods (i.e. *Centropages typicus*, *Metridia lucens*, *Oithona spp.*, and *Paracalunus spp.*), with cycles that can be explained in part by the NAO (Kane *et al.* 2007, Kane *et al.* 2011a, Morse *et al.* 2017). Top down control (predator grazing) was not incorporated into this study, but could affect the distribution and inter-annual abundance changes of *L. retroversa.* In the Northwest Atlantic, predators of pteropods include mackerel (Ackman *et al.* 1972), cod (Levasseur *et al.* 1994) and bowhead whales (Pomerleau *et al.* 2012), and likely others.

In sum, *L. retroversa* in the GOM did not show evidence of being adversely affected by a changing environment. Instead, *L. retroversa* had population cycles that may relate to increased productivity, the favorability of conditions for pteropod physiology, advection, or top down control. All of these factors could be affected by climate change. It is important to continue monitoring marine systems with long-term observations to investigate how climate variability and anthropogenic climate change might affect pteropods and other marine species.

Supplementary Materials

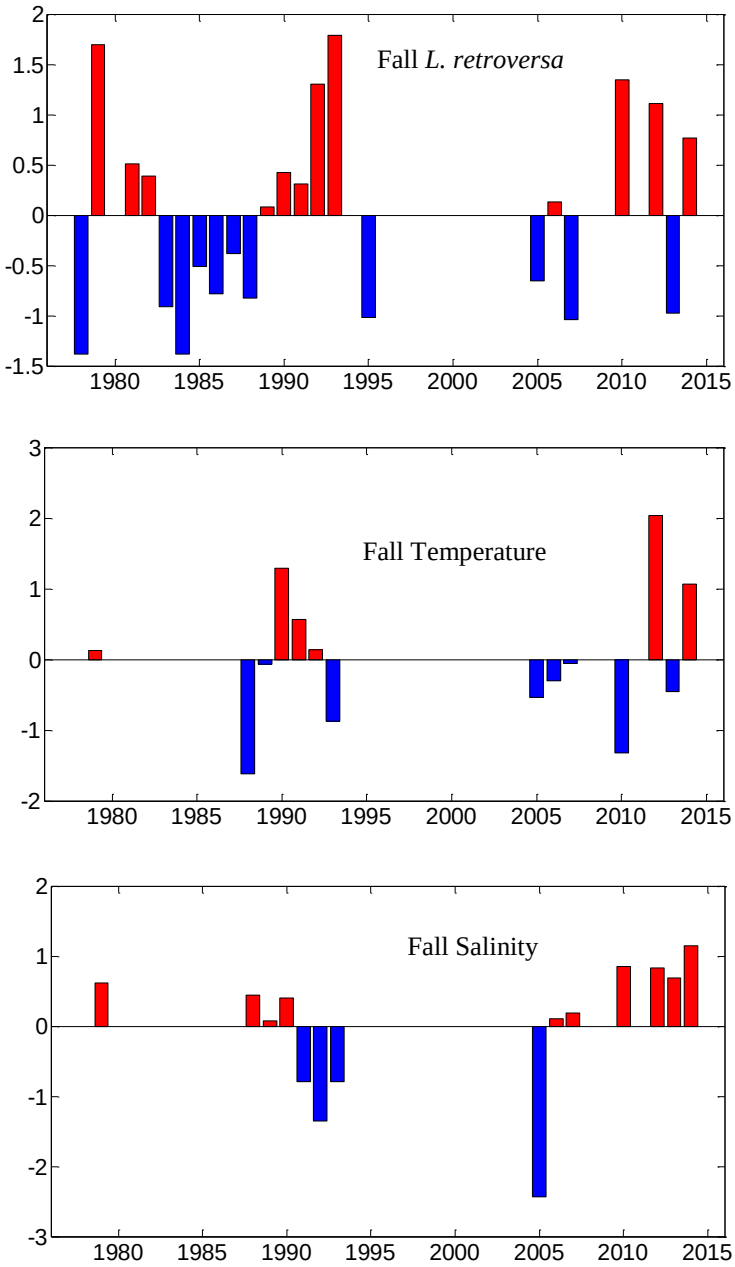

Figure S1. Annual anomalies in *L. retroversa* abundance, temperature, and salinity from fall months in the CCMB. a. Abundance anomaly, b. temperature anomaly, and c. salinity anomaly. Only years with 5 or more observations in the CCMB are shown.

Chapter 5

Conclusions

Laboratory experiments with elevated carbon dioxide (CO_2) have shown that pteropod shells begin to dissolve at concentrations of dissolved CO_2 expected in the surface ocean by the end of the century (Comeau *et al.* 2009, Comeau *et al* 2010a, Lischka *et al.* 2011, Bednaršek *et al.* 2012a, Comeau *et al.* 2012a, Lischka and Riebesell 2012, Bednaršek *et al.* 2014b). However there is uncertainty about the real world consequences of ocean acidification to pteropods, such as how individual fitness and population dynamics could be affected. The possibility of specificity in the responses of different pteropod species to ocean acidification is also important to consider when extrapolating from one species to the broader taxon, but relatively little research has been done on this topic. There is also the need for more research concerning whether pteropods have already been suffering from the effects of ocean acidification and other environmental change in the modern ocean. This thesis was motivated by these gaps in knowledge, and more specifically I aimed to 1) identify possible fitness effects of ocean acidification on pteropods, 2) investigate the response of wild populations of pteropods to regional variability in aragonite saturation state (Ω_A), 3) examine a time-series dataset to determine whether population scale changes have already occurred in the Gulf of Maine, and 4) describe how local conditions affect the presence and abundance of pteropods. Additionally, I developed more quantitative tools to allow for the assessment of pteropod shell condition and locomotion that can facilitate comparisons between species, regions, and future studies. In this chapter, I will relate my findings to the goals of this thesis while addressing limitations and avenues for future work.

Pteropod Fitness and Ocean Acidification

The fitness of pteropods could be affected by ocean acidification via changes in appearance and locomotion, which might make pteropods more susceptible to predation. In the present work, the shells of *Limacina retroversa* became less transparent after exposure to elevated CO_2. More transparent shells might be advantageous for reducing visibility to visual predators, such as fish (LeBrasseur 1966, Ackman *et al.* 1972, Levasseur *et al.* 1996, Pakhomov *et al.* 1996, Armstrong *et al.* 2005, Hunt *et al.* 2008, Sturdevant *et al.* 2013). A loss of transparency could affect open ocean camouflage and lead to higher mortality due to predation. The sinking rates of live *L. retroversa* were slower after exposure to elevated CO_2. Sinking may be a predatory evasion behavior for pteropods, and slower speeds may make them easier to capture. Changes to predator-prey relationships could be an indirect effect of ocean acidification. A future avenue of research might be to directly test whether the susceptibility of pteropods to predators is affected after exposure to elevated CO_2. This might be accomplished by combining shelled pteropods exposed to different concentration of CO_2 with visual predators (e.g. small fish) or non-visual predators (e.g. gymnosome pteropods) in feeding experiments in order to measure the consumption rates and assess the efficacy of the anti-predator behaviors of pteropods.

Changes were observed in the sinking rates of *L. retroversa* after exposure to elevated CO_2 that could have been caused by observed differences in shell condition. Three explanations could explain why pteropods sink more slowly after exposure to elevated CO_2: the shells could be less dense, thinner, or have increased roughness that affects the shell's hydrodynamics. Howes *et al.* (2017) speculated that there is not enough shell production or loss during acute

periods of pteropod exposure (≤4 weeks) to change the density or thickness, and hence mass, of a shell even in under-saturated conditions. Furthermore, I did not observe differences between the masses or the mass/length ratios of individuals between the treatments from the April 2015 experiment. I conducted preliminary investigations into the thickness of *L. retroversa* using micro-computed tomography (micro-CT) after 7 days of exposure to ambient and high CO_2 levels. I did not observe clear differences in shell thickness between the treatments, albeit with only two individuals per treatment. Imaging the shell with scanning electron microscopy revealed that the *L. retroversa* had rougher shell surfaces in the elevated CO_2 treatments due to dissolution, consistent with other studies (Lischka *et al.* 2011, Bednaršek *et al.* 2012a, Bednaršek *et al.* 2014b, Peck *et al.* 2016). I propose that this roughness of the surface makes the shells less transparent and is responsible for slowing the sinking rates of individuals from the elevated CO_2 treatments. However, it is also possible that discoloration of the shell is the result of changes to the organic matrix in the shell, assuming that the organic material imbedded in the shell is not removed during the 24–48 hour soak in bleach. Byrne *et al.* (1984) described a different link between sinking rates and shell condition and attributed slower pteropod sinking rates to bulk loss of aragonite due to dissolution, which leads to a reduction in mass. Bulk dissolution might be an important factor controlling the post mortem sinking rates of shells whereas the roughness of the surface might affect the sinking of live animals while they live in the upper ocean. Additional studies using micro-CT and more sophisticated video analyses of sinking shells (i.e. particle image velocimetry) could be used to further examine the relationship between shell condition and sinking rates.

Swimming ability appeared to be mostly unaffected by enhanced CO_2. The differences between speeds, wing beat frequencies, and path tortuosity between treatments were not

consistent across experiments, were only occasionally significant, and generally were not significantly different during the later weeks (two and three weeks). It is possible that large individual ability in swimming performances masked an effect from elevated CO_2 or that longer exposures to elevated CO_2 would have elicited a treatment effect. If there were to have been a directional change in swimming speed, it could hypothetically be towards faster or slower speeds under elevated CO_2. Decreased calcification and increased dissolution might lead to lighter shells which could reduce the effort of swimming and possibly increase the speed in higher CO_2 conditions. Another possibility is that changes to the ballast of the shell could disrupt the ability of pteropods to rotate the shell between the power and recovery strokes, leading to slower and less efficient swimming (Murphy *et al.* 2016). The stress of low pH (acidosis) might reduce the physiological health of the pteropods and therefore reduce swimming speed. Alternatively, swimming ability might only respond to changes in CO_2 (and pH) when synergistic stressors are present such as changes in salinity (freshening) as was found in another study (Manno *et al.* 2012). In this case, swimming speed decreased while mortality increased in treatments that had reduced pH and reduced salinity in combination, which suggests that slowed swimming might be a response that precedes death. The authors speculated that reduction in salinity affects the seawater density, which affects the swimming ability of the pteropods. This has implications for pteropod swimming in the context of the real density gradients that exist in the wild.

One limitation of laboratory experiments is that the health, physiology, and behavior of the pteropods can be affected in captivity. Experiments with pteropods can only accomplish acute exposures durations because of the limited amount of time that pteropods remain alive and healthy in a laboratory setting. In the wild there is a lifetime of exposure to *in situ* conditions. The drawback of acute exposures is that we might miss real consequences of environmental

change that take a long time to manifest. The lack of a clear swimming response to elevated CO_2 might also relate to the overall attrition of pteropods in captivity, which seemed to be largely stochastic across the treatments and replicates. Whenever possible, multiple independent pteropod experiments should be executed in order to assess whether differences in organismal responses are consistent between experiments or whether they might be spurious.

As our culturing ability improves, so can the complexity or our experiments. In the experiments that I conducted with *L. retroversa,* the pteropods were given ample concentrations of algal food. A future study could vary the food concentrations along with the concentrations of CO_2 to see if food availability modulates the effect of Ω_A on shells and locomotion. Next, experiments that examine the shells, sinking, and swimming of pteropods should be conducted with species with different shell morphologies to understand how the fitness of other species might respond to ocean acidification. It will also be important to improve the control of the carbonate system in the experiments. Small differences in Ω_A could be affecting the present observed responses of shells and locomotion, particularly in the medium treatment since Ω_A=1 might be an important threshold for pteropods. With more precise control of Ω_A, experiments could be conducted that vary Ω_A and temperature on daily schedules to mimic the fluctuating conditions experienced by a vertically migrating pteropods. Additionally, changing a treatment from low Ω_A to high Ω_A could reveal whether the shells and sinking of pteropods can recover after exposure to elevated CO_2.

Additional behavioral experiments or *in situ* imaging systems could be ways to investigate further the swimming of pteropods and whether it is affected by ocean acidification. The swimming cues for pteropods are not known, such as whether or not pteropod swimming is affected by light or physical and chemical gradients. Future experiments could try to control for

these factors and in particular investigate how pteropods behave in density stratified tanks. Since laboratory experiments currently depend upon confining pteropods with rigid boundaries, observations of *in situ* behavior could be more revealing. This could be accomplished with imaging systems designed for mesoplankton, such as the video plankton recorder or a system that can image an animal over successive frames.

Another behavior that has been relatively under studied is the feeding of pteropods with mucous nets. Mucous nets have not been observed with laboratory experiments, and therefore may benefit from *in situ* imaging techniques. When pteropods have been observed with mucous webs, the pteropods reportedly hang nearly motionless without sinking or swimming (Gilmer and Harbison 1986). Understanding the alternation between feeding, sinking, and swimming behaviors could help with constructing an energy budget for wild pteropods and identifying the fitness effect of ocean acidification.

Shells from Wild Populations of Pteropods

Regional variability in the dissolution of the shells of wild *Limacina helicina* and *Clio pyramidata* from the open ocean was observed but did not seem to be strongly correlated to Ω_A. The patterns that I observed in the shell condition of *C. pyramidata* were consistent with regional differences in Ω_A, but the differences were not significant, possibly due to large individual variability and relatively small sample sizes. The samples sizes used in this study were between 7 and 12 to facilitate a large number of comparisons, including across sizes and depths for *L. helicina*. Similar sample sizes have been used in other studies concerning regional differences in shell condition, yet in those studies large and significant differences in shell condition were observed (Bednaršek *et al.* 2012b, Bednaršek *et al.* 2014a, Bednaršek and Ohman 2015, Johnson

et al. 2016). The other studies were conducted in upwelling coastal regions, which might result in larger differences in Ω_A and more pronounced shell condition patterns. Larger sample sizes are recommended for examining *in situ* shell condition where differences might be slight or individual variability might be large.

The shell condition of *L. helicina* had more complicated spatial patterns that could not be explained only by Ω_A. The *L. helicina* shells from below 200 m depth where the Ω_A was substantially below one were dissolving as was expected. However at intermediate Ω_A (ca. 1.7–2.4), the shell condition of *L. helicina* was quite variable. It is possible that shell construction and maintenance is not hindered for this species at this range of Ω_A. Other studies of *in situ* dissolution of pteropods were conducted in regions where coastal upwelling decreased the Ω_A beyond what I observed in the upper 100 m of the open ocean sites. For *L. helicina antarctica*, dissolution was prominent for wild-caught individuals at Ω_A from 1–1.2 (Bednaršek *et al.* 2012b, Johnson *et al.* 2016). In the upwelling coastal region along the U.S. West Coast, the surface Ω_A drops as low as 0.8, and dissolution on *L. helicina* was clearly related to the percent of the water column (0-100 m) that was under-saturated (Bednaršek *et al.* 2014a). In another study that used depth-stratified pteropod sampling, the authors found that dissolution was most pronounced near the saturation horizon (Ω_A<1.2), but some dissolution was still found where Ω_A was ~2 (Bednaršek and Ohman 2015). In the present study, shell condition was apparently reduced in two different regions (47°N and 45°N) where *in situ* Ω_A ~2, yet at lower Ω_A (1.68) the shells were in better condition. These patterns suggest that the shell condition of *L. helicina* is not simply determined by Ω_A when Ω_A>1.7 and that other factors could be affecting the variability in shell condition.

Food availability is a potential variable that could explain some of the spatial patterns in the shell condition of *L. helicina*. Regional differences in shell conditions of wild caught *L. helicina* were similar to patterns in fluorescence which is an index of chlorophyll concentrations. Generally, fluorescence values and shell condition of *L. helicina* had a positive relationship at the four North Pacific sites. For pteropods, food availability has been observed to modulate the physiological response of pteropods to ocean acidification (Siebel *et al.* 2012), and the effects of food availability on calcification has been observed for corals and mussels (Langdon and Atkinson 2005, Cohen and Holcomb 2009, Melzner *et al.* 2011, Drenkard *et al.* 2013, Thomsen *et al.* 2013).

Earlier life stages of pteropods may be more vulnerable to shell dissolution than adults. A significant relationship was observed between shell condition and the size of *L. helicina*, where the individuals with shell lengths larger than 1 mm had better shell condition and less variability than the smaller size class. This size dependency was fairly slight and should be tested in lower Ω_A environments. Laboratory experiments can also be used to compare the shells of different sized pteropods under the same conditions. One experiment did this, comparing adult and juvenile *L. helicina* shells after 14 days at transitional Ω_A (~1) and observed slightly less dissolution on the shells of adults (Bednaršek *et al.* 2014b). Larger organisms may be more efficient at feeding or have larger energy reserves that allow them to allocate more energy towards shell maintenance (Lischka *et al.* 2011). If the shell condition improves throughout the development of a pteropod into an adult, this indicates that shell repair is taking place. Evidence of shell repair was observed during the calcein staining experiments with *L. retroversa* and in another study using *L. helicina* (Lischka *et al.* 2011). Alternatively, pteropods with poor shell condition might be selectively removed from the population, possibly due to predation, leading

to an adult population with good shell condition. Future studies should account for size based differences in shell condition within a species.

Variability in shell condition could occur on fine spatial or temporal scales, which might be a source of uncertainty when trying to describe regional differences. Large differences were measured in the shell conditions of *L. helicina* caught at the same depth range (25-50 m) and the same broad region (47°N) between tows that were about 10 km and 11 hours apart. Although there was a day/night difference in the timing of the tows, the pattern in shell dissolution was not consistent with the expectation that a diel vertical migration (DVM) would bring *L. helicina* with greater shell dissolution into the surface layers at night since the shell condition was actually much lower during the day. It may be necessary to conduct more spatially extensive shell sampling to adequately characterize regional differences. Nearby groups of *L. helicina* could have had different shell conditions due to different histories of environmental conditions or feeding histories. The *in situ* conditions that an individual experiences are dependent upon its trajectory through the ocean, which is mostly controlled by ocean currents. While ocean circulation modeling was outside of the scope of this thesis, future work should consider constraining the location of pteropods using hind-cast ocean modeling.

Uncertainty about the vertical migratory behavior of these species makes it difficult to know what Ω_A they actually experience and for what proportion of the time. The DVM is fairly uncertain for *L. helicina* and *L. retroversa*, with suspected forma differences in the DVM of *L. helicina* (McGowan 1963) and reverse diel vertical migratory behavior observed for *L. retroversa* only during part of the year (Wormuth *et al.* 1985). Even within a vertically migrating pteropod population, such as *C. pyramidata*, individuals may travel to different depths during the day, which could cause individual variability in shell condition within a region. In this work,

some of the variability in shell condition within a location could be due to individual differences in environmental history stemming from different migratory habits. Region-specific information on the DVM of pteropods could improve our understanding of the conditions experienced by pteropod populations. By engaging in a diel vertical migration, pteropods will experience environmental fluctuation on daily cycles. There is evidence from $\delta^{18}O$ measurements of pteropod shells, that the shells of migrating species are mostly produced in the surface layer, where temperature is higher and Ω_A is higher (Fabry and Deuser 1992). Periodic relief from low Ω_A might be important for vertically migrating species to maintain shells, although this has not yet been tested.

In the *L. retroversa* experiments, seasonal differences were observed in the shells of the ambient treatments that might relate to the temporal changes of *in situ* Ω_A, with lower shell condition in months when the Ω_A was lower. These shells were assessed after four days in captivity at the ambient CO_2 concentration. The next step is to examine shell transparency using *L. retroversa* that were preserved immediately after capture during the seasonal cruises. There was no evidence of differences in the sensitivity of *L. retroversa* shells to elevated CO_2 between seasons but it is hard to draw definitive conclusions because of differences in the carbonate chemistry between experiments. Improved control over the carbonate parameters in the treatments would be needed to ascertain if the magnitude of the response of *L. retroversa* to elevated CO_2 varies seasonally.

Investigating how the shells of live pteropods might be affected by ocean acidification can be done with individuals from laboratory experiments or with wild-caught individuals, and both are important tools. With laboratory experiments, I was able to simulate the effects of ocean acidification in the future, while with the *in situ* examination of pteropod shells, I was able to

address the sensitivity of pteropod species to variability in current conditions. In the surface layers of the open ocean, the differences in Ω_A (ca. 1.6–3.3) corresponded to slight differences in the shells of *C. pyramidata*, and Ω_A (ca. 1.7–2.4) did not have a clear effect on the shells of *L. helicina*. By the end of the century, the Ω_A in the upper 200 m is projected to decrease between 0.2–1.9, depending on the region (Comeau *et al.* 2012c). Therefore, *C. pyramidata* and *L. helicina* in the North Pacific may experience threshold or under-saturated Ω_A near the surface by the end of the century and ocean acidification could cause these pteropods to exhibit dissolution similar to what was observed on the shells of *L. retroversa* after exposure to elevated CO_2. Dissolution of the shell could affect the locomotion of pteropods, visibility to predators, or have other fitness consequences. On the population scale, large decreases to Ω_A are likely to negatively impact pteropods. More work is needed before we can predict when and where possible changes to pteropod shells and populations will take place.

Population Changes

In the fourth chapter, I examined the variability in space and time of *L. retroversa* in the Gulf of Maine (GOM). My overall goals were to determine if the population had declined in response to environmental change, characterize associations with the physical conditions in the GOM, and relate population cycles to changes in conditions that could be driven by large scale climate oscillations. I examined data collected from 1977 to 2015, which is currently the most up-to-date study using a pteropods time series, but I found no evidence of decline in the abundance of *L. retroversa*.

The ability for pteropods to respond to gradual environmental change may be different than the ability to deal with the immediate changes associated with laboratory experiments.

Although no population decline was observed for *L. retroversa* in the GOM, at some time in the future there could be a decline in response to changing conditions. Alternatively, there might not be population changes if pteropod populations can adapt at a rate that matches the environmental changes or if conditions do not ever exceed their tolerances. The timescale at which pteropod populations can adapt and the existing genetic and phenotypic variability are not well known. A parental effect is when adults that have been exposed to certain conditions confer some heritable advantage or disadvantage to their offspring. One study examined whether eggs laid by pteropods exposed to elevated CO_2 had some resilience to ocean acidification and found that the eggs were more susceptible to ocean acidification (Manno *et al.* 2016). While this did not seem to be a beneficial mechanism for pteropod adaptation, populations can adapt/evolve by other mechanisms including natural selection. Multi-generational studies on pteropods could more realistically inform on population scale effects of environmental stressors, but would require improved culturing techniques.

Changes to food availability may relate to changes in water mass circulation and stratification, since these will affect the nutrients that are available to primary producers (Greene *et al.* 2013). There were apparent associations between years when *L. retroversa* abundances were high and the average salinities were low, which could cause stratification in the water column in a way that supports higher primary productivity. In the GOM, the amount of chlorophyll in the surface ocean has generally increased over the past decades (Kane 2011b, O'Brien *et al.* 2013). The slight increase in abundance of *L. retroversa* in the fall over the time series observed in this study could relate to an overall increase in phytoplankton. The regional variability in shell condition of North Pacific *L. helicina* had an apparent relationship to the chlorophyll fluorescence, suggesting that the amount of food available might affect the fitness of

pteropods. Increased food availability might ameliorate the effects of environmental stressors, including ocean acidification.

Future work on the time series of *L. retroversa* in the GOM could benefit from estimates of the carbonate chemistry. Relating changes in pteropod abundances directly to ocean acidification was not possible due to the lack of an adequate time-series of pCO_2, pH, or Ω_A. In the same way that co-located temperature, salinity, and pteropod density data was important for describing habitat conditions, NESFC surveys should also measure carbonate chemistry associated with each net tow, preferably with enough parameters to calculate Ω_A (e.g. DIC and TA). There is a buoy in the Western GOM that has been taking measurements of pCO_2 since 2006 and pH since 2010, which could be used to generally describe how the carbonate chemistry in the GOM is changing once the time-series becomes long enough (Sutton *et al.* 2013).

Broader View

This thesis focused on pteropods and spanned the scale from the small pores on the surface of the shell to the inter-annual changes in the abundance of pteropods in the Gulf of Maine. Changes to the shell due to ocean acidification could affect the sinking rates of pteropods, which matters at the individual level as a pteropod tries to avoid predation and perform diel vertical migrations and furthermore could affect the global sequestration of carbon to the deep ocean. Pteropods may be responsible for 20-42% of the carbonate that sinks out of the euphotic zone (Bednaršek *et al.* 2012c). When carbon is stored in the deep ocean, it spends a long time before it exchanges with the atmosphere (hundreds to thousands of years, Fortier *et al.* 1994). The sequestration of carbon to depth via pteropods depends on abundances as well. Although, I did not find evidence of a declining population of pteropods in the GOM, long-term

declines have been observed in other regions (Mackas and Galbraith 2011, Beare *et al.* 2013, Beaugrand *et al.* 2013).

It is difficult to predict how ecological interactions between pteropods and their prey and predators will be affected by environmental change. If pteropods are negatively affected by ocean acidification, their role as predators could be reduced. A release of pteropod prey (e.g. tintinnids and dinoflagellates) from pteropod grazing pressure could cause complicated changes in pelagic food webs (Gilmer and Harbison 1991). The mortality of pteropods to predators might increase due to greater visibility and slower escape responses. Furthermore, pteropod shells might serve as protection from predators, and have decreased effectiveness from ocean acidification (Teniswood *et al.* 2013). A disruption to these predator prey dynamics could decrease the abundance of both pteropods and their predators. Although pteropods are sometimes found to be important to certain predators (e.g. juvenile pink salmon, Armstrong *et al.* 2005), it is possible that some predators can switch to other prey in the absence of pteropods. Studies on the predator-prey dynamics of pteropods could help fill some of these gaps in knowledge.

In this thesis, I set out to employ a multi-faceted approach towards studying the fate of pteropods in the face of ocean acidification and other environmental change. Overall, there is the potential for pteropods to be negatively affected by ocean acidification, particularly as CO_2 concentrations increase throughout this century. Wild populations seem to have some degree of resiliency to ocean acidification so far, since two species of pteropod were not strongly sensitive to regional variability in Ω_A and the population of pteropods in the GOM remained robust over 39 years. However, changing environmental conditions, including ocean acidification and warming, could have negative impacts on pteropods in the future. Since pteropods are important to marine ecosystems, the importance of this topic transcends this one taxon. Given their

widespread distributions, changes in the abundance of pteropod species could have global impacts on marine food webs and the carbon cycle.

References

Accornero, A., Manno, C., Esposito, F., and Gambi, M. C. 2003. The vertical flux of particulate matter in the polynya of Terra Nova Bay. Part II. Biological components. *Antarctic Science.* 15(2): 175-188.

Ackman, R.G., Hingley, J., and MacKay, K.T. 1972. Dimethyl sulfide as an odor component in Nova Scotia fall mackerel. *Journal of Fisheries Research Board of Canada*. 29: 1085-1088.

Almogi-Labin, A., Luz, B., Duplessy, J.-C. 1986. Quaternary paleo-oceanography, pteropod preservation and stable-isotope record of the Red Sea. *Palaeogeography, Palaeoclimatology, Palaeoecology*. 57: 195-211.

Amaral, V., Cabral, H. N., and Bishop, M. J. 2011. Resistance among wild invertebrate populations to recurrent estuarine acidification. *Estuarine, Coastal and Shelf Science.* 93: 460-467.

Armstrong, J. L., Boldt, J. L., Cross, A. D., Moss, J. H., Davis, N. D., Meyers, K. W., Walker, R. V., *et al*. 2005. Distribution, size, and interannual, seasonal and diel food habits of northern Gulf of Alaska juvenile pink salmon, *Oncorhynchus gorbuscha*. *Deep-Sea Research II: Tropical Studies in Oceanography.* 52: 247-265.

Bathmann, U. V., Noji, T. T., and Bodungen, B. V. 1991. Sedimentation of pteropods in the Norwegian Sea in autumn. Deep-Sea Research. 38(10): 1341-1360.

Bé, A. W. H., MacClintock, C., and Currie, D. C. 1972. Helical shell structure and growth of the pteropod *Cuverina columnella*. *Biomineralization Reseach Reports*. 4: 47-79.

Beare, D., McQuatters-Gollop, A., van der Hammen, T., Machiels, M., Teoh, S. J., and Hall-Spencer, J. M. 2013. Long-term trends in calcifying plankton and pH in the North Sea. *PLoS ONE*. 8(5): e61175 doi: 10.1371/journal.pone.0061175.

Beaugrand, G., McQuatters-Gollop, A., Edwards, M., and Goberville, E. 2013. Long-term responses of North Atlantic calcifying plankton to climate change. *Nature Climate Change*. 3: 263-267.

Beckmann, W., Auras, A., and Hemleben, C. 1987. Cyclonic cold-core eddy in the eastern North Atlantic. III. Zooplankton. *Marine Ecology Progress Series*. 39: 165-173.

Bednaršek, N., Tarling, G. A., Bakker, D. C., Fielding, S., Cohen, A., Kuzirian, A., McCorkle, D., Lézé, B., and Montagna, R. 2012a. Description and quantification of pteropod shell dissolution: a sensitive bioindicator of ocean acidification. *Global Change Biology*. 18(7): 2378-2388.

Bednaršek, N., Tarling, G. A., Bakker, D. C., Fielding, S., Jones, E. M., Venables, H. J., Ward, P., *et al*. 2012b. Extensive dissolution of live pteropods in the Southern Ocean. *Nature Geoscience*. 5: 881-885.

Bednaršek, N., Možina, J., Vogt, M., O'Brien, C., and Tarling, G. A. 2012c. The global distribution of pteropods and their contribution to carbonate and carbon biomass in the modern ocean. *Earth System Science Data.* 4: 167-186.

Bednaršek, N., Feely, R. A., Reum, J. C. P., Peterson, B., Menkel, J., Alin, S. R., and Hales, B. 2014a. *Limacina helicina* shell dissolution as an indicator of declining habitat suitability owing to ocean acidification in the California Current Ecosystem. *Proceedings of the Royal Society B.* 281: 20140123.

Bednaršek, N., Tarling, G. A., Bakker, D. C. E., Fielding, S., and Feely, R. A. 2014b. Dissolution dominating calcification process in polar pteropods close to the point of aragonite undersaturation. *PLoS ONE.* 9(10): e109183. doi:10.1371/journal.pone.0109183

Bednaršek, N., and Ohman, M.D. 2015. Changes in pteropod distributions and shell dissolution across a frontal system in the California Current System. *Marine Ecology Progress Series*. 523: 93-103.

Bednaršek, N., Harvey, C. J., Kaplan, I. C., Feely, R. A., and Možina, J. 2016a. Pteropods on the edge: cumulative effects of ocean acidification, warming, and deoxygenation. *Progress in Oceanography.* 145: 1-24.

Bednaršek, N., Johnson, J., and Feely, R. A. 2016b. Comment on Peck *et al*: Vulnerability of pteropod (*Limacina helicina)* to ocean acidification: shell dissolution occurs despite an intact organic layer. *Deep Sea Research Part II*. 127: 53-56.

Bednaršek, N., Klinger, T., Harvey, C. J., Weisberg, S., McCabe, R. M., Feely, R. A., Newton, J., and Tolimierir, N. 2017. New ocean, new needs: application of pteropod shell dissolution as a biological indicator for marine resource management. *Ecological Indicators*. 76: 240-244.

Berger, W. H. 1987. Deep-sea carbonate: pteropod distribution and aragonite compensation depth. *Deep-sea Research.* 25: 447-452.

Berner, R.A., and Honjo, S. 1981. Pelagic sedimentation of aragonite: its geochemical significance. *Science*. 211(4485): 940-942.

Bigelow, H. B. 1924. Plankton of the offshore waters of the Gulf of Maine. *Bulletin of the Bureau of Fisheries*. 40(2): 1-528.

Burridge, A. K., Goetze, E., Raes, N., Huisman, J., and Peijnenburg, K. T. C. A. 2015. Global biogeography and evolution of *Cuverina* pteropods. *BMC Evolutionary Biology*. 15:39 doi:10.1186/s12862-015-0310-8.

Busch, D.S., Maher, M., Thibodeau, P., and McElhany, P. 2014. Shell condition and survival of Puget Sound pteropods are impaired by ocean acidification conditions. *PLoS ONE*. 9(8): e105884. doi: 10.1371/journal.pone.0105884.

Byrne, R.H., Acker, J.G., Betzer, P.R., Feely, R.A., and Cates, M.H. 1984. Water column dissolution of aragonite in the Pacific Ocean. *Nature.* 312: 322-326.

Chan, K.Y.K., Grünbaum, D., and O'Donnell, M.J. 2011. Effects of ocean acidification induced morphological changes on larval swimming and feeding. *The Journal of Experimental Biology.* 214: 3857-3867.

Chang, Y., and Yen, J. 2012. Swimming in the intermediate Reynolds range: kinematics of the pteropod *Limacina helicina*. *Integrative and Comparative Biology*. 52(5): 597-615.

Chen, C., and Bé, A. W. H. 1964. Seasonal distributions of euthecosomatous pteropods in the surface waters of five stations in the Western North Atlantic. *Bulletin of Marine Science of the Gulf and Caribbean*. 14(2): 185-220.

Chu, S. N., Wang, Z. A., Doney, S. C., Lawson, G. L., Hoering, K. A. 2016. Changes in anthropogenic carbon storage in the Northeast Pacific in the last decade. *Journal of Geophysical Research: Oceans.* 121: 4618-4632.

Clark, D., Lamare, M., and Barker, M. 2009. Response of sea urchin pluteus larvae (Echinodermata: Echinoidea) to reduced seawater pH: a comparison among a tropical, temperate, and a polar species. *Marine Biology*. 156: 1125-1137.

Cohen, A. L. and Holcomb, M. 2009. Why corals care about ocean acidification, uncovering the mechanism. *Oceanography.* 22(4): 118:127.

Comeau, S., Gorsky, G., Jeffree, R., Teyssié, J. L., and Gattuso, J. P. 2009. Key arctic pelagic mollusk (*Limacina helicina*) threatened by ocean acidification. *Biogeosciences*. 6: 1877-1882.

Comeau, S., Jeffree, R., Teyssié, J. L., and Gattuso, J. P. 2010a. Response of the Arctic pteropod *Limacina helicina* to projected future environmental conditions. *PLoS ONE*. 5(6): e11362. doi:10.1371/journal.pone.0011362.

Comeau, S., Gorsky, G., Alliouana, S., and Gattuso, J. P. 2010b. Larvae of the pteropod *Cavolinia inflexa* exposed to aragonite undersaturation are viable but shell-less. *Marine Biology.* doi: 10.1007/s00227-010-1493-6

Comeau, S., Alliouane, S., and Gattuso, J. P. 2012a. Effects of ocean acidification on overwintering juvenile Arctic pteropods *Limacina helicina*. *Marine Ecology Progress Series*. 456: 279-284.

Comeau, S., Gattuso, J. P., Jeffree, R., and Gazeau, F. 2012b. Effect of carbonate chemistry manipulations on calcification, respiration, and excretion of a Mediterranean pteropod. *Biogeosciences Discuss*. 9: 6169-6189.

Comeau, S., Gattuso, J. P., Nisumaa, A. M., and Orr, J. 2012c. Impacts of aragonite saturation state changes on migratory pteropods. *Proceedings of the Royal Society B.* 279: 732-738.

Conover, J. R., and Lalli, C. M. 1974. Feeding and growth in *Clione limacina*, a pteropod mollusk. II. Assimilation, metabolism, and growth efficiency. *Journal of Experimental Marine Biology and Ecology.* 16: 131-154.

Dadon, J. R. 1990. Annual cycle of *Limacina retroversa* in Patagonian waters. *American Malacological Bulletin*. 18(1): 77-84.

Dadon, J. R., and Masello, J. F. 1999. Mechanisms generating and maintaining the admixture of zooplanktonic molluscs (Euthcosomata: Opistobranchiata: Gastropoda) in the subtropical front of the South Atlantic. *Marine Biology.* 135: 171-179.

Davenport, J., and Bebbington, A. 1990. Observations on the swimming and buoyancy of some thecosomatous pteropod gastropods. *Journal of Molluscan Studies*. 56: 487-497

de Moel, H., Ganssen, G. M., Peeters, F. J. C., Jung, S. J. A., Brummer, G. J. A., snf Zeebe, R. E. 2009. Planktonic foraminiferal shell thinning in the Arabian Sea due to anthropogenic ocean acidification? *Biogeosciences.* 6: 1917-1925.

Dickinson, G. H., Matoo, O. B., Tourek, R. T., Sokolova, I. M., and Beniash, E. 2013. Environmental salinity modulates the effects of elevated CO_2 levels on juvenile hard-shell clams, *Mercenaria mercenaria*. *The Journal of Experimental Biology.* 216: 2607-2618.

Dickson, A.G., and Millero, F.J. 1987. A comparison of the equilibrium constants for the dissociation of carbonic acid in seawater media. *Deep Sea Research.* 34: 1733-1743.

Dickson, A.G. 1990. Thermodynamics of the dissociation of boric acid in synthetic seawater from 273.15 to 318.15 K. *Deep Sea Research.* 37: 755-766.

Diester-Haass, L. 1973. Holocene climate in the Persian Gulf as deduced from grain-size and pteropod distribution. *Marine Geology*. 14: 207-223.

Doney, S. C., Fabry, V. J., Feely, R. A., and Kleypas, J. A. 2009. Ocean acidification: the other CO_2 Problem. *Annual Review of Marine Science.* 1: 169-192.

Drenkard, E. J., Cohen, A. L., McCorkle, D. C., de Putron, S. J., Starczak, V. R., and Zicht, A. E. 2013. Calcification by juvenile corals under heterotrophy and elevated CO_2. *Coral Reefs.* 32: 727-735.

Emerson, E., and Hedges. J. 2008. Chemical Oceanography and the Marine Carbon Cycle. Cambridge University Press, Cambridge. 407 pp.

Fabry, V. J., and Deuser, W. G. 1992. Seasonal changes in the isotopic compositions and sinking fluxes of euthecosomatous pteropod shells in the Sargasso Sea. *Paleoceanography.* 7(2): 195-213.

Fabry, V.J., Seibel, B.A., Feely, R.A., and Orr, J.C. 2008. Impacts of ocean acidification on marine fauna and ecosystem processes. *ICES Journal of Marine Science*. 65: 414 -432.

Fanelli, E., Cartes, J. E., and Papiol, V. 2011. Food web structure of deep-sea macrozooplankton and micronekton off the Catalan slope: insight from stable isotopes. *Journal of Marine Systems*. 87(1): 79-89.

Feely, R. A., Sabine, C. L., Lee, K., Berelson, W., Kleypas, J., Fabry, V. J., and Millero, F. J. 2004. Impact of anthropogenic CO_2 on the $CaCO_3$ system in the oceans. *Science.* 305: 362-366.

Fernández-Reiriz, M. J., Range, P., and Álvarez-Salgado, X. A. 2012. Tolerance of juvenile *Mytilus galloprovincialis* to experimental seawater acidification. *Marine Ecology Progress Series*. 454: 65-74.

Fortier, L, Le Fèvre, J., and Legendre, L. 1994. Export of biogenic carbon to fish and to the deep ocean: the role of large planktonic microphages. *Journal of Plankton Research.* 16(7): 809-839.

Gallager, S. M., Davis, C. S., Epstein, A. W., Solow, A., and Beardsley, R. C. 1996. High-resolution observations of plankton spatial distributions correlated with hydrography in the Great South Channel, Georges Bank. *Deep-Sea Research II.* 43(7-8): 1627-1663.

Gasca, R., and Janssen, A. W. 2014. Taxonomic review, molecular data and key to the species of Creseidae from the Atlantic Ocean. *Journal of Molluscan Studies*. 80(1): 35-42.

Gazeau, F., Quiblier, C., Jansen, J. M., Gattuso, J. P., Middelburg, J. J., and Heip, C. H. R. 2007. Impact of elevated CO_2 on shellfish and calcification. *Geophysical Research Letters.* 34: L07603, doi:10.1029/2006GL028554

Gazeau, F., Parker, L. M., Comeau, S., Gattuso, J. P., O'Connor, W. A., Martin, S., Pörtner, H. O., and Ross, P. M. 2013. Impacts of ocean acidification on marine shelled molluscs. *Marine Biology*. 160: 2207-2245.

Gerhardt, S., Groth, H., Rühlemann, C., and Henrich R. 2000. Aragonite preservation in late Quaternary sediment cores on the Brazilian Continental Slope: implications for intermediate water circulation. *International Journal of Earch Science.* 88: 607-618.

Gerhardt, S., and Henrich, R. 2001. Shell preservation of *Limacina inflata* (Pteropoda) in surface sediments from the Central and South Atlantic Ocean: a new proxy to determine the aragonite saturation state of water masses. *Deep-Sea Research I.* 48: 2051-2071.

Geyer, W. R., Signell, R. P., Fong, D. A., Wang, J., Anderson, D. M., and Keafer, B. A. 2004. The freshwater transport and dynamics of the western Maine coastal current. *Continental Shelf Research.* 24. 1339-1357.

Gilmer, R. W., and Harbison, G. R. 1986. Structure and field behavior of pteropod molluscs: feeding methods in the families Cavoliniidae, Limacinidae, and Peraclididae (Gastropoda: Thecosomata). *Marine Biology*. 91: 47-57.

Gilmer, R. W., and Harbison, G. R. 1991. Diet of *Limacina helicina* (Gastropoda: Thecosomata) in Arctic waters in midsummer. *Marine Ecology Progress Series.* 77: 125-134.

Glendill, D. K., White, M. M., Salisbury, J., Thomas, H. Mlsna, I., Liebman, M., Mook, B., *et al.* 2015. Ocean and coastal acidification off New England and Nova Scotia. *Oceanography*. 28(2): 182-197.

Greene, C. H., Pershing, A. J., Conversi, A., Blanque, B., Hannah, C., Sameoto, D., Head, E., *et al.* 2003. Trans-Atlantic responses of *Calanus finmarchicus* populations to basin-scale forcing associated with the North Atlantic Oscillation. *Progress in Oceanography.* 58: 301-312.

Greene, C. H., and Pershing, A. J. 2007. Climate drives sea change. *Science.* 315(5815): 1084-1085.

Greene, C. H., Meyer-Gutbrod, E., Monger, B. C., McGarry, L. P., Pershing, A. J., Belkin, I, M., Frantantoni, P. S., *et al.* 2013. Remote climate forcing of decadal-scale regime shifts in Northwest Atlantic shelf ecosystems. *Limnology and Oceanography*. 58(3): 803-816.

Gruber, N. 2011, Warming up, turning sour, losing breath: ocean biogeochemistry under global change. *Philosophical Transactions of the Royal Society.* 369: 1980-1996.

Haddad, G.A., and Droxler, A.W. 1996. Metastable $CaCO_3$ dissolution at intermediate water depths of the Caribbean and western North Atlantic: Implications for intermediate water circulation during the past 200,000 years. *Paleoceanography.* 11(6): 701-716.

Head, E. J. H., and Pepin, P. 2010. Spatial and inter-decadal variability in plankton abundance and composition in the Northwest Atlantic (1958-2006). *Journal of Plankton Research.* 32(12): 1633-1648.

Hiebenthal, C., Philipp, E. E. R., Eisenhauer, A., and Wahl, M. 2013. Effects of seawater pCO_2 and temperature on shell growth, shell stability, condition and cellular stress of Western Baltic Sea *Mytilus edulis* and *Arctica islandica*. *Marine Biology.* 160: 2073-2087.

Howes, E. L., Bednaršek, N., Büdenbender, J., Comeau, S., Doubleday, A., Gallager, S. M., Hopcroft, R. R., et al., 2014. Sink and swim: a status review of thecosome pteropod culture techniques. Journal of Plankton Research. 36(2): 299-315.

Howes, E. L., Stemmann, L., Assailly, C., Irisson, J. O., Dima, M., Bijma, J., and Gattuso, J. P. 2015. Pteropod time series from the North Western Mediterranean (1967-2003): impacts of pH and climate variability. *Marine Ecology Progress Series.* 531: 193-206.

Howes, E. L., Eagle, R. A., Gattuso, J. P., and Bijma, J. 2017. Comparison of Mediterranean pteropod shell biometrics and ultrastructure from historical (1910 and 1921) and present day (2012) samples provides baseline for monitoring effects of global change. *PLoS ONE.* 12(1): e0167891. doi: 10.1371/journal.pone.0167891.

Hsiao, S. C. T. 1939. The reproductive system and spermatogenesis of *Limacina (Spiratella) retroversa*. *Biological Bulletin*. 76(2): 280-303.

Hunt, B. P. V., Pakhomov, E. A., Hosie, G. W., Siegel, V., Ward, P., and Bernard. K. 2008. Pteropods in the southern ocean ecosystems. Progress in Oceanography. 78: 193-221.

Hunt, B., Strugnell, J. Bednaršek, N., Linse, K, Nelson, R. J. Pakhomov, E., Seibel, B., Steinke, D., and Würzberg, L. 2010. Poles apart: the "biopolar" pteropod species *Limacina helicina* is genetically distinct between the Arctic and Antarctic Oceans. *PLoS ONE.* 5(3): e9835. doi:10.1371/journal.pone.0009835.

Hurrell, J. W. 1995. Decadal trends in the North Atlantic Oscillation: regional temperatures and precipitation. *Science.* 269(5224): 676-679.

Ivanina, A. V., Dickinson, G. H., Matoo, O. B., Bagwe, R., Dickinson, A., Beniash, E., and Sokolova, I.M. 2013. Interactive effects of elevated temperature and CO_2 levels on energy metabolism and biomineralization of marine bivalves *Crassostrea virginica* and *Mercenaria mercenaria. Comparative Biochemistry and Physiology, Part A.* 166: 101-111.

Johnson, K. M., Hoshijima, U., Sugano, C. S., Nguyen, A. T., and Hofmann, G. E. 2016. Shell dissolution observed in *Limacina helicina antarctica* from the Ross Sea, Antarctica: paired shell characteristics and *in situ* seawater chemistry. *Biogeosciences Discuss.* doi:10.5194/bg-2016-467, in review.

Kane, J. 2007. Zooplankton abundance trends on Georges Bank, 1977-2004. *ICES Journal of Marine Science*. 64(5): 909-919.

Kane, J. 2011a. Inter-decadal variability of zooplankton abundance in the Middle Atlantic Bight. *Journal of Northwest Atlantic Fisheries Science.* 43: 81-92.

Kane, J. 2011b. Multiyear variability of phytoplankton abundance in the Gulf of Maine. *ICES Journal of Marine Science.* 68(9): 1833-1841.

Karnovsky, N.J., Hobson, K.A., Iverson, S., and Hunt, G.L. 2008. Seasonal changes in diets of seabirds in the North Water Polynya: a multiple-indicator approach. *Marine Ecology Progress Series.* 357: 291-299.

Kornicker, L. S. 1959. Observations on the behavior of the pteropod *Creseis acicula*. *Bulletin of Marine Science of the Gulf and Caribbean*. 9(3): 331-336.

Kroeker, K.J., Kordas, R. L., Crim, R. N., and Singh, G. G. 2010. Meta-analysis reveals negative yet variable effects of ocean acidification on marine organisms. *Ecology Letters*. 13: 1419-1434.

Kurihara, H. 2008. Effects of CO_2-driven ocean acidification on the early development of stages of invertebrates. *Marine Ecology Progress Series*. 373: 275-284.

Kurihara, H., Asai, T., Kato, S., and Ishimatsu, A. 2009. Effects of elevated pCO_2 on early development in the mussel *Mytilus galloprovincialis*. *Aquatic Biology*. 4: 225-233.

Lalli, C. M. 1972. Food and feeding of *Paedoclione doliiformis* Danforth, a neotenous gymnosome pteropod. *Biological Bulletin.* 143: 392-402.

Lalli, C.M., and Gilmer, R.W. 1989. Pelagic snails: the biology of holoplanktonic gastropod mollusks. *Stanford University Press*, Los Altos. 259 pp.

Langdon, C., and Atkinson, M. J. 2005. Effect of elevated pCO_2 on photosynthesis and calcification of corals and interactions with seasonal change in temperature/irradiance and nutrient enrichment. *Journal of Geophysical Research*. 110: C09S07, doi: 10.1029/2004JC002576.

LeBrasseur, R. J. 1966. Stomach contents of salmon and steelhead trout in the Northeastern Pacific Ocean. *Journal of Fisheries Research Board of Canada*. 23(1): 85-100.

Letessier, T. B., Pond, D. W., McGill, R. A. R., William, W. D. K., and Brierley, A. S. 2012. Trophic interactions of invertebrate zooplankton on either side of the Charlie Gibbs Fracture Zone/Subpolar Front of the Mid-Atlantic Ridge. *Journal of Marine Systems*. 94: 174-184.

Levasseur, M., Keller, M. D., Bonneau, E., D'Amours, D., and Bellows, W. K. 1994. Oceanographic basis of a DMS-related Atlantic cod (Gadus morhua) fishery problem: blackberry feed. *Canadian Journal of Fisheries and Aquatic Sciences*. 51: 881-889.

Li, L., Weaver, J. C., and Ortiz, C. 2015. Hierarchical structural design for fracture resistance in the shell of the pteropod *Clio pyramidata*. *Nature Communications.* doi:10.1038/ncomms7216.

Lischka, S., Büdenbender, J., Boxhammer, T., and Riebesell, U. 2011. Impact of ocean acidification and elevated temperatures on early juveniles of the polar shelled pteropod *Limacina helicina*: mortality, shell degradation, and shell growth. *Biogeosciences*. 8: 919-932.

Lischka, S., and Riebesell, U. 2012. Synergistic effects of ocean acidification and warming on overwintering pteropods in the Arctic. *Global Change Biology*. 18: 3517-3528.

Lischka, S., and Riebesell, U. 2016. Metabolic response of Arctic pteropods to ocean acidification and warming during the polar night/twilight phase in Kongsfjord (Spitsbergen). *Polar Biology*. doi:10.1007/s00300-016-2044-5.

Loeb, V. J., and Santora, J. A. 2013. Pteropods and climate off the Antarctic Peninsula. *Progress in Oceanography.* 116: 31-48.

Maas, A.E., Wishner, K.F., and Seibel, B.A. 2012. Metabolic suppression in thecosomatous pteropods as an effect of low temperature and hypoxia in the eastern tropical North Pacific. *Marine Biology*. 159: 1955-1967.

Maas, A. E., Blanco-Bercial, L., and Lawson, G. L. 2013. Reexamination of the Species Assignment of Diacavolinia Pteropods Using DNA Barcoding. *PLoS ONE.* 8(1): e53889. doi:10.1371/journal.pone.0053889.

Maas, A. E., Lawson, G. L., and Wang, Z. A. 2016. The metabolic response of thecosome pteropods from the North Atlantic and North Pacific oceans to high CO_2 and low O_2. *Biogeosciences*. 13: 6191-6210.

Mackas, D. L., and Galbraith, M. D. 2011. Pteropod time series from the NE Pacific. *ICES Journal of Marine Science*. 69: 448-459.

Manno, C., Sandrini, S., Tositti, L., and Accornero, A. 2007. First stages of degradation of *Limacina helicina* shells observed above the aragonite chemical lysocline in Terra Nova Bay (Antarctica). *Journal of Marine Systems.* 68: 91-102.

Manno, C., Morata, N., and Primicerio, R. 2012. *Limacina retroversa's* response to combined effects of ocean acidification and sea water freshening. *Estuarine, Coastal and Shelf Science*. 113: 163-171.

Manno, C., Peck, V. L., and Tarling, G. A. 2016. Pteropod eggs released at high pCO_2 lack resilience to ocean acidification. *Nature: Scientific Reports.* 6: 25752. doi:10.1038/srep25752.

Matoo, O. B., Ivanina, A. V., Ullstad, C., Beniash, E., and Sokolova, I.M. 2013. Interactive effects of elevated temperature and CO_2 levels on metabolism and oxidative stress in two common marine bivalves (*Crassostrea virginica* and *Mercenaria mercenaria*). *Comparatice Biochemistry and Physiology, Part A.* 164: 545-553.

Matsumoto, K. 2007. Radiocarbon-based circulation age of the world oceans. *Journal of Geophysical Research*. doi:10.1029/2007JC004095

McGowan, J.A. 1963. Geographical variation in *Limacina helicina* in the North Pacific. *Speciation in the sea. Systematics Association Publication No. 5*, 109-128.

Mehrbach, C., Culberson, C. H., Hawley, J. E., and Pytkowicz, R. M. 1973. Measurement of apparent dissociation constants of carbonic acid in seawater at atmospheric pressure. *Limnology and Oceanography*. 18: 897-907.

Melzner, F., Stange, P., Trübenbach, K., Thomsen, J., Casties, I., Panknin, U., Gorb, S. N., Gutowska, M.A. 2011. Food supply and seawater pCO_2 impact calcification and internal shell dissolution of the blue mussel *Mytilus edulis*. *PLoS ONE*. 6(9): e24223. doi:10.1371/journal.pone.0024223

Miller, A. W., Reynolds, A. C., Sobrino, C., Riedel. G. F. 2009. Shellfish face uncertain future in high CO_2 world: influence of acidification on oyster larvae calcification and growth in esutaries. *PLoS ONE.* 4(5): e5661. doi:10.1371/journal.pone.0005661

Millman, J. D., Troy, P. J., Balch, W. M., Adams, A. K., Li, Y. H., and Mackenzie, F. T. 1999. Biologically mediated dissolution of calcium carbonate above the chemical lysocline? *Deep-Sea Research I*. 46: 1653-1669.

Morse, R. E., Friedland, K. D., Tommasi, D., Stock, C., and Nye, J. 2017. Distinct zooplankton regime shift patterns across ecoregions of the U.S. Northeast continental shelf Large Marine Ecosystem. *Journal of Maine Systems.* 165: 77-91.

Mountain, D. G. 2012. Labrador slope water entering the Gulf of Maine – response to the North Atlantic Oscillation. *Continental Shelf Research.* 47: 150-155.

Mucci, A. 1983. The solubility of calcite and aragonite in seawater at various salinities, temperatures, and one atmospheric total pressure. *American Journal of Science*. 283: 780-799.

Murphy, D.W., Adhikari, D., Webster, D.R., and Yen, J. 2016. Underwater flight by the planktonic sea butterfly. *Journal of Experimental Biology.* 219: 535-543.

Noji, T. T., Bathmann, U. V., von Bodungen, B., Voss, M., Anita, A., Krumbholz, M., *et al.* 1997. Clearance of picoplankton-sized particles and formation of rapidly sinking aggregates by the pteropod, *Limacina retroversa*. *Journal of Plankton Research*. 19(7): 863-875.

Nye, J. A., Link, J. S., Hare, J. A., and Overholtz, W. J. 2009. Changing spatial distributions of fish stocks in relation to climate and population size on the Northeast United States continental shelf. *Marine Ecology Progress Series.* 393: 111-129.

Nye, J. A., Baker, M. R., Bell, R., Kenny, A., Halimeda Kilbourne, K., Friedland, K. D.,Martino, E., *et al.* 2014. Ecosystem effects of the Atlantic Multidecadal Oscillation. *Journal of Marine Systems.* 133: 103-116.

O'Brien, T. D., Wiebe, P. H., and Faulkenhaug, T. 2013. ICES zooplankton status report 2010/2011. ICES Cooperative Research Report No. 318. 208 pp.

Ohman, M. D., Lavaniegos, B. E., and Townsend, A. W. 2009. Multi-decadal variations in calcareous holozooplankton in the California Current System: thecosome pteropods, hteropods, and foraminifera. *Geophysical Research Letters*. 36(18): L18608, doi:10.1029/2009GL039901.

Orr, J.C., Fabry, V.J., Aumont, O., Bopp, L., Doney, S.C., Feely, R.A., and Gnanadesikan, A., *et al*. 2005. Anthropogenic ocean acidification over the twenty-first century and its impacts on calcifying organism. *Nature.* 437(29): 681-686.

Owen, J.P., and Ryu, W.S. 2015. The effects of linear and quadratic drag on falling spheres: an undergraduate laboratory. *European Journal of Physics.* 26: 1085-1091.

Pakhomov, E.A., Perissinotto, R., and McQuaid, C.D. 1996. Prey composition and daily rations of myctophid fishes in the Southern Ocean. *Marine Ecology Progress Series.* 134: 1-14.

Parker, L. M., Ross, P. M., and O'Connor, W. A. 2010. Comparing the effect of elevated pCO_2 and temperature on the fertilization and early development of two species of oysters. *Marine Biology.* 157: 2435-2452.

Parker, L. M., Ross, P. M., and O'Connor W. A. 2011. Populations of the Sydney rock oyster, *Saccostrea glomerata*, vary in response to ocean acidification. *Marine Biology*. 158: 689-697.

Passow, U., and Carlson, C. A. 2012. The biological pump in a high CO_2 world. *Marine Ecology Progress Series.* 470: 249-271.

Peck, V. L., Tarling, G. A., Manno, C., Harper, E. M., and Tynan, E. 2016. Outer organic layer and internal repair mechanism protects pteropod *Limacina helicina* from ocean acidification. *Deep-Sea Research II.* 127: 41-52.

Pershing, A. J., Head, E. H. J., Greene, C. H., and Jossi, J. W. 2010. Pattern and scale of variability among Northwest Atlantic shelf plankton communities. *Journal of Plankton Research.* 32(12): 1661-1674.

Pershing, A. J., Alexander, M. A., Hernandez, C. M., Kerr, L. A., Le Bris, A., Mills, K. E., Nye, J. A., *et al.* 2015. Slow adaptation in the face of rapid warming leads to collapse of the Gulf of Maine cod fishery. *Science.* 350(6262): 809-812.

Pettigrew, N. R., Churchill, J. H., Janzen, C. D., Mangum, L. J., Signell, R. P., Thomas, A. C., Townsend. D. W., Wallinga, J. P., and Xue, H. 2005. The kinematic and hydrographic structure of the Gulf of Maine coastal current. *Deep-Sea Research II.* 52: 2369-2391.

Pierrot, D., Lewis, E., and Wallace, D. 2006. Co2sys DOS Program developed for CO_2 system calculations. Carbon Dioxide Information anlysis Center, Oak Ridge National Laboratory, US Department of Energy ORNL/CDIAC-105.

Pomerleau, C., Lesage, V., Ferguson, S.H., Winkler, G., Petersen, S.D., and Higdon, J.W. 2012. Prey assemblage isotopic variability as a tool for assessing diet and the spatial distribution of bowhead whale *Balaena mysticetus* foraging in the Canadian eastern Arctic. *Marine Ecology Progress Series.* 469: 161-174.

Range, P., Piló, D., Ben-Hamadou, R., Chícharo, M. A., Matias, D., Joaquim, S., Oliveira, A. P., and Chícharo, L. 2012. Seawater acidification by CO_2 in a coastal lagoon environment: effects on life history traits of juvenile mussels *Mytilus galloprovincialis*. *Journal of Experimental Marine Biology and Ecology.* 424-425: 89-98.

Raven, J., Caldeira, K., Elderfield, H., Hoegh-Guldberg, O., Liss, P., Riebesell, U., Shepherd, J., Turley, C. and Watson, A. 2005. Ocean acidification due to increasing atmospheric carbon dioxide. Policy Document 12/05, The Royal Society, London. 60 pp.

Redfield, A. C. 1939. The history of a population of *Limacina retroversa* during its drift across the Gulf of Maine. *Biological Bulletin.* 76(1): 26-47.

Richoux, N. B., and Froneman, P. W. 2009. Plankton trophodynamics at the subtropical convergence, Southern Ocean. *Journal of Plankton Research*. 31(9): 1059-1073.

Ries, J. B., Cohen, A. L., and McCorkle, D. C. 2009. Marine calcifiers exhibit mixed responses to CO_2 induced ocean acidification. *Geology*. 37(12):1131-1134.

Roberts, D., Howard, W. R., Moy, A. D., Roberts, J. L., Trull, T. W., Bray, S. G., and Hopcroft, R. R. 2011. Interannual pteropod variability in sediment traps deployed above and below the aragonite saturation horizon in the Sub-Antarctic Southern Ocean. *Polar Biology*. 34: 1739-1750.

Roger, L. M., Richardson, A. J., McKinnon, A. D., Knott, B., Matear, R., and Scadding, C. 2012. Comparison of the shell structure of two tropical *Thecosomata* (*Creseis acicula* and *Diacavolinia longirostris*) from 1963 to 2009: potential implications of declining aragonite saturation. *ICES Journal of Marine Science*. 69(3): 465-474.

Sabine, C. L., Feely, R. A., Gruber, N., Key, R. M., Lee, K., Bullister, J. L., Wanninkhof, *et al.* 2004. The oceanic sink for anthropogenic CO_2. *Science*. 305(5682): 367-371.

Salisbury, J., Vandemark, Hunt, C., Campbell, J., Jonsson, B., Mahadevan, A., McGills, W., and Xue, H. 2009. Episodic riverine influence on surface DIC in the coastal Gulf of Maine. *Estuarine, Coastal and Shelf Science.* 82: 108-118.

Seibel, B. A., Maas, A. E., and Dierssen, H. M. 2012. Energetic plasticity underlies a variable response to ocean acidification in the pteropod, *Limacina helicina antarctica. PLoS ONE.* 7(4): e30464. doi: 10.1371/journal.pone.0030464.

Sturdevant, M. V., Orsi, J. A., and Fergusson, E. A. 2013. Diets and trophic linkages of epipelagic fish predators in coastal Southeast Alaska during a period of warm and cold climate years, 1997-2011. *Marine and Coastal Fisheries: Dynamics, Management, and Ecosystem Science*. 4: 526-545.

Sutton, A., Sabine, C., Salisbury, J., Vandemark, D., Musielewicz, S., Maenner, S., Dietrich, C., Bott, R., and Osborne, J. 2013. High-resolution ocean and atmosphere pCO2 time series measurements from mooring NH_70W_43N. http://cdiac.esd.ornl.gov/ftp/oceans/Moorings/NH_70W_43N/. Carbon Dioxide Information Analysis Center, Oak Ridge National Laboratory, US Department of Energy, Oak Ridge, Tennessee. doi: 10.3334/CDIAC/OTG.TSM_NH_70W_43N.

Talley L.D., G.L. Pickard, W.J. Emery, J.H. Swift. 2011. Descriptive Physical Oceanography: An Introduction (Sixth Edition). *Elsivier*. Boston, MA. 555 pp.

Talmage, S. C., and Golber, C. J. 2011. Effects of elevated temperature and carbon dioxide on the growth and survival of larvae and juveniles of three species of Northwest Atlantic bivalves. *PLoS ONE*. 6(10): e26941. doi:10.1371/journal.pone.0026941

Teniswood. C.M.H., D. Roberts, W.R. Howard, and J.E. Bradby. 2013. A quantitative assessment of the mechanical strength of the polar pteropod *Limacina helicina antarctica* shell. *ICES Journal of Marine Science.* 70(7): 1499-1505.

Thabet, A.A., Maas, A.E., Lawson, G.L., and Tarrant, A.M. 2015. Life cycle and early development of the thecosomatous pteropod *Limacina retroversa* in the Gulf of Maine, including the effect of elevated CO_2 levels. *Marine Biology.* 162: 2235-2249.

Thomsen, J., Casties, I., Pansch, C., Körtizinger, A., and Melzner, F. 2013. Food availability outweighs ocean acidification effects in juvenile *Mytilus edulis*: laboratory and field experiments. *Global Change Biology*. 19: 1017-1027.

Townsend, D. W., Rebuck, N. D., Thomas, M. A., Karp-Boss, L., and Gettings, R. M. 2010. A changing nutrient regime in the Gulf of Maine. 30: 820-823.

Townsend, D., W., Pettigrew, N. R., Thomas, M. A., Neary, M. G., McGillicuddy, D. J., and O'Donnell, J. 2015. Water masses and nutrient sources to the Gulf of Maine. *Journal of Marine Research.* 73: 93-122.

Van der Spoel, S. 1969. The shell of *Clio pyramidata* forma *Lanceolata* and forma *convexa* (*Gastropoda, Pteropoda*). *Vidensk. Meddr dansk naturh. Foren.* 132: 95:114.

Vecchione, M., and Grant, G. C., 1983. A multivariate analysis of planktonic molluscan distribution in the Middle Atlantic Bight. 1(4): 405-424.

Vinogradov, M. Y. 1961. Food sources of the deep-water fauna. Speed of decomposition of dead Pteropoda. *Doklady Akademii Nauk SSSR.* 138: 1439-1442.

Waldbusser, G. G., Steenson, R. A., and Green, M. A. 2011. Oyster shell dissolution rates in estuarine waters: effects of pH and shell legacy. *Journal of Shellfish Research.* 30(3): 659-669.

Walker, J. A. 2002. Functional Morphology and Virtual Models: Physical Constraints on the Design of Oscillating Wings, Fins, Legs, and Feed at Intermediate Reynolds Numbers. *Integrative and Comparative Biology.* 42: 232-242.

Wall-Palmer, D., Smart, C. W., and Hart, M. B. 2013. In-life pteropod dissolution as an indicator of past ocean carbonate saturation. *Quaternary Science Reviews.* 81: 29-34.

Wang, Z. A., and Cai W. J. 2004. Carbon dioxide degassing and inorganic carbon export from a marsh-dominated estuary (the Duplin River): a marsh CO_2 pump. *Limnology and Oceanography.* 49: 341-354.

Wang, Z. A., Wanninkhof, R., Cai, W. J., Byrne, R. H., Hu, X., Peng, T. H., and Huang, H. J. 2013. The marine inorganic carbon system along the Gulf of Mexico and Atlantic coasts of the United States: insights from transregional coastal carbon study. *Limnology and Oceanography*. 58(1): 325-342.

Wang, Z. A., Lawson, G. L., Pilskaln, C. H., and Maas, A. E. 2017. Seasonal controls of aragonite saturation states in the Gulf of Maine. *Journal of Geophysical Research: Oceans.* 122(1): 372-389.

Wanninkhof, R., Barbero, L., Byrne, R., Cai, W. J., Huang, W. J., Zhang, J. Z., Baringer, M., and Langdon, C. 2015. Ocean acidification along the Gulf Coast and East Coast of the USA. *Continental Shelf Resesarch*. 98: 54-71.

Wessel, P., and Smith, H. H. F. 1996. A global self-consistent, hierarchical, high-resolution shoreline database. *Journal of Geophysical Research.* 101(4): 8741-8743.

Wheeler, J. D., Helfrich, K. R., Anderson, E. J., McGann, B., Staats, P., Wargula, A. E., Wilt, K., and Mullineaux, L. S. 2013. Upward swimming of competent oyster larvae *Crassostrea virginica* persists in highly turbulent flow as detected by PIV flow subtraction. *Marine Ecology Progress Series.* 488: 171-185.

White, A. W. 1977. Dinoflagellate toxins as probable cause of an Atlantic herring (*Clupea harengus harengus*) kill, and pteropods as apparent vector. *Journal of Fisheries Research Board of Canada.* 34: 2421-2424.

White, M. M., McCorkle, D. C., Mullineaux, L. S., and Cohen, A. L. 2013. Early exposure of bay scallops (*Argopecten irradians*) to high CO_2 causes a decrease in larval shell growth. *PLoS ONE.* 8(4): e61065. doi:10.1371/journal.pone.0061065

Wiebe, P. H. 1970. Small-scale spatial distribution in oceanic zooplankton. *Limnology and Oceanography.* 15(2): 205-217.

Wormuth, J. H. 1981. Vertical distributions and diel migrations of *Euthecosomata* in the northwest Sargasso Sea. *Deep-sea Research*. 28A(12): 1493-1515.

Wormuth, J. H. 1985. The role of cold-core Gulf Stream rings in the temporal and spatial patterns of euthecosomatous pteropods. *Deep-Sea Research*. 32(7): 773-788.

Zhang, T., Ma, Y., Chen, K., Kunz, M., Tamura, N., Qiang, M., Xu, J., and Qi, L. 2011. Structure and mechanical properties of a pteropod shell consisting of interlocked helical aragonite nanofibers. *Angewandte Chemie International Edition*. 50: 10361-10365.